

# **TGF- $\beta$ signaling at the cellular junctions**

DISSERTATION

Zur Erlangung des akademischen Grades

**Doctor rerum naturalium**

**(Dr. rer. nat.)**

vorgelegt

der Fakultät Mathematik und Naturwissenschaften

der Technischen Universität Dresden

von

Dipl.-Biochem. **Veronica Dudu**

geboren am 12.10.1976 in Bukarest

# **TGF- $\beta$ signaling at the cellular junctions**

DISSERTATION

Zur Erlangung des akademischen Grades

**Doctor rerum naturalium**

**(Dr. rer. nat.)**

vorgelegt

der Fakultät Mathematik und Naturwissenschaften

der Technischen Universität Dresden

von

Dipl.-Biochem. **Veronica Dudu**

geboren am 12.10.1976 in Bukarest

Gutachter: Dr. Marcos González-Gaitán

Prof. Dr. Gerold Barth

Prof. Dr. Christian Klämbt

Eingereicht: 22.02.2005

Tag der Verteidigung:



## SUMMARY

During cell communication, cells produce secreted signals termed morphogens, which traffic through the tissue until they are received by target, responding cells. Using the fruit fly *Drosophila melanogaster* as a model organism, I have studied transforming growth factor- $\beta$  (TGF- $\beta$ ) signal from the secreting to the receiving cells in the developing wing epithelial cells and at the neuromuscular junctions. Cell culture studies have suggested that cells modulate morphogenetic signaling by expressing the receptors and secreting the ligand in spatially defined areas of the cell. Indeed, I have found that TGF- $\beta$  ligands, receptors and R-Smads show a polarized distribution both in the epithelial cells and at the synapses. My results indicate that the cellular junctions define a signaling domain within the plasma membrane, to which TGF- $\beta$  signaling machinery is targeted.

In the context of epithelial cells, the junctions play a role in TGF- $\beta$  signaling regulation through their component  $\beta$ -cat. A complex forms between  $\beta$ -cat and the R-Smad Mad, but the mechanism by which  $\beta$ -cat modulates signaling is not yet understood.

At the synapse, the sub-cellular localization of TGF- $\beta$  pathway components indicates the occurrence of an anterograde signal. Moreover, my results suggest a scenario in which TGF- $\beta$  signaling is coupled with synaptic activity: quanta of growth factor, released upon neurostimulation together with neurotransmitter quanta, could modulate therefore the development and the function of the synapse.

## TABLE OF CONTENTS

<b>SUMMARY</b> .....	I
<b>TABLE OF CONTENTS</b> .....	II
<b>INTRODUCTION</b> .....	1
<b>TGF-<math>\beta</math> signaling in wing imaginal discs</b> .....	2
Patterning wing imaginal discs in <i>Drosophila</i> .....	2
TGF- $\beta$ signaling pathway.....	4
Dpp morphogenetic gradient .....	7
Apico-basal polarity and cell junctions.....	9
Do the cell junctions play a role in TGF- $\beta$ signaling? .....	12
<b>TGF-<math>\beta</math> signaling at the neuromuscular junction</b> .....	13
<i>Drosophila</i> neuromuscular junction (NMJ).....	13
Control of synapse growth and function .....	16
Morphogens at the synapse.....	17
TGF- $\beta$ signaling at the synapse.....	17
Wingless pathway at the synapse.....	20
Goal of the project .....	22
<b>MATERIALS AND METHODS</b> .....	23
Fly stocks .....	23
Constructs and transgenic flies .....	23
GAL4-mediated ectopic gene expression .....	23
Mosaic analysis: FLP-FRT mitotic recombination .....	24
GFP-Mad rescue .....	25
Dissection and mounting.....	25
Larval body wall preparation.....	25
Imaginal wing discs .....	26
Antibodies .....	26
Immunocytochemistry .....	27
Larval preparation.....	27
Immunostaining of imaginal discs .....	27
Extracellular immunostaining of imaginal discs .....	28
Electronmicroscopy .....	28
Immuno-electronmicroscopy.....	29
Cryosectioning.....	29
In vivo imaging.....	29
Quantifications.....	30
Reverse transcriptase-combined polymerase chain reaction (RT-PCR) .....	30
Immunoprecipitation .....	31
Western blotting .....	31
GST pull-downs .....	32
GST-fusion protein expression.....	32
In vitro transcription/ translation .....	32

GST pull-down assay .....	32
<b>RESULTS .....</b>	<b>34</b>
<b>TGF-<math>\beta</math> signaling at cell junctions in the <i>Drosophila</i> wing epithelium .....</b>	<b>34</b>
Junctional confinement of TGF- $\beta$ receptor .....	34
Junctional localization of the morphogen Dpp .....	38
Targeting of R-Smad Mad to the junctional area.....	40
$\beta$ -cat regulates Dpp signaling read-out.....	42
Mad forms a complex with $\beta$ -cat .....	44
<b>TGF-<math>\beta</math> signaling at <i>Drosophila</i> NMJ.....</b>	<b>45</b>
Postsynaptic TGF- $\beta$ signal transduction machinery.....	45
R-Smad postsynaptic phosphorylation .....	50
R-Smad accumulation at the synapse depends on synaptic stimulation .....	54
<b>DISCUSSION .....</b>	<b>56</b>
<b>TGF-<math>\beta</math> signaling at the epithelial cell junctions .....</b>	<b>56</b>
Extracellular Dpp is targeted to the junctional area of receiving cells	56
Cell-surface TGF- $\beta$ type I receptor accumulates at the junctions.....	57
The R-Smad Mad is recruited to the junctional area.....	58
$\beta$ -cat regulates Dpp signaling read-out.....	58
<b>TGF-<math>\beta</math> signaling at the neuromuscular junction .....</b>	<b>59</b>
Presynaptic TGF- $\beta$ localization .....	60
Postsynaptic pool of TGF- $\beta$ type I receptor .....	60
An anterograde TGF- $\beta$ signal at the synapse .....	61
Sub-cellular localization of TGF- $\beta$ components indicative of their role at the synapse? .....	61
R-Smad accumulation at the synapse is dependent on synaptic activity.....	62
<b>ABBREVIATIONS.....</b>	<b>64</b>
<b>ACKNOWLEDGEMENTS.....</b>	<b>65</b>
<b>REFERENCES.....</b>	<b>67</b>
Statement / Versicherung .....	79
Publications during PhD.....	80

## INTRODUCTION

The development of an organism from a single cell to a multi-cellular ensemble with a characteristic shape and size is the result of coordinated gene activities that direct the developmental fate of individual cells. Cell proliferation, growth, differentiation, migration, and death coordinate the precise behavior of single cells to constitute functional organisms. Both factors acting cell-autonomously as well as secreted signaling molecules functioning non-cell-autonomously guide cells through distinct developmental paths. Secreted signals traffic through the tissue until they are received by the responding target cells. Using the fruit fly *Drosophila melanogaster* as a model organism, I have studied transforming growth factor- $\beta$  (TGF- $\beta$ ) signaling from secreting to receiving cells.

In polarized epithelia, the apical and baso-lateral plasma membrane domains are characterized by different sets of membrane lipids, trans-membrane proteins and associated cortical proteins. In *Drosophila*, studies of the lineage that gives rise to the sensory organs suggested that, in non-signaling cells, the ligand Delta may be segregated by the cell junctions to the baso-lateral membranes where it cannot interact with its receptor Notch, found at the apical surface of the cells (François Schweisguth, unpublished data). Consistently, cell culture studies have showed that MDCK cells regulate TGF- $\beta$  signaling by expressing the receptors and secreting the ligand in spatially defined areas of the cell, separated by cell junctions (Murphy et al., 2004).

I have analyzed the relevance for signal transduction of the sub-cellular localization of the TGF- $\beta$  pathway core components, in the context of two communication processes: during morphogenetic signaling in the epithelial cells of wing imaginal discs, and during synaptic transmission at the neuromuscular junction. In the wing imaginal disc epithelia, the cellular junctions separate the apical and baso-lateral plasma membrane domains. The junctional area ensures, thus, a spatial barrier between the two domains. Consistently, the neuromuscular junction provides a spatial separation between the pre- and postsynaptic membranes. *Drosophila* motoneurons, with their somas in the ventral cord and their axons extended to make synapses with the body wall muscles, are polarized

cells as well. TGF- $\beta$  signaling was studied and compared in the context of these two types of polarized cell junctions.

## TGF- $\beta$ signaling in wing imaginal discs

### Patterning wing imaginal discs in *Drosophila*

During pattern formation and morphogenesis, cells acquire positional information and differentiate according to their locations into distinct functional structures (Wolpert, 1969). “Positional information” is provided by signaling molecules termed morphogens, which are secreted from a source, traffic across the target field and form long-range concentration gradients. The receiving cells interpret the gradients by activating target gene expression at discrete concentration thresholds thereby acquiring positional information (Turing, 1952) (Wolpert, 1969).

An extensively studied model organism for identifying and analyzing morphogens and their function during pattern formation and morphogenesis is *Drosophila*. The *Drosophila* adult epidermis develops through the combined activity of different morphogens in distinct sets of larval epidermal cells, known as imaginal discs. They arise as pockets in the embryonic ectoderm and grow inside the body until the larva becomes a pupa, at which point they turn inside out to form the body wall and appendages. In a *Drosophila* larva there are 19 imaginal discs (Fig. 1). Nine pairs form the head and the thorax, and a medial disc forms the genitalia. The abdominal epidermis of the adult is derived from separate cell clusters called histoblasts. Unlike discs, the histoblasts remain superficial during larval life, staying integrated in the epidermis of the larva, and do not grow until the pupal stage when they replace the epidermis of the larva.

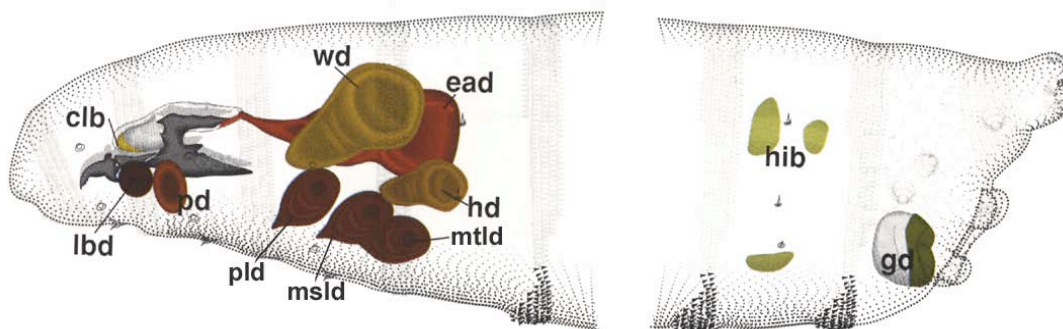


**Figure 1. Schematic representation of imaginal discs in third instar *Drosophila* larva:** lbd (labial disc), clb (clypeolabral disc/bud), pd (prothorax/humeral disc), wd (wing disc), ead (eye-antennal disc), hd (halter disc), pld (pro-thoracic leg disc), mslid (meso-thoracic leg disc), mtld (metathoracic leg disc), hib (histoblasts), gc (genital disc).



(meta-thoracic leg disc), gd (genital disc). Hib (abdominal histoblasts) are also depicted (modified after Hartenstein, 1993)

The wing disc epithelium, like the rest of the discs, is a single cell epithelium that forms a flattened hollow sac (Fig. 2). One side of the disc thickens into a columnar epithelium that will secrete the adult cuticle of the mesothorax, while most of the other side forms a squamous peripodial epithelium (Bryant, 1975). Topologically, the wing imaginal disc can be subdivided into four compartments: the anterior (A), posterior (P), dorsal (D) and ventral (V) compartments (Garcia-Bellido et al., 1973) (Fig. 2).

Different morphogens specify the cell fates in the wing imaginal disc: Hedgehog (Hh), Wingless (Wg) and TGF- $\beta$  family member Decapentaplegic (Dpp) (Fig. 2). Of them, Wg seems not to be a classical morphogen, since its concentration gradient does not directly activate different genes above different concentration thresholds, but maintains distinct gene expressions in a concentration-dependent manner (Martinez Arias, 2003).

Hh is expressed by all the cells of the P compartment (Tabata and Kornberg, 1994) and activates *dpp* expression in the A compartment, as well as enhances the expression of *patched* (*ptc*) (Maschat et al., 1998) (Strigini and Cohen, 1997) (Vervoort et al., 1999) (Wang and Holmgren, 1999). Hh also activates *engrailed* (*en*) in the late 3<sup>rd</sup> instar disc (Blair, 1992) (Guillen et al., 1995) (Sanicola et al., 1995) (Tabata and Kornberg, 1994). Dpp, which is expressed in an anterior stripe of cells adjacent to the A/P boundary, functions as well as a morphogen, inducing in both compartments the expression of the target genes *spalt* (*sal*), *optomotor-blind* (*omb*) and *vestigial* (*vg*) (Kim et al., 1995) (Kim et al., 1996) (Lecuit et al., 1996) (Nellen et al., 1996).

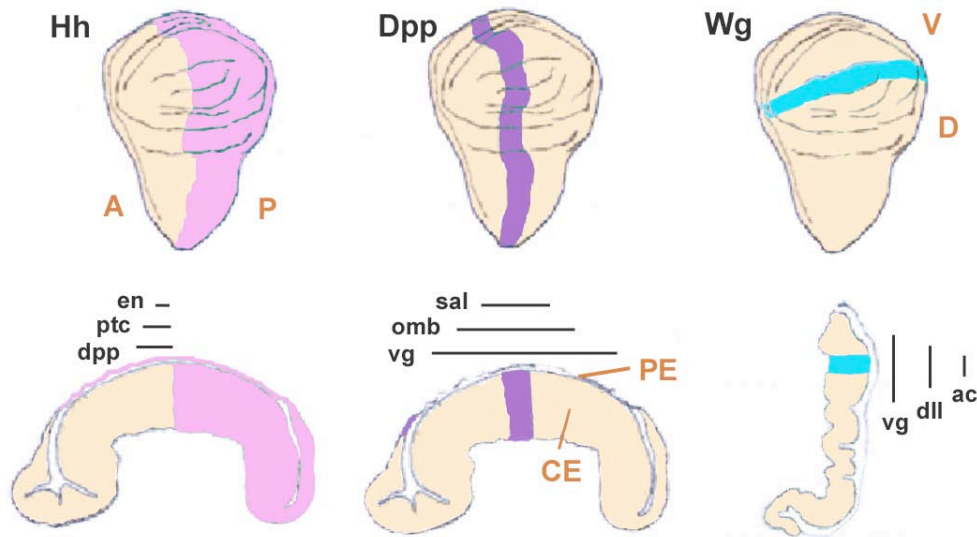


**Figure 2. Schematic representation of morphogens patterning the wing imaginal disc.** Hh is expressed in the posterior compartment (P) from where induces the expression of *dpp* and *en*, and enhances the expression of *ptc* in a concentration dependent manner in the anterior (A) compartment. Dpp induces the expression of *vg*, *omb* and *sal* in a concentration dependent manner along the A/P axis. Wg is expressed by cells at the ventral (V)/ dorsal (D) border and maintains the expression of *vg*, *dll* and *ac* in a concentration dependent manner along the D/V axis. PE- peripodial epithelium; CE- columnar epithelium

Wg expression is induced at the D/V border (Neumann and Cohen, 1996), where it maintains the differential expression of target genes (Martinez Arias, 2003): *achaete* (*ac*), *distalless* (*dll*) and *vg* (Cubas et al., 1991) (Diaz-Benjumea and Cohen, 1995) (Kim et al., 1995) (Neumann and Cohen, 1996) (Skeath and Carroll, 1992) (Zecca et al., 1996).

### TGF- $\beta$ signaling pathway

The mechanisms of morphogenetic TGF- $\beta$  signal transduction are evolutionarily conserved (Fig. 3). The mature TGF- $\beta$  ligands are secreted as disulfide-linked dimers that are derived from the carboxy-terminal region of precursor proteins after the cleavage of a prodomain (Derynck et al., 1985) (Gentry et al., 1988). The ligand dimer signals through serine/threonine kinase receptors termed type I and type II (reviewed in Massague, 2000). Two general modes of ligand binding have been observed (reviewed in Shi Y., 2003). One mode involves direct binding of the ligand dimer to the type II receptor serine/threonine kinases and subsequent interaction of this complex with the type I receptor at the cell surface. The second binding mode is cooperative, involving type I and II receptors that bind the ligand dimer with high affinity. After the ligand binds the receptors, the

type II receptor phosphorylates the type I receptor kinase domain within a specific domain termed GS (Glycine-Serine-rich) box located N-terminal to the kinase domain (Wrana et al., 1994). The type I receptors, then, propagate the signal through phosphorylation of a subset of Smad transcription factors (see next).

There are three functional classes of Smad proteins: the receptor-regulated Smads (R-Smads), the co-mediator Smads (co-Smads) and the inhibitory Smads (i-Smads). R-Smads are directly phosphorylated and activated by the type I receptor kinases and undergo formation of heteromeric complexes with the co-Smad (Chacko et al., 2001) (Kretzschmar et al., 1997) (Macias-Silva et al., 1996). The activated Smad complexes are then translocated into the nucleus and, in conjunction with other nuclear cofactors, regulate the transcription of target genes (Lagna et al., 1996). In the basal state the R-Smads are retained in the cytoplasm, possibly by interaction with Smad anchor for receptor activation (SARA). Receptor-mediated phosphorylation decreases their affinity for SARA and also increases the affinity of R-Smads for the co-Smad (Xu et al., 2000). The i-Smads negatively regulate TGF- $\beta$  signaling by either binding to the activated type I receptor and thus interfering with the phosphorylation of R-Smads (Kavsak et al., 2000) (Suzuki et al., 2002) or by direct binding to the phosphorylated R-Smads thereby competing with the co-Smad (Hata et al., 1998). The pathway is also downregulated by targeting the R-Smads for degradation through Smurfs (Smad ubiquitylation regulatory factors) (Zhu et al., 1999). The Smurfs, in complex with i-Smads, also mediate ubiquitination of activated receptors, leading to their degradation in the proteasome (Ebisawa et al., 2001) (Tajima et al., 2003). i-Smads themselves undergo ubiquitination and degradation in this process.

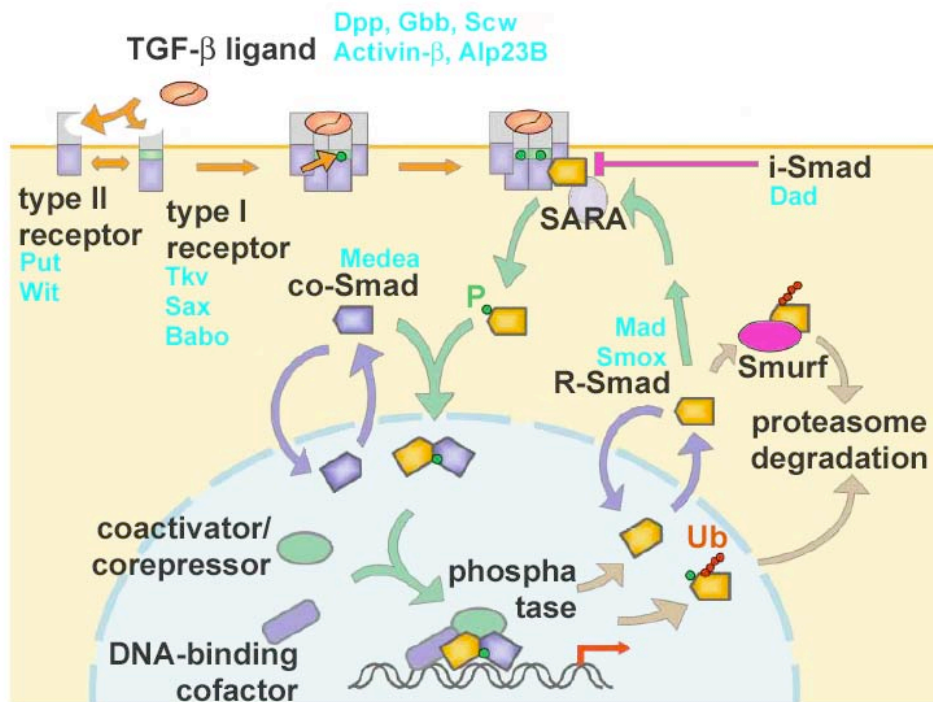


**Figure 3. Schematic representation of TGF- $\beta$  signaling pathway in *Drosophila*.** The BMP ligands (Dpp, Gbb, Scw) act through the type I receptors Tk or Sax, resulting in phosphorylation of the R-Smad Mad, its association with the co-Smad Medea, translocation of the complex to the nucleus, and regulation of the target genes expression together with different co-activators/repressors. The type II receptors Put and Wit display dual specificity and function in both the BMP and activin pathway. An activin pathway initiated by Activin- $\beta$  or Alp23B signals through the type I receptor Babo, triggering the phosphorylation of the R-Smad Smox. Both pathways are negatively regulated by the i-Smad Dad and by the ubiquitin ligase Smurf. Green and red circles depict phosphate and ubiquitin groups (modified after Shi Y., 2003)

The TGF- $\beta$  family comprises two subfamilies: the bone morphogenetic proteins (BMPs) and the activins. In *Drosophila* the BMP-like ligands Dpp (Spencer et al., 1982), Screw (Scw) (Arora et al., 1994) and Glass bottom boat 60A (Gbb) (Doctor et al., 1992) (Wharton et al., 1991) signal through Thick veins (Tk) or Saxophone (Sax) type I receptors, while the activin ligands dActivin- $\beta$  (Kutty et al., 1998) and Activin-like protein at 23B (Alp23B) (Faucheux et al., 2001) signal through Baboon (Babo) type I receptor (Brummel et al., 1994) (Nellen et al., 1994) (Penton et al., 1994) (Xie et al., 1994). Both subfamilies share the type II receptors: Punt (Put) or Wishful thinking (Wit) (Aberle et al., 2002) (Letsou et al., 1995) (Marques et al., 2002) (Ruberte et al., 1995). Two additional ligands have been identified: Myoglianin (Myo) (Lo and Frasch, 1999) and Maverick (Mav) (Nguyen et al., 2000). Their receptor specificity is not known and the phylogenetic analysis and sequence comparison do not assign these ligands to a particular pathway.

All BMP ligands trigger the phosphorylation of the R-Smad Mothers against Dpp (Mad) (Sekelsky et al., 1995), while the activins signal through Smad on X (Smox) (Henderson and Andrew, 1998). Downstream of R-Smad, both pathways share the same co-Smad: Medea (Rafferty et al., 1995), and are negatively regulated by the same i-Smad: Daughters against Dpp (Dad) (Tsuneizumi et al., 1997). The contrast between the wide spectrum of cellular and developmental responses attributed to TGF- $\beta$  ligands and the fact that they signal through relatively few (and shared) core components imply that there is an extensive regulation controlling the different biological responses. The association with various DNA-binding cofactors, activators or repressors (Fig. 3), tightly regulates the stage and cell-type specificity of TGF- $\beta$  family gene responses.

### **Dpp morphogenetic gradient**

Dpp is a member of the TGF- $\beta$  family of secreted signaling factors that control a diverse set of cellular processes in species ranging from flies to worms to mammals. In *Drosophila*, among the processes that require Dpp signaling are: oogenesis, specification of cell fates along the dorsal-ventral axis during embryogenesis, subdivision of the dorsal mesoderm, dorsal closure, regional identity of the gut visceral mesoderm and endoderm, development of the heart, gastric caecae, salivary glands and trachea, growth and patterning of the wing disc (reviewed in Parker et al., 2004).

According to the model of positional information, a morphogen is produced and secreted from a restricted group of cells and spreads through the target field to make a concentration gradient (Wolpert, 1969). The endogenous Dpp distribution in the receiving tissue has not been detected in *Drosophila*, due to lack of sensitive antibodies for immunofluorescence. To investigate the Dpp morphogen gradient in the wing imaginal disc, functional GFP-tagged Dpp fusions were generated (Entchev et al., 2000) (Teleman and Cohen, 2000). Driven by the *dpp* wing enhancer, GFP-Dpp spreads beyond the Dpp expressing cells and is detectable up to 40 cell diameters away from the source, forming a gradient of concentration (Fig. 4). Gradient formation is very rapid: the Dpp gradient expands initially at a rate of around five cell diameters per hour. The morphogen moves in all directions. The gradient expands until a steady-state situation is reached at about 6-8 hours after beginning of a GFP-Dpp expression pulse.

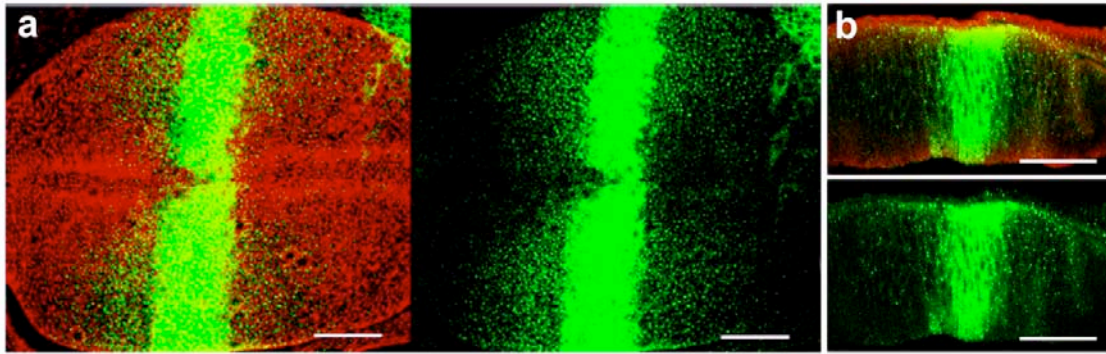


**Figure 4. Dpp gradient in *Drosophila* wing imaginal discs.** GFP-Dpp (green) establishes a concentration gradient in the receiving tissue, phalloidin (red) labels cell profiles. **a)** an apical XY section (modified after Kruse et al., 2004); **b)** a cryostat XZ section (scale bars: 50 $\mu$ m) (genotype: *dpp-GAL4/ UAS-GFP-Dpp*)

The mechanisms that control the movement and spreading of the morphogen through the tissue regulate both the shape and the slope of the gradient. In principle, several processes can account for the morphogen spreading through the tissue: i) free diffusion through the extracellular space; ii) dilution of the morphogen: the morphogen is retained in the cells which are displaced from the source into the target tissue by successive rounds of cell division; iii) active cell mediated processes like transport of the morphogen along cell extensions that bring in contact the source and target (cytonemes), or planar transcytosis (reviewed in González-Gaitán, 2003).

According to the planar transcytosis model of morphogen transport (Entchev et al., 2000), Dpp is internalized by each cell via receptor-mediated endocytosis, traffics through the endocytic pathway controlled by small GTPases of the Rab (Ras-related in the brain) family, and it is released to signal in the next cells, moving further into the target tissue. Therefore, the receiving cells determine the shape of the gradient. Dpp localizes at the receiving cells in intracellular punctuate structures mainly confined to the apical part of the columnar epithelium, while some staining is also detected more baso-laterally (Fig. 4). Apical Dpp in the receiving cells can be seen far away from the source, while in a more basal position it is observed only in cells nearby the source (Fig. 4b). The apical localization of the morphogen suggests a scenario in which the trafficking of the growth factor at the receiving cells is confined to the apical side of the cell. We wanted to study the relationship between the asymmetric apico-basal

localization of Dpp and the apico-basal organization of the developing epithelial wing cells, in which apical and baso-lateral plasma membrane domains, separated by the junctions, are characterized by different sets of membrane lipids, trans-membrane proteins and associated cortical proteins.

### Apico-basal polarity and cell junctions

Epithelial cells are connected to one another by specialized junctions, which are essential for epithelial integrity and the establishment of the apico-basal polarity. Two major types of junctions are found in both vertebrates and invertebrates cells: adherens junctions (AJs) and tight junctions (TJs).

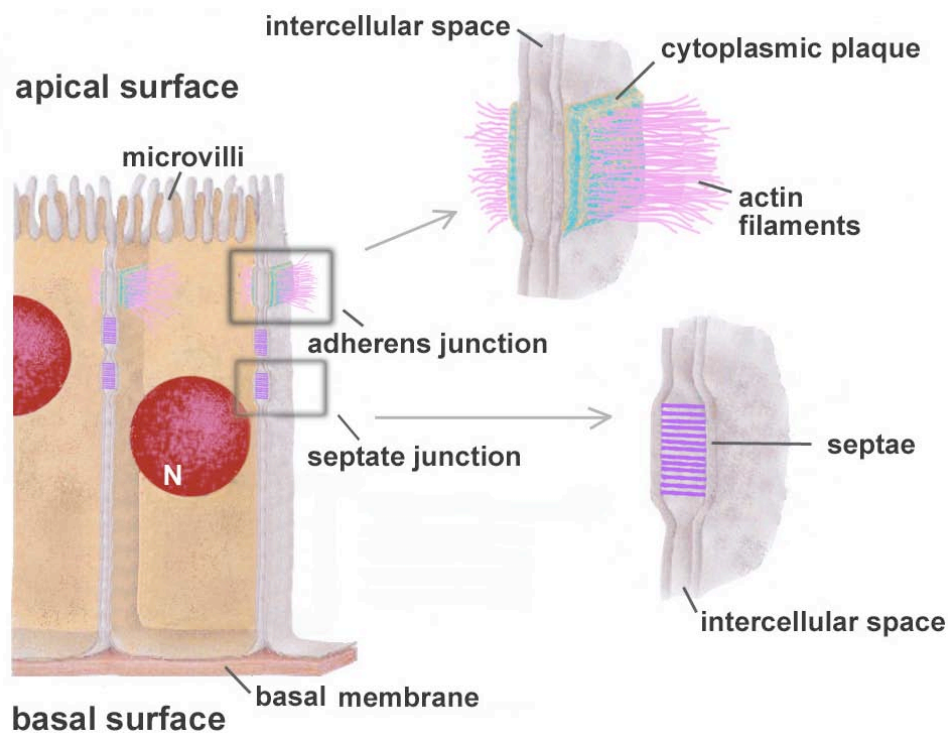


**Figure 5. Schematic representation of cell junctions in *Drosophila*.** The adherens junctions through the connected actin filaments play an active role in cell shape and polarity. The septate junctions form an impermeable barrier between cell membranes. N- nucleus

AJs consist of an electron-dense cytoplasmic plaque, called the undercoat, which is connected to an actin filament network (Fig. 5). They form a complete belt around the cell at the level of the junctions. In both mammals and *Drosophila*, the proteins concentrated at AJs include E-Cadherin (E-Cad),  $\beta$ -catenin ( $\beta$ -cat) (named Armadillo (Arm) in *Drosophila*) and  $\alpha$ -catenin ( $\alpha$ -cat).

E-Cad is a calcium-dependent homophilic cell adhesion trans-membrane protein. It binds through its cytoplasmic domain to the catenins, which provide a link to the cytoskeleton by binding to actin filaments (Tepass et al., 1996).

$\beta$ -cat/Arm plays a dual role: one in cell adhesion at the AJs and the second one in Wnt/Wg signaling. Mutational studies suggest that different functions are mediated by different protein domains (Orsulic and Peifer, 1996). The  $\beta$ -cat/Arm structure consists of acidic N and C termini, and a highly basic central region containing twelve imperfect sequence repeats, known as Arm repeats.  $\alpha$ -cat binds to the acidic N terminus domain, which, together with the first six Arm repeats are involved in the protein function in the junctions. The repeats provide binding sites for APC, Axin (both involved in the degradation pathway of  $\beta$ -cat/Arm), E-Cad and TCF (a co-factor in Wnt/Wg signaling), which bind competitively to this region (Hulsken et al., 1994) (Omer et al., 1999). The C terminus part is important in binding Teashirt, a Zinc-finger transcription factor that helps mediating Wg signaling (Cox et al., 1999). This terminal domain also regulates the protein stability and the intramolecular interactions. 70% of the cellular  $\beta$ -cat/Arm is E-Cad-associated; when the cadherin binding sites are saturated, the excess  $\beta$ -cat/Arm binds APC/Axin, which leads to its degradation. The  $\beta$ -cat/Arm binding sites of APC are rapidly saturated, allowing TCF to effectively compete for binding to  $\beta$ -cat/Arm (Cox et al., 1999). Formation of this complex triggers nuclear translocation of  $\beta$ -cat/Arm and activation of Wnt/Wg target genes (reviewed in Bienz, 2005).

Just above the AJs and just below the apical side of the cell lies the sub-apical region (SAR), which has an organizing role in epithelial polarization. Studies in *Drosophila* established that two protein complexes are localized to the SAR: the Crumbs/ Patj/ Stardust complex and the Bazooka/ aPKC/ PAR-6 complex. Proteins of the Bazooka complex associate with the SAR and the apical plasma membrane and regulate early phases of AJs assembly (Wodarz et al., 2000). Proteins from the Crumbs complex localize apical to the AJs and regulate later phases of AJs maturation and stabilization (Bachmann et al., 2001).

TJs mediate cell-cell adhesion, maintain a diffusion barrier between apical and baso-lateral surfaces of the epithelial sheet ('gate' function), and maintain a barrier within the plane of plasma membrane to prevent diffusion of lipids and



membrane-bound proteins between the apical and baso-lateral membrane domains ('fence' function) (Lamb et al., 1998).

Unlike the vertebrates TJs, which are apical to the AJs, in *Drosophila* they form basal to the AJs on the laterally plasma membrane of the epithelial cells (Fig. 5). They are called septate junctions (SJs) because of the characteristic ladder-like array of cross-bridges or septa that span the 15-20 nm inter-membranar space between neighboring cells (Lane and Swales, 1982). SJs are analogous to TJs: both have similar barrier and fence properties and homologous proteins composition. Fly proteins like Discs large (Dlg), Coracle (Cora), Scribble (Scrib), Discs lost (Dlt), Lethal giant larvae (Lgl) and Neurexin IV (NeurIV) have vertebrate homologs in the TJs (reviewed in Knust and Bossinger, 2002).

The molecular composition of the septa is unknown. Of the known factors associated to the SJs, only NeurIV is a trans-membrane protein. Mutations in *neurIV* lead to loss of the septae, together with a mislocalization of Cora (Baumgartner et al., 1996). However, the epithelial polarity and adhesion in the embryo are not affected. *NeurIV* mutant embryos also show defective dorsal closure, as seen in *cora* mutants. Consistently, NeurIV binds through its cytoplasmic tail the amino terminal domain of Cora (Ward et al., 2001). Cora itself is required for the maintenance of the SJs, since mutations of the protein result in a breakdown of the barrier function, without affecting the apico-basal polarity of the epithelium (Ward et al., 2001).

Scrib is a multi-PDZ cytoplasmic protein localized at the SJs. *scrib* mutants have aberrant cell shapes and loose the monolayer organization of the epithelia (Bilder and Perrimon, 2000). In a complex together with Dlg and Lgl, Scrib function in restricting the apical membrane identity and correctly placing AJs.

Dlg is localized on the cytoplasmic face of the SJs and is required for their maintenance, as well as for proper organization of the cytoskeleton and the apico-basal polarity of epithelial cells (Woods et al., 1996). These functions are mediated by different domains of the protein. Dlg has in the N terminus three PDZ domains, which are likely to bind to an unknown trans-membrane partner involved in SJ assembly, since mutations of these domains lead to loss of epithelial structure. The C terminus contains a GUK (guanylate kinase-homologous) domain, shown to mediate an unknown signaling pathway involved in proliferation control (reviewed in Bryant, 1997). Mutations inactivating this

domain cause excess cell proliferation, without affecting apical-baso polarity (Woods and Bryant, 1991).

### **Do the cell junctions play a role in TGF- $\beta$ signaling?**

According to the model of Dpp gradient formation by planar transcytosis, the morphogen secreted by the producing cells diffuses extracellularly only at short-range, while long-range distribution requires Dpp internalization and re-secretion. Dpp is internalized by receptor-mediated endocytosis into the cells of the target tissue, traffics intracellularly through endosomal compartments and the non-degraded ligand is released to signal in the neighboring cells. The rate of transcytosis is dependent among other things on the rate of endocytosis, which is determined not by the absolute number of receptors, but by their concentration. Since a single molecule of Dpp travels very fast across a single cell (less than two minutes) (Lander et al., 2002) (Bollenbach et al., 2005) (Kruse et al., 2004) the rate of endocytosis must also be very fast to account for the transport by planar transcytosis. A possible way by which a fast endocytosis rate could be achieved is by concentrating the receptors to a specific area of the cells. This scenario would imply that the ligand, while trafficking from one cell to the next, should be secreted also at the same specific area of the cell where the receptors are concentrated. Thus, the apical concentration of Dpp might reflect its secretion in the junctional area. In order to study the role of cell junctions in TGF- $\beta$  signal transduction pathway I have performed experiments to address the following questions:

Is the Dpp signaling machinery localized at the junctions?

If so, by which means the signal transduction components are retained at the junctions?

Does this localization control the level of Dpp signaling read-out?

## **TGF- $\beta$ signaling at the neuromuscular junction**

Epithelial cell junctions constituents like  $\beta$ -cat, Dlg and Scrib were found as well localized at a specialized type of junction: the neuromuscular junction of *Drosophila*, where they are involved in the maturation and the plasticity of the glutamatergic synapses (Roche et al., 2002) (reviewed in Koh et al., 2000). On the other hand, TGF- $\beta$  was shown to be involved in synaptic growth and function (reviewed in Keshishian and Kim, 2004). Do the TGF- $\beta$  signaling pathway components localize at the junction between the motoneurons and muscles, like their function suggests?

### ***Drosophila* neuromuscular junction (NMJ)**

The NMJ is a specialized synapse devoted to the communication between motor neurons and muscles. This communication is essential for proper development and function of the synapse.

Both the pattern of the muscles and the motoneurons in *Drosophila* larvae are well characterized (reviewed in Bate et al., 1999) (Chiba, 1999). The body wall musculature is organized in a stereotyped and segmentally repeated pattern of multinucleated muscle cells. Each abdominal hemisegment from A2 to A7 contains 30 muscle fibers (Fig. 6). The pattern in A1 is slightly different, and there are other specialized muscles in the more anterior and posterior segments. Each muscle fiber has a characteristic position, orientation, morphology, size, body wall insertion site and innervation pattern (Bate, 1990) (Johansen et al., 1989) (Keshishian et al., 1996) (Hoang and Chiba, 2001).

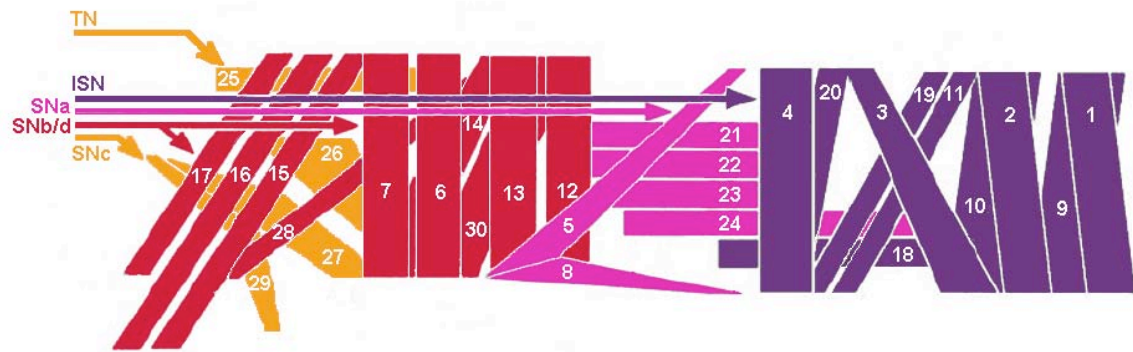


**Figure 6. Schematic representation of the muscle pattern in an abdominal right half-segment.** Anterior is to the top, ventral to the left. Thirty muscles (1-30) are innervated through six nerve branches: ISN, SNa, SNb, SNc, SNd and TN, components of motoneuron axons of the CNS (modified after Hoang and Chiba, 2001)

40 motoneurons innervate the 30 muscle fibers in each abdominal segment. These motoneuron axons are grouped into six major nerve branches: ISN (intersegmental nerve branch), SNa (segmental nerve branch a), SNb, SNc, SNd and TN (transverse nerve) (Fig. 6). Their cell bodies are located within the central nervous system (CNS) and they project in a stereotypic manner to the muscle fibers, generating a precise and invariant innervation pattern (Broadie and Bate, 1993) (Halpern et al., 1991) (Sink and Whitington, 1991). Each motoneuron axon can be identified based on its specific contacts on particular target muscles, the degree of terminal branching, the bouton morphology and the neurotransmitters contained (Johansen et al., 1989) (Hoang and Chiba, 2001). The entire motoneuron population uses glutamate as the excitatory neurotransmitter (Jan and Jan, 1976) (Johansen et al., 1989). Different motoneuron subsets express co-transmitters including octopamine (Monastirioti et al., 1995) and the peptide neurotransmitters proctolin (Anderson et al., 1988), insulin-like peptide (Gorczyca et al., 1993) and leukokinin I-like peptide (Cantera et al., 1992).

The *Drosophila* body wall muscle fibers are poly-innervated. Some motoneurons innervate only a single muscle fiber, whereas others project to muscle fiber pairs or even to larger subsets of the body wall muscles. The axon endings can be divided into three morphologically defined classes: type I, II and III (Fig. 7).

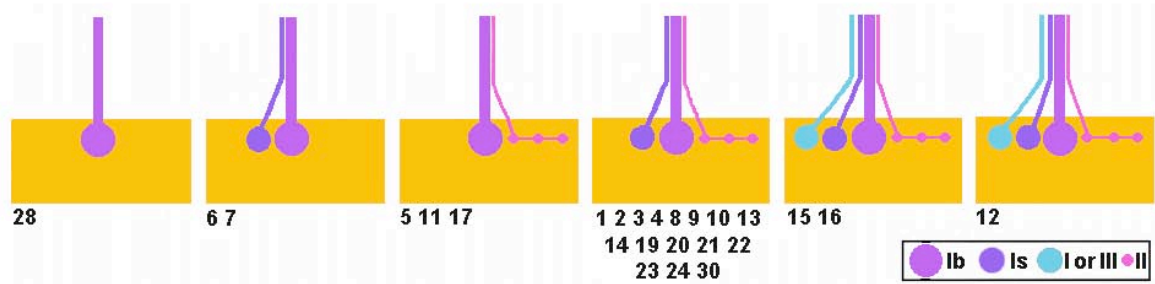


**Figure 7. Schematic representation of the motoneuron types (Ib, Is, II and III) and the muscles innervated by them (1-30).** The number of motoneurons that innervate a given muscle varies from 1 to 4 (modified after Hoang and Chiba, 2001)

Type I boutons innervate all body wall muscles. The boutons are round in shape and enclosed by a prominent subsynaptic reticulum (SSR): a postsynaptic specialization made by the highly folded sarcolemma of the muscle (Fig. 8), where many molecules required for neurotransmission and neurotransmitter uptake are clustered (Atwood et al., 1993). Type I boutons are filled with synaptic vesicles (SVs) that contain glutamate. Type I boutons are further subdivided according to their size into I big (Ib) and I small (Is) (Budnik et al., 1996). Type Ib boutons are 3 to 6  $\mu\text{m}$  in diameter, whereas type Is boutons are 2 to 4  $\mu\text{m}$  in diameter. In addition, type Is boutons contain less SVs (sometimes with peptide neurotransmitters) and are surrounded by less developed SSR than type Ib boutons. The type Is terminals can be often longer and more elaborated than those bearing type Ib boutons.

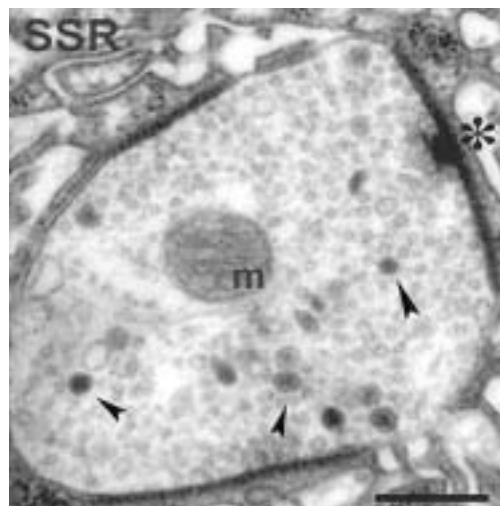


**Figure 8. Type I synaptic bouton morphology.** The synaptic bouton is enveloped into the subsynaptic reticulum (SSR) of the muscle. The bouton is nearly filled with small clear synaptic vesicles that contain glutamate. Vesicles with neuropeptide are also observed (arrowheads). Active zones of synaptic release are characterized by an electron-dense T bar composed of a stem associated with the presynaptic membrane and a bar perpendicular to the distal end of the stem (star) (m: mitochondria) (scale bar: 400nm) (modified after Guichet et al., 2002)

Type II boutons are small (1-2 $\mu\text{m}$ ) and the terminals bearing them are very long and the most elaborate of all axon terminals. They are localized to superficial grooves in the surface of the muscle fiber, with little or no surrounding SSR (Jia

et al., 1993). These boutons contain both clear SVs with glutamate, as well as dense core vesicles with octopamine (Jia et al., 1993).

Type III boutons are of medium size (2-3 $\mu$ m) and the terminals bearing them are of medium length. Similar to type II endings, they have a superficial localization on the muscle cell surface and almost lack SSR (Jia et al., 1993). In addition to SVs with glutamate, they contain large round vesicles with a varying degree of electron density filled with insulin-like peptide, a putative neural cotransmitter (Gorczyca et al., 1993).

### **Control of synapse growth and function**

The communication between motoneurons and the muscles is essential for proper development and function of the synapse. Synaptogenesis starts about 13 hours after egg laying (AEL), as motor neuron growth cones begin to make contact with their target muscles. Each growth cone extends filopodial processes that explore the muscle fiber in search for the appropriate target muscle. The embryonic synapses are formed at about 14.5 hours AEL and the superfluous contacts are pruned back.

When the first instar larva hatches, the synapse is relatively rudimentary, comprising only a few boutons with no SSR. Larval motor synapses grow progressively in size and strength as the innervated larval muscle expands in size during development (Schuster et al., 1996). From the first to the third instar larvae, the surface area of the muscles increases 100 folds. Concomitantly, the nerve terminals also grow, with an increase of 10 fold of the number of synaptic boutons and 10-fold increase of the active zones per bouton. The initial formation of correctly positioned NMJs is an activity-independent process based on molecular recognition cues and interactions between growth cones and target (Broadie and Bate, 1993). However, the later synaptic flexibility of the synapses is a dynamic, activity-dependent process involving lasting structural and physiological alteration.

Several studies have identified a number of mediators of synaptic growth and plasticity. These include the potassium channel proteins Eag and Shaker (Budnik et al., 1990), cAMP pathway members (Zhong et al., 1992), cell adhesion molecules: Fasciclin II (Schuster et al., 1996), Discs large (Budnik et al., 1996), Scribble (Roche et al., 2002), the extracellular matrix adhesion molecule  $\beta$ PS

Integrin (Beumer et al., 1999), the microtubule-associated protein Futsch (Roos et al., 2000), the ubiquitin ligase Highwire (Wan et al., 2000), and the deubiquitinating protease Fat Facets (DiAntonio et al., 2001).

### **Morphogens at the synapse**

#### **TGF- $\beta$ signaling at the synapse**

Activity-responsive retrograde signals from muscle were believed since a long time to act via presynaptic receptors to regulate transmitter release, likely by modulating genes and molecules that control functional properties of the motor neuron. Recent reports provided evidence that the TGF- $\beta$  pathway is involved in a retrograde signal from the muscle that regulates synapse size and the transmitter release from the neuron (Marques et al., 2002) (Aberle et al., 2002) (Sweeney and Davis, 2002) (McCabe et al., 2003) (Rawson et al., 2003) (McCabe et al., 2004). According to the current model (Fig. 9), at *Drosophila* NMJ, the BMP ligand Gbb is secreted by the muscles and signals upon binding to a neural receptor dimer formed by the type II receptor Wit and the type I receptors Sax/Tkv. The activation of the receptors results in phosphorylation of the transcription factor Mad. Phospho-Mad, together with the co-Smad Medea, modulate the expression of unknown TGF- $\beta$ -responsive genes in the neuron somas, influencing the growth and strength of the motor synapses.

How is actually the signal from the synaptic boutons transmitted to the motoneural soma, in the ventral cord? It seems that activation of BMP signaling is dependent on axonal retrograde transport, which conveys the activated proteins to the cell body. In a dominant-negative inhibitor of the dynein-dynactin complex microtubule motor p150/glued ( $\Delta$ -Gl) that disrupts retrograde axonal transport, phospho-Mad accumulation in the motoneuron nuclei is lost (McCabe et al., 2003).

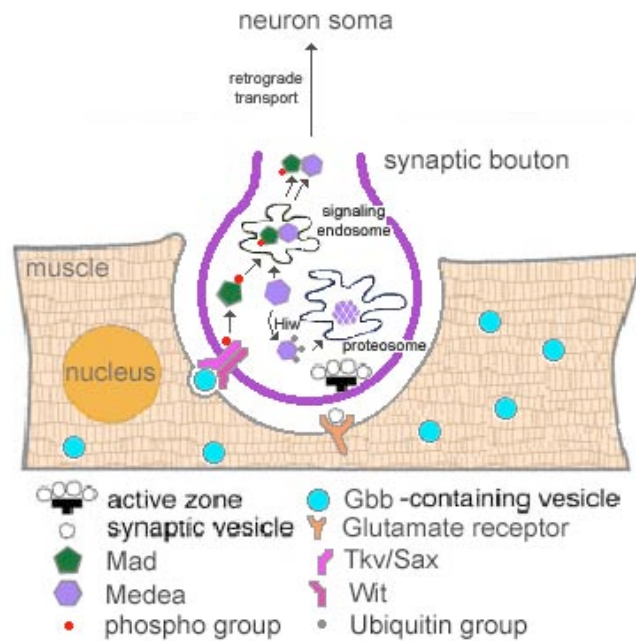


**Figure 9. Schematic representation of TGF- $\beta$  signaling components at the synapse.** Muscle secreted Gbb ligand binds to a presynaptic complex formed between type I (Tkv or Sax) and type II (Wit) receptors. Upon phosphorylation by the type II receptor, the type I phosphorylates the transcription factor Mad. Activated Mad binds to the co-Smad Medea, and through retrograde transport, possibly via a signaling endosome, reaches the nucleus in the neural soma to modulate transcription of specific genes. Down-regulation of signaling is achieved by ubiquitylation (by the ubiquitin-ligase Highwire, Hiw) and proteosome-dependent degradation of Medea or targeting of the signaling complex for lysosomal degradation (regulated by Spinster, not depicted)

Loss-of-function mutants of the TGF- $\beta$  signaling pathway components (*gbb*, *tkv*, *sax*, *wit*, *mad*, *med*) have reduced number of synaptic boutons, phenotype accompanied by a reduction of transmitter release. Consistently, activation of the pathway has opposite effects. Mutations in Dad, a negative regulator of TGF- $\beta$  pathway, as well as the expression in the neurons of a constitutively active form of Tkv induce synaptic overgrowth (Sweeney and Davis, 2002) (Rawson et al., 2003).

After receptor activation in the synaptic boutons, TGF- $\beta$  signaling may be prolonged by the transport of the receptors to signaling endosomes (Shi Y., 2003) or limited by targeting them to degradative compartments via the endosomal protein Spinster (Spin), a multipass transmembrane protein that localizes to the late endosomal and lysosomal compartment (Sweeney and Davis, 2002). A parallel degradative mechanism is suggested by the observation that the co-Smad Medea can form a complex with Highwire (Hiw), a presynaptically enriched ubiquitin-ligase (McCabe et al., 2004). Both loss-of-function mutations in *spin* and *hiw* lead to greatly expanded synapses, the predicted consequence of enhanced TGF- $\beta$  signaling. These phenotypes are suppressed in a dose-dependent



manner by TGF- $\beta$  signaling mutants (*med*, *mad*, *tkv*, *sax*, *wit*), while the activation of the pathway in the mutant background results in additional overgrowth (Marques et al., 2002) (Aberle et al., 2002) (Sweeney and Davis, 2002) (McCabe et al., 2003) (Rawson et al., 2003) (McCabe et al., 2004).

The reduced NMJ phenotype of *gbb* mutants is rescued by expressing Gbb in muscles, suggesting that its presence there is important for normal NMJ development (McCabe et al., 2003). Nevertheless, the phenotypic rescue improves when Gbb is expressed both by muscles and neurons. This indicates that normal NMJ development requires TGF- $\beta$  activity both at the muscle and at the neuron. Consistently, the *spin* mutant phenotype is fully rescued when a wild-type transgene is expressed ubiquitously, but only partially rescued when the transgene is expressed just in the neurons or muscles (Sweeney and Davis, 2002). These results suggest that an anterograde TGF- $\beta$  signaling emanating from the neuron is involved in synaptic growth and synaptic strength regulation, in parallel with the documented retrograde signal. Alternatively, an autocrine signaling event might occur at the muscle.

Retrograde Gbb signaling through a presynaptic receptor dimer was shown recently to regulate the expression of the neuropeptide FMRFamide (FMRFa) in peptidergic Tv neurons of the *Drosophila* CNS (Allan et al., 2003). The Tv neurons express both Apterous, a LIM-domain transcription factor, and Squeeze, a zinc-finger transcription factor (Allan et al., 2003) (Benveniste and Taghert, 1999). Both factors are found elsewhere in the CNS but their expression overlaps in the Tv neurons. The coordinate expression of the two transcription factors predeterminates the dependence of the cell on TGF- $\beta$  signaling for FMRFa expression. When the transcription factors are ectopically expressed in non-FMRFa-positive neurons, the cells become competent for FMRFa expression. However, the ectopic FMRFa expression occurs only in the presence of Gbb, recapitulating the situation in Tv cells (Allan et al., 2003). This suggests a critical role between combinatorial transcription factor codes and signal transduction pathways in diversifying the response of the neurons to retrograde TGF- $\beta$  signaling. Given the large number of diverse cell types in the CNS, what may appear to be an almost excessive complexity of combinatorial coding may be in fact essential for high fidelity gene expression.

Synaptic homeostasis seems to be not the only neuronal function of the TGF- $\beta$  pathway in *Drosophila*; recently, this signaling pathway was shown to be involved also in neuronal differentiation and remodeling (Zheng et al., 2003). During metamorphosis, the Kenyon cells in the mushroom body (MB, the olfactory learning and memory center) are remodeled from their larval form, in which they innervate both medial and dorsal lobes of the MB, to the adult form, in which they innervate only the medial lobe. Larval axons retract from both lobes and then re-grow into the medial  $\gamma$  lobe by a mechanism that involves regulation by the steroid hormone ecdysone. In this process, TGF- $\beta$  controls the expression of the ecdysone receptor, rendering larval neurons responsive to the steroid that directs axonal remodeling. Tzumin Lee's group found that loss of the Activin/TGF- $\beta$  signaling components Babo, Wit/ Punt, Smox and Activin itself leads to the persistence of the larval Kenyon cells morphology. Ecdysone receptor expression is suppressed in the mutant neurons, but ectopic expression of the receptor significantly rescues the remodeling defects, bypassing the requirement for TGF- $\beta$  signaling. Thus, the TGF- $\beta$ /Activin pathway plays a permissive function in upregulating the expression of ecdysone receptor that confers responsiveness to ecdysone, a primary regulator of axonal remodeling (Zheng et al., 2003).

### **Wingless pathway at the synapse**

Another morphogen, Wingless (Wg, a *Drosophila* Wnt), provides an essential cue for the coordinated development of pre- and post-synaptic structures, possibly through a combined anterograde and retrograde signal (Packard et al., 2002). Both Wg and its receptor Frizzled2 (Fz2) are expressed at the glutamatergic NMJ. Wg is secreted by the synaptic boutons and accumulates at the postsynaptic side, being then uptaken by the muscle. Blocking Wg secretion by using mutations in *porcupine* (*porc*, which encodes an endoplasmic reticulum protein required for Wg processing and trafficking (Kadowaki et al., 1996) or a thermosensitive allele *wg<sup>ts</sup>* severely reduces muscle-dependent formation of new synaptic boutons. In mammals, the Wnt pathway has been implicated in cytoskeleton reorganization during growth-cone extension (Salinas and Hall, 1999). Activation of Wnt pathway results in inhibition of GSK-3 $\beta$ , which is believed to destabilize microtubules through phosphorylation of the microtubule associated protein MAP1B (Goold et al., 1999), which is the homologue of Futsch

in *Drosophila*. Indeed, most of the  $wg^{ts}$  mutant boutons have splayed or disintegrated microtubule filaments, suggesting that synaptic expansion is arrested.

At the ultrastructural level, defective Wg function prevents formation of active zones and postsynaptic structures (SSR is not present around the synapse) in many boutons (Packard et al., 2002). Mutant boutons that develop active zones exhibit dramatic defects in active zone shape and in postsynaptic area directly apposed to the active zones. In wild-type boutons the T bars of the active zones consist of a stem associated with the presynaptic membrane and a bar perpendicular to the distal end of the stem. In  $wg$  mutants the T bars appear as amorphous dense areas, or contain aberrantly shaped stems with little or no bar. Opposing these modified active zones, the SSR detaches from the presynaptic compartment, forming enlarged pockets.

Based on the study of the role of Wg at *Drosophila* NMJ, two models were proposed to explain how the morphogen is involved in pre- and postsynaptic differentiation (Fig. 10). The first model (Fig. 10a) assumes a parallel anterograde and autocrine signaling. The Wg receptor, Fz2, is localized both pre- and postsynaptically and interacts with Wg secreted by the synaptic bouton. This triggers independent pre- and postsynaptic transduction cascades leading to the proper positioning and morphology of active zones and to proper development of the postsynaptic apparatus.

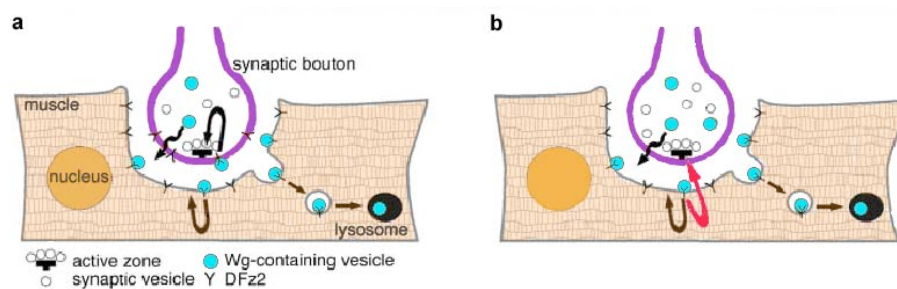


**Figure 10. Schematic representation of Wg signaling at the NMJ. a)** an anterograde/autocrine Wg pathway versus **b)** an anterograde Wg signal and a retrograde unknown signal (red arrow) (modified after Packard et al., 2002)

According to the second model (Fig. 10b) there is just an anterograde Wg signal. Fz2 is located exclusively at the postsynaptic junctional region. The interaction of Fz2 with Wg results in proper formation and positioning of the postsynaptic apparatus and elicits an unidentified retrograde message that signals the proper

formation and positioning of active zones. According to both models, secreted Wg is removed from the membrane by endocytosis.

### **Goal of the project**

TGF- $\beta$  retrograde signaling is involved in synaptic development and function (Marques et al., 2002) (Aberle et al., 2002) (Sweeney and Davis, 2002) (McCabe et al., 2003) (Rawson et al., 2003) (McCabe et al., 2004). Nevertheless, the mechanisms by which TGF- $\beta$  modulates NMJ development and function are not clarified yet. Previous reports (see above) suggest a parallel anterograde TGF- $\beta$  signal at the NMJ. In order to elucidate the means of TGF- $\beta$  function at the synapse, I have performed experiments to address the following questions:

Which is the sub-cellular localization of TGF- $\beta$  signaling components at the synapse?

Are they involved in an anterograde signal?

## MATERIALS AND METHODS

### Fly stocks

The following fly stocks have been used: wild-type OreR, *dpp*<sup>d12</sup> (St Johnston et al., 1990), *dpp*<sup>d8</sup> (St Johnston et al., 1990), *mad*<sup>12</sup> (Sekelsky et al., 1995), *mad*<sup>B1</sup> (Wiersdorff et al., 1996), *arm*<sup>XM19</sup> (Perrimon and Mahowald, 1987), *dlg*<sup>m52</sup> (Woods and Bryant, 1991), *cora*<sup>5</sup> (Lamb et al., 1998), *scrib*<sup>1</sup> (Bilder and Perrimon, 2000), *shg*<sup>H</sup> (Tepass et al., 1996), *shg*<sup>G29</sup> (Tepass et al., 1996), *UAS-GFPDpp* (Entchev et al., 2000), *UAS-Dad* (Tsuneizumi et al., 1997), *UAS-GFPgpi* (Greco et al., 2001), *UAS-GluRIIA-GFP* and *UAS-GluRIIA-mRFP* (Stephan Sigrist, Max Planck Institute, Göttingen Germany), *UAS-GFP* (Barry Dickson, Institute of Molecular Pathology, Vienna Austria).

### Constructs and transgenic flies

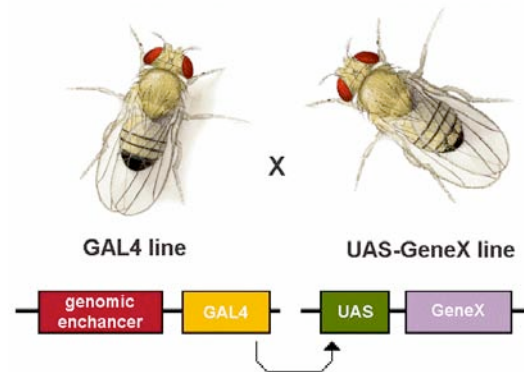
*UAS-TkvGFP* flies were generated by subcloning the coding sequence of Tkv (LD15534 of the fly genome project) into the poly-linker of the vector pUAST containing EGFP downstream of the insertion. For the *UAS-GFPMad* flies, the coding sequence of Mad (RE72705 of the fly genome project) was subcloned into the poly-linker of the vector pUAST containing EGFP upstream of the insertion. *UAS-GFPActivin* flies were generated by cloning the coding sequence of Activin (RE37047 of the fly genome project) into the poly-linker of the vector pUAST containing EGFP downstream of the insertion, the same for: *UAS-GFPAlp23B* (GH14433 of the fly genome project), *UAS-GFPGbb* (with the difference that Scw was amplified from genomic DNA) and *UAS-GFPScw* (Scw was amplified from genomic DNA). For the *UAS-HRPDpp* flies, the HRP replaced GFP in the pUAST-GFPDpp construct.

### GAL4-mediated ectopic gene expression

For the selective ectopic expression of the above transgenic constructs in different tissues of *Drosophila*, GAL4-mediated expression system (Brand and Perrimon, 1993) was used. GAL4 is a yeast transcription factor, which activates transcription in *Drosophila* (Fischer et al., 1988). For its expression, the *GAL4*

gene is integrated at sites that are under temporal and spatial control of various genomic enhancers. GAL4 can bind to an *upstream activator sequence (UAS)* and initiate the transcription of target gene of interest present downstream of the *UAS* sequence (Fig. 11). The targeted ectopic gene expression occurs in the progeny of the cross between the transgenic line expressing GAL4 and the line carrying the target gene downstream of the *UAS*.

**Figure 11. GAL4-mediated expression system.** Protein X expression is driven in the progeny of flies carrying the GAL4 coding sequence downstream a genomic enhancer and flies carrying the Gene X coding sequence downstream of an *UAS (upstream activator sequence)*. In the cells containing both transgenes, GAL4 binds to the UAS and promotes the transcription of Gene X



### Mosaic analysis: FLP-FRT mitotic recombination

Mutant homozygotic cells can be generated in heterozygotic flies by inducing recombination between homologous chromosomes. Heat-shock-induced expression of the site-specific recombinase FLP leads to the recombination between Flipase Recombination Targets (FRTs) that have been inserted in identical positions on both homologs. With the appropriate developmental time point and level of heat-shock, mitotic recombination can produce a patch of cells (clone) of mutant tissue (Fig. 12).

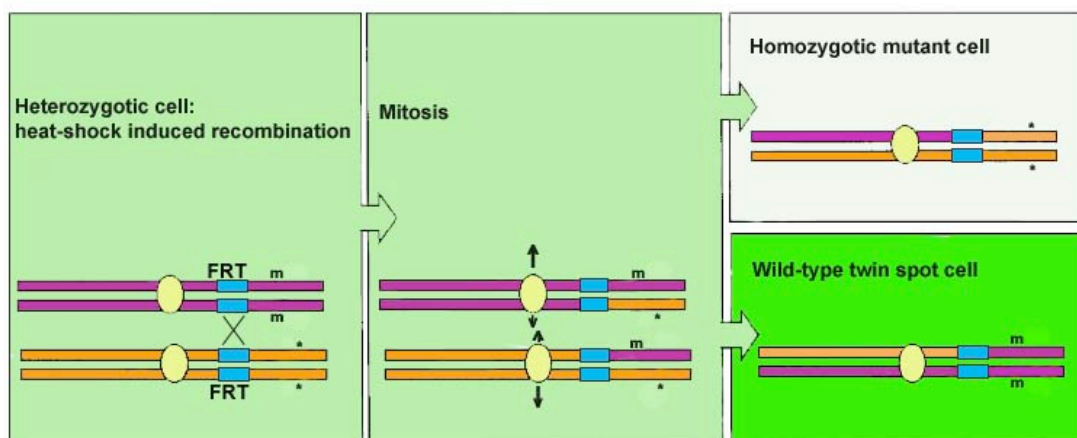


**Figure 12. The FLP-FRT system.** From a cell heterozygous for a certain mutation (\*), through mitotic recombination arise two daughter cells: a homozygous cell for the mutation ( $^{*}/^{*}$ ) and a homozygous cell for the wild type allele. If a marker (m) is present in the initial cell in trans and

proximal to the mutation, on the sister chromatide, the daughter cell homozygous for the wild-type allele will also be homozygous for the marker. The resulting daughter cells of this cell will form the so called 'twin spot'. The resulting daughters of the \*/\* cell will produce a clone of mutant cells

The location of the mutant clone can be identified by the use of genetic (Ub-GFP, tub-DsRed) or histological markers (PMyc epitope marker construct detected by anti-Myc staining). To analyze the role of various adherens and septate junctions components on Dpp signalling read-out, clones of Arm, E-Cad, Cora, Dlg and Scrib were generated in the wing imaginal discs. Larvae of the following genotypes were studied: *Ub-GFP FRT101/arm<sup>XM19</sup> FRT101;;hs-FLP*, *hs-FLP/+;Ub-GFP FRTG13/shg<sup>IG29</sup> FRTG13* or *hs-FLP/+;hs-Pmyc FRTG13/shg<sup>IG29</sup> FRTG13*, *hs-FLP/+;cora<sup>5</sup> FRT43D/Pmyc FRT43D*, *FRT101 dlg<sup>m52</sup>/Ub-GFP FRT101;;hs-FLP* or *FRT18A dlg<sup>m52</sup>/tub-DsRed FRT18A;;hs-FLP/+*, *hs-FLP/+;; FRT82B scrib<sup>1</sup>/tub-DsRed FRT82B*. Three days old larvae (grown at RT) were heat-shocked at 38°C for 2hr, left 1hr at RT to recover and raised at 18°C until they reached the third instar stage. To induce *PMyc* transcription, the larvae were heat shocked at 37°C for 1hr followed by 1hr at RT to allow the translation of the *PMyc* transcript prior to fixation.

### GFP-Mad rescue

The GFP-Mad chimera was expressed in *mad<sup>B1</sup>* mutant background and tested for viability rescue. *mad<sup>B1</sup>/mad<sup>B1</sup>; da-GAL4/UAS-GFPMad* larvae and adults were analyzed.

### Dissection and mounting

#### Larval body wall preparation

Preparation of the larval body wall was performed as described (Estes et al., 1996) with some modifications. Wandering third instar larvae were picked from the food and dissected to expose body wall muscles and innervating motoneurons. For dissection, larvae were placed in a drop of cold ice-cold Ca<sup>2+</sup>-free normal saline (Jan and Jan, 1976) (130mM NaCl, 5mM KCl, 5mM HEPES, 2mM MgCl<sub>2</sub>, 2mM CaCl<sub>2</sub>, 36mM sucrose pH 7.3) in a 35mm diameter Petri dish covered with a thin layer of transparent sylgard resin (RTV615A + RTV615B, GE Bayer Silicones). The larval head and tail were pinned to the sylgard resin using insect pins (Fine Science Tools), the body was stretched and dissected

opened along the dorsal midline using a hypodermic needle (BD Microlance 3, Becton Dickinson). The preparation was then pinned out flat to the sylgard resin and internal organs were removed to expose the body wall muscles and the innervating motoneurons. Analysis was restricted to synapses of muscles 6 and 7 in abdominal segments 2 to 4 (A2-A4).

### **Imaginal wing discs**

*Drosophila* third instar larvae were collected in a glass dish. Dissection of wing imaginal discs was performed in PEM (80mM Na-PIPES, 5mM EGTA, 1mM MgCl<sub>2</sub>, pH 7.4); when submitted for E-Cad staining, larvae were dissected in PBS buffer (137mM NaCl, 2.68mM KCl, 10.14mM Na<sub>2</sub>HPO<sub>4</sub>, 1.76mM KH<sub>2</sub>PO<sub>4</sub>, pH 7.4) supplemented with 0.9mM CaCl<sub>2</sub> and 0.5mM MgCl<sub>2</sub>. The larval cuticle was inverted in such manner so that the attached imaginal discs are exposed to the solution.

### **Antibodies**

#### Antibodies generated

Rabbit anti-*Drosophila* SARA was generated against two peptides: H<sub>2</sub>N-LSEESSPSREPETEMC-CONH<sub>2</sub> and H<sub>2</sub>N-CQAESSTPSQDENPEI-CONH<sub>2</sub>, dilution 1:1000. Rabbit anti-*Drosophila* Mad was generated against two peptides, one corresponding to the linker and the other one to the MH2 domain (H<sub>2</sub>N-PSEDGNSNNPNDGGQC-CONH<sub>2</sub> and H<sub>2</sub>N-NRNSTIENTRRHIGKC-CONH<sub>2</sub>), dilution 1:1000. The immune sera were affinity chromatography purified using the corresponding peptides coupled to CNBr-activated Sepharose 4B (Amersham Biosciences). The specificity of the antibodies was tested by pre-incubating the purified antibody with 100 µg/ml of the respective peptide for 30 minutes at room temperature and performing subsequently an antibody staining on wild-type discs. No fluorescent signal was detected under these conditions.

Other antibodies used: rabbit anti-iTkV 1:1250 (Kruse et al., 2004), rabbit anti-luminalTkV (eTkV) 1:10 (Kruse et al., 2004), mouse anti-Arm 1:100 (7A22, Hybridoma Bank), guinea-pig anti-Cora 1:100 (Ward et al., 2001), mouse anti-Dlg 1:500 (4F3, Hybridoma Bank), rabbit anti-Mad 1:100 (Sutherland et al., 2003), rabbit anti-PMad 1:1000 (Tanimoto et al., 2000), goat anti-GFP 1:10 (Kruse et al., 2004), anti-Myc 1:250 (CalBiochem), mouse anti-CSP 1:100 (Zinsmaier et al., 1994), mouse anti-nc82 1:100 (Heimbeck et al., 1999), rat anti-E-Cad 1:20 (Oda



et al., 1994), mouse anti- $\beta$ PSInt 1:1000 (CF.6G11, Hybridoma Bank), mouse anti-Lamin 1:500 (ADL67.10, Hybridoma Bank). Corresponding secondary Alexa 488, 546, 633 (Molecular Probes) or Cy5 (Dianova)-conjugated antibodies were used 1:500 diluted. Polyclonal primary and all secondary antibodies were preabsorbed using an excess of fixed *Drosophila* embryos prior to use in order to reduce the background. PreadSORption was performed by incubating the antibody diluted 1:10 in BBT (10mM Tris, 55mM NaCl, 40mM KCl, 7mM MgCl<sub>2</sub>, 5mM CaCl<sub>2</sub>, 20mM glucose, 50mM sucrose, 10% bovine serum albumin (BSA), 0.1% Tween20, pH 6.95) with 400  $\mu$ l of fixed embryos ON at 4 °C.

## **Immunocytochemistry**

### **Larval preparation**

Immunofluorescence of third instar larvae NMJs was performed as described (Wucherpfennig et al., 2003). Briefly, larvae were dissected and fixed in 4% paraformaldehyde (PFA) in PEM for 90-120 min at RT. The subsequent incubation steps were performed on a rocking platform. The preparation was first permeabilized at RT in PEM containing 0.1% IGEPAL (Sigma). The incubation with the primary antibody was ON at 4°C, followed by incubation with the secondary antibodies for 2h at RT (both primary and secondary antibodies diluted in PEM containing 0.1% IGEPAL and 0.1% BSA). Specimens were embedded in MOLWOL anti-fade embedding medium (Bohringer).

### **Immunostaining of imaginal discs**

Imaginal discs were subsequently fixed in 4 % PFA in PEM and permeabilized in 4% PFA in PEMT (PEM with 0.1-0.2% Triton X100) for 40 min each. The dissected wing discs were washed twice with PEMT for 10 min, interrupted by a wash with 50mM NH<sub>4</sub>Cl in PEM for 10 min to remove as well as to quench free aldehydes. The tissue was then incubated in blocking solution (PEMT with 0.1%BSA) ON at 4 °C. After blocking, the samples were incubated with primary antibodies diluted in PEMT for 2hr at RT. Unbound primary antibodies were removed by washes with PEMT. Subsequent incubation with the appropriate secondary antibodies diluted in PEMT for 2hr at RT was followed by washes with PEMT and PEM, respectively. Finally, the wing imaginal discs were removed from the cuticle and mounted in MOLWOL.

### **Extracellular immunostaining of imaginal discs**

Extracellular GFP-Dpp and cell-surface associated Tkv were detected by incubating the dissected wing imaginal discs prior to fixation (Strigini and Cohen, 2000) with goat anti-GFP antibody and rabbit anti-eTkv, respectively. Third instar larvae were dissected in Shields and Sang M3 Insect Medium (Sigma) and incubated, on ice for two hours, with the primary antibody diluted in M3 medium. The samples were then washed with M3 medium to remove the unbound antibody, fixed in 4% PFA in PEM and permeabilized in 4% PFA in PEMT for 40 min each. Subsequent procedure was according to the intracellular immunostaining (without blocking and primary antibody incubation).

Fluorescent phalloidin 488, 546 or 647 (Molecular Probes) staining was sometimes performed after the secondary antibody step in order to monitor cell profiles, and DAPI (Sigma) or Hoechst (Molecular Probes) were applied to visualize the cells nuclei.

### **Electronmicroscopy**

For electron microscopy, wing imaginal discs of *UAS-HRPDpp; apt-GAL4/+* third instar larvae grown at 29°C were used. After dissection, the preparations were fixed in 1% glutaraldehyde in PBS for 2 min. The fixation was interrupted by brief wash in PBS, and then the preps were permeabilized with PBST (PBS with 0.2% Triton X100). The samples were saturated with DAB (Sigma, 1mg/ml). The peroxidase reaction was developed by adding of H<sub>2</sub>O<sub>2</sub> to final dilution of 0.003% for 30 min. In order to stop the reaction, the preparations were washed with PBS. The tissue was postfixed in 1% glutaraldehyde in PBS at 4°C overnight. After brief washes with PBS and distilled water, the samples were contrasted with 1% OsO<sub>4</sub> in dH<sub>2</sub>O. For post-staining 1% uranylacetate in dH<sub>2</sub>O for 1h at 4°C was applied. After several washes with dH<sub>2</sub>O, the samples were dehydrated by ethanol serial washes (50%, 70%, 100%) and washed shortly with propylene oxide, followed by incubation in mixture of propylene oxide/EPON 1:1, and then incubation in EPON overnight at RT. The imaginal discs were dissected out and mounted in EPON in flat embedding molds. The resin was polymerized at 65°C for 48 hr. Serial thin sections were collected and analyzed on Phillips TEM.

### Immuno-electronmicroscopy

For immuno-EM wing imaginal disc preparations of third instar larvae of *hh-GAL4/ UAS-Tkv-GFP*, *tub-GAL4/ UAS-GFP-Mad* and *MS1096-GAL4/ UAS-GFP-Dpp* were fixed in 4% PFA and 0.05 or 0.2% glutaraldehyde, embedded in 10% gelatine, and infiltrated in 2.3M sucrose. Specimens were quickly frozen in liquid nitrogen and cryo-sectioned at a Leica ultracut UCT/FCS microtome at  $-105^{\circ}\text{C}$ . 80nm cryosections were retrieved in 1% methylcellulose (Sigma-Aldrich)/1.3M sucrose (Merck). Cryosections were incubated with anti-GFP antibody and 10 nm gold-coupled secondary antibody. Subsequently, sections were postfixed in 1% glutaraldehyde, contrasted in 0.3% uranylacetate/1.8% methylcellulose, and imaged with a Morgagni electron microscope (FEI Co.).

### Cryosectioning

Cryostat XZ-sections at Cryo-Star HM 560 (Microm) were performed with 4% PFA-fixed wing discs incubated at  $4^{\circ}\text{C}$  ON in 30% sucrose solution in PBS, after immunostaining procedure, and mounted in Tissue-Tek (Sakura). This approach confers a better XZ resolution than Z sections acquired by confocal microscopes (see Fig. 13).

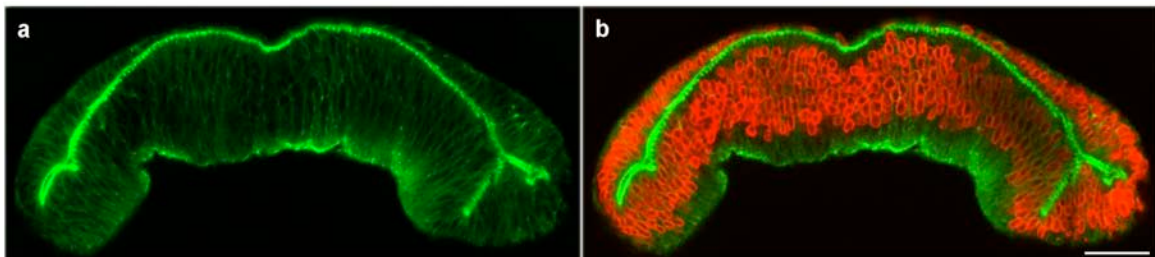


**Figure 13. Cryostat XZ section of a wild-type disc. a)** phalloidin staining (green) labels cell profiles; **b)** laminin (red) labels the nuclear envelope; the pseudo-stratified aspect of the columnar epithelium is due to the different levels occupied by its nuclei (scale bar:  $20\mu\text{m}$ )

### In vivo imaging

For in vivo imaging of the NMJ, third instar *MHC-GAL4/ UAS-GFP<sup>Mad</sup>* larvae were dissected and imaged in ice-cold  $\text{Ca}^{2+}$ -free saline to prevent movement. The GFP fluorescence at the synapse was imaged at a Zeiss confocal microscope with a 40x/1.3 numerical aperture (NA) Plan-Apochromat water objective. Stimulation was performed in high  $\text{K}^{+}$  saline (80mM NaCl, 60mM KCl,

5mM HEPES, 2mM MgCl<sub>2</sub>, 2mM CaCl<sub>2</sub>, 36mM sucrose, pH 7.3) for 5 min. The increased in fluorescence at the NMJ following stimulation was analyzed in ImageJ, after normalization to the background.

For in vivo imaging of the wing imaginal discs, larvae were dissected in cold M3 medium, the discs were transferred to a chamber filled with M3 medium and lypophillic dye FM4-64 (Molecular Probes, dilution 1:2000), and imaged at a Zeiss confocal microscope with a 40x/1.3 numerical aperture (NA) Plan-Apochromat water objective.

### Quantifications

The postsynaptic localization of Tkv, Tkv-GFP, Mad, GFP-Mad and SARA was confirmed by quantifying their immunofluorescence signal with LSM5 Image Examiner, along diameters across 5-10 boutons (the diameter spans 0.5 μm more on each side of the postsynaptic fluorescence, see figures), belonging to at least 3 different preparations. CSP and Dlg immuno-fluorescence were used as pre- and postsynaptic markers, respectively. The signal was normalized and plotted as arbitrary fluorescence units across the bouton diameter.

The signal of PMad fluorescence was analyzed in at least 7 synapses belonging to at least 3 preparations of WT, *mad*<sup>12</sup>/*mad*<sup>12</sup> and *MHC-GAL4/ UAS-Dad*. The average intensity of the signal was measured in ImageJ and normalized to the synapse area. The background fluorescence was extracted.

IEM pictures (2 to 4 cells per picture, 4 to 6 pictures per genotype) were analyzed in order to quantify the density of the proteins in different areas of the cell. For the plasma membrane-associated proteins quantification, gold particles found at 30 nm proximity on each side of the plasma membrane were counted. The number was normalized then to the area (length of the plasma membrane multiplied by 60 nm). For the nuclei and cytoplasm (area of the mitochondria was subtracted), the number of gold particles was normalized to the area analyzed.

For all the graphs the standard errors are plotted. The statistical significance of the data was analyzed with GraphPad InStat.

### Reverse transcriptase-combined polymerase chain reaction (RT-PCR)

Third instar larvae were dissected as described for the flat preparation. The brains together with the ventral cord were removed from the opened larvae and

collected (30 brains/tube). The body walls- muscles plus epidermis- were also collected (10 preparations/tube). From each sample RNA was purified with RNeasy Mini Kit (Quiagen). RT-PCR was performed for detection of Activin- $\beta$ , Alp23B, Scw, Gbb, Dpp, Tkv, Babo, Put, Wit, Sax, Mad, Smox, SARA, and Rab5 as a control. The PCR primers were designed in such manner to amplify common exons of eventually more isoforms of these proteins and also to distinguish between amplicons derived from the target mRNA and contaminating genomic DNA.

### **Immunoprecipitation**

Klorix dechorionated embryos (15-17hr AEL) (50-100 $\mu$ l) were homogenized in lysis buffer (50mM Tris-HCl, 50mM NaCl, 1% IGEPAL, inhibitor-mix tablet (Roche), pH 8) in 1ml donce homogeniser (Wheaton). The homogenate was centrifugated and the supernatant containing the proteic (and lipidic) fraction was incubated with the appropriate antibody 3-4hr at 4°C (mouse anti-Arm 1.5:100, rabbit anti-Mad 1:100). After incubation, Protein A-Agarose or Protein G-Sepharose beads (Amersham Life Sciences) (previously equilibrated with lysis buffer) were added, and mixed ON at 4°C. Next day the excess unbound proteins and antibodies were washed with lysis buffer. The bound proteins were eluted from the beads by boiling them in SDS-sample buffer and submitted to SDS-PAGE.

### **Western blotting**

The proteins from polyacrylamide matrixes were transferred to a polyvinylidene difluoride (PVDF) membrane inside a semi-dry Western Blot apparatus (BioRad). The PVDF membrane was then submerged with blocking solution (TBST buffer: 154mM Tris, 10mM NaCl, 0.05% Tween20, pH 7.4, with 5% milk) overnight at 4°C. The detection of membrane-bound proteins was carried out next day with an enhanced-chemiluminescence (ECL) detection kit (Amersham Life Science) using rabbit anti-Mad 1:1 000 and mouse anti-Arm 1:100. The membranes were incubated with the primary antibody in blocking solution for 1.5hr. Subsequent membrane washes with TBST buffer were followed by incubation with the horseradish peroxidase (HRP)-coupled secondary antibody in blocking solution

for 30min. The ECL reaction was visualized by placing an X-ray film (Biomax ML, Kodak) onto the membrane.

## **GST pull-downs**

### **GST-fusion protein expression**

Arm-Myc and GFP-Mad were cloned into pGEX-3-6P vector. The pGEX-GST-construct vectors were transformed in BL21 *E.coli* strain. A pre-culture was prepared by picking a single colony incubated ON at 37°C in 5ml LB medium with 1mM Ampicillin. The day after, a main-culture was started (1l LB medium with 1mM Ampicillin and the 5ml of pre-culture) and incubated at 37°C while shaking until  $OD_{600nm}=0.8$ . When the right concentration was reached, 1mM IPTG (MBI Fermentas) for induction of GST-fusion expression was added and the cultures were shaken at 20°C ON. The cultures were centrifuged the next day at 5000g for 10min at 4°C and the supernatant discarded. The pellet was resuspended in 20ml lysis buffer (10 ml PBS, 1 mM DTT, 1 mM CLAAP protease inhibitor cocktail (Sigma)), transferred to a 50 ml Falcon tube and shock-frozen with liquid nitrogen. The sample was afterwards defrosted at 37°C and 20 ml lysis buffer added. The bacteria were lysed at Emulsiflex (3 times), centrifuged at 13000g for 45 minutes at 4°C. Meanwhile Glutathione Sepharose beads (Amersham Bioscience) were equilibrated with wash buffer (PBS and 0.5% BSA). The supernatant, which contains the GST-fusion proteins, was added to the equilibrated beads and incubated for 2hr at 4°C. The mixture was then centrifuged at 500g for 5min at 4°C. The pellet representing the immobilized GST-fusion proteins on the beads was then washed four times with wash buffer and left ON at 4°C in 1ml wash buffer.

### **In vitro transcription/ translation**

Arm-Myc and GFP-Mad were cloned into the pCRBlunt vector (which contains the T7 promoter). The constructs were expressed in vitro using the TNT Coupled Reticulocyte Lysate System (Promega) and a radioactive Easy Tag protein labelling mix (Perkin Elmer).

### **GST pull-down assay**

The hot proteins were incubated for 2hr at 4°C together with the GST-fusion proteins immobilized on the beads. For the elution of the immobilized GST-fusion proteins from the beads (together with bound hot proteins), elution buffer (10mM

Glutathione in 50mM Tris, pH 8) was added for 20 minutes at 25°C. The mixture was then shortly centrifuged at 13000g, the resulting supernatant containing the GST-fusions plus complexed hot proteins being concentrated by acetone precipitation. Proteins were re-suspended in sample buffer and run on a SDS-PAGE gel. As a negative control just GST protein was used. The gel was coloured in Coomassie Brilliant-Blue to detect the GST-fusions, fixed in a 20% methanol/ 7% acetic acid solution and the signal was amplified by incubation in Amplify (Amersham Biosciences). The gel was dried and the protein complexes were detected by autoradiography.

## RESULTS

I have studied here the relevance of the sub-cellular localization of TGF- $\beta$  pathway core components for the signal transduction, in the context of two communication processes in polarized cells: during morphogenetic signaling in the epithelial cells of wing imaginal discs and during synaptic transmission at the neuromuscular junction. For both processes, TGF- $\beta$  ligands, receptors and R-Smads show a polarized localization within the cells. My results indicate that the junctional area between the secreting and the receiving cell functions as a signaling domain. In the case of epithelial cells, the level of TGF- $\beta$  signal is regulated by  $\beta$ -cat, an AJs component, probably in a complex together with the R-Smad Mad. At the neuromuscular junctions, an anterograde TGF- $\beta$  signal seems to be coupled with synaptic activity. The possibility of quanta of neurotransmitter released simultaneously with quanta of growth factor might explain, thus, the documented role of TGF- $\beta$  signaling during synaptic function and development.

### **TGF- $\beta$ signaling at cell junctions in the *Drosophila* wing epithelium**

#### **Junctional confinement of TGF- $\beta$ receptor**

The localization of the type I receptor Tkv was monitored by immunodetection of the endogenous protein and visualization of a Tkv-GFP chimera. Using an antibody recognizing the cytoplasmic tail of TGF- $\beta$  type I receptor Tkv (Kruse et al., 2004), the receptor is detected in vesicular structures within the wing disc cells (Fig. 14a, a' circles). Tkv is enriched in an apical region of the epithelial cells; moreover, it is associated with the junctional area of the plasma membrane as monitored in double immunostainings with  $\beta$ -cat and Cora as markers of the AJs and SJs, respectively (Fig. 14a', arrowheads).



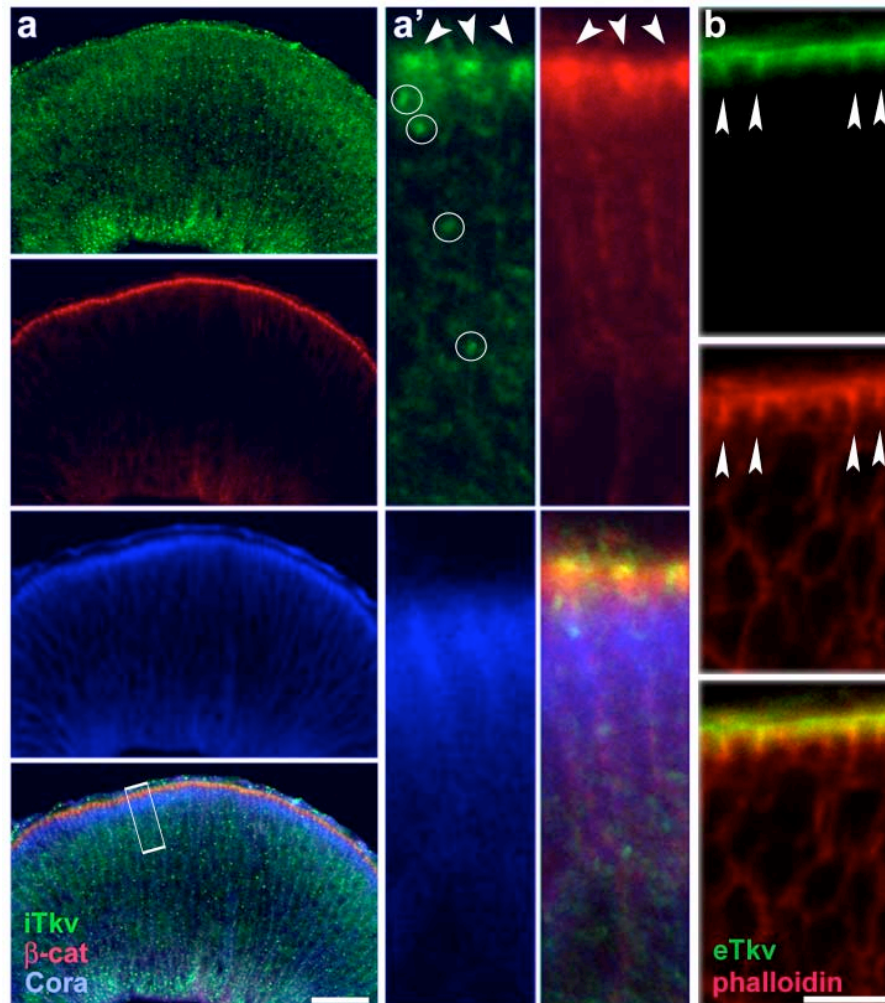


**Figure 14. Plasma membrane-associated TGF- $\beta$  type I receptor Tkv is concentrated at cell junctions.** Cryostat XZ sections of wild-type discs. **a)** whole receptor population stained by the intracellular antibody (green),  $\beta$ -cat (red) labels the AJs, Cora (blue) labels the SJs; **a')** magnification of the region boxed in **a**, Tkv vesicular structures are encircled, arrowheads point to the Tkv population associated to the junctions; **b)** plasma membrane-associated receptor labeled by the luminal antibody (green) according to the extracellular staining protocol, phalloidin (red) marks the junctional cortical actin ring; arrowheads point to the plasma-membrane associated Tkv present at the junctions (scale bars: **a**: 10 $\mu$ m, **b**: 5 $\mu$ m)

In order to distinguish the receptor found at the plasma membrane from the internalized pool, an extracellular staining protocol (Strigini and Cohen, 2000) (see Materials and Methods) was performed, making use of an antibody that recognizes the luminal part of Tkv (Kruse et al., 2004). In short, the antibody was applied without permeabilization and prior to fixation, at 4°C when no endocytosis takes place. This way the antibody reaches only to the cell-surface receptors. The receptor population detected through this protocol is confined to the apical cell junctions (Fig. 14b, arrowheads).

To confirm the specificity of the extracellular staining protocol, the Tkv antibody recognizing the intracellular tail of the receptor was used as a negative control. In this condition, no signal is detected (Fig. 15a). This result validates the exclusive detection of cell-surface proteins by this method. The method allows the detection of basal and apical plasma membrane associated proteins, too. Integrins are transmembrane receptors involved in the interaction of the epithelial cells with the extracellular matrix. They are distributed over the basal cell surface of the wing disc (Brower et al., 1995) (Fig. 15b, arrows) and they are indeed detected performing an extracellular staining with an antibody recognizing their extracellular domain (Brower et al., 1995) (Fig. 15b', arrow). Apical plasma membrane associated proteins are as well detected performing the extracellular staining protocol. To confirm this, the localization of a GFPgpi (glycophosphatidylinositol) chimera (Greco et al., 2001) was analyzed. Gpi anchors target proteins to the outer leaflet of the plasma membrane. In our hands, GFPgpi is targeted to the apical surface of the developing wing cells. Indeed, the extracellular staining protocol detected the apical localized GFPgpi (not shown).

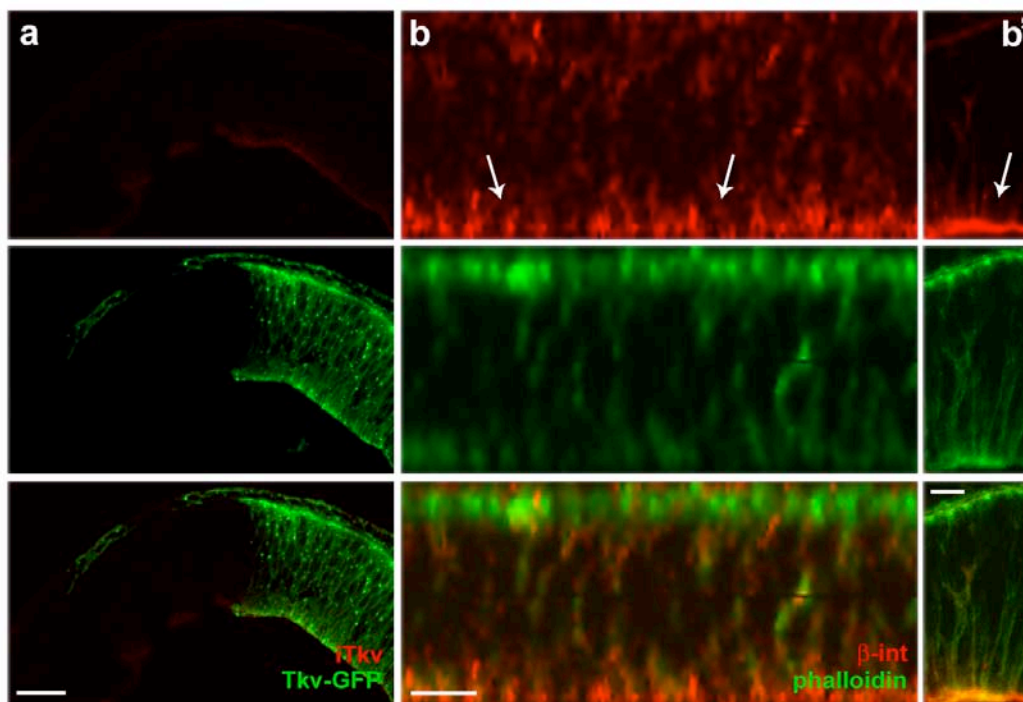


**Fig. 15. Extracellular staining allows detection of both apical and basal plasma membrane associated proteins.** **a**) Tkv (red) is not detected by the antibody generated against the cytoplasmic tail when an extracellular protocol is performed (the faint basal signal represents background), Tkv-GFP (green); **b**) conventional staining protocol:  $\beta$ -integrin (red) is associated with the baso-lateral membranes of the wing disc cells (arrows), some staining is detected also inside the cells; phalloidin (green) labels the apical actin ring; **c**) extracellular staining protocol

detects surface-associated  $\beta$ -integrin (red) (arrow), phalloidin (green) (genotypes: **a** *hh-GAL4/UAS Tkv-GFP*, **b** and **c**: WT) (scale bars: **a**: 20 $\mu$ m, **b**, **c**: 5 $\mu$ m)

The accumulation of cell-surface receptors was confirmed at the ultrastructural level. For that, a C terminus Tkv-GFP fusion was generated. Functionality of the chimera was confirmed by rescuing the lethality of *tkv<sup>8</sup>/tkv<sup>7</sup>* mutants (Nellen et al., 1994) (Penton et al., 1994) (Periklis Pantazis, personal communication). Like the endogenous protein, the chimera is detected in association with the apical junctional area at the confocal microscopy level (Fig. 16a, arrows). Immunoelectronmicroscopy (IEM) studies revealed that inside the cells the receptor is found in multivesicular structures (Fig. 16d', d''), while at the plasma membrane Tkv is associated with both septate and adherens junctions (Fig. 16b, c, stars). AJs can be recognized morphologically at EM level by a cytoplasmic electron-dense plaque on the sides of the two apposing membranes (Fig. 16b, arrow), while the SJs are recognized by electron-dense material spanning the cleft between two apposing membranes (Fig. 16c, arrows). Out of 19 junctions, 7 were Tkv-positive. The plasma membrane associated receptors are concentrated by a 4-fold factor at the AJs and SJs, with respect to other plasma membrane domains (i. e. microvilli) (Fig. 16e).

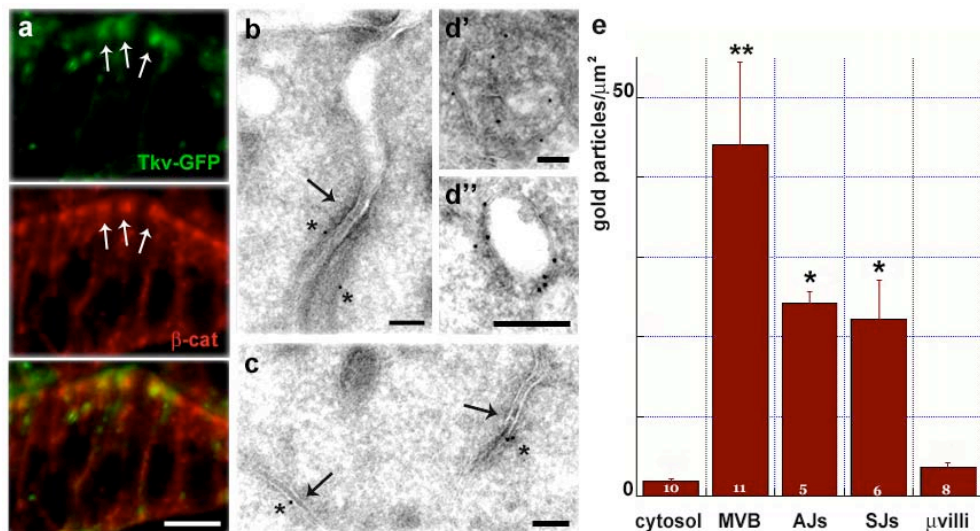


**Figure 16. Ultrastructural characterization of Tkv localization.** **a**) cryostat XZ section showing that functional Tkv-GFP (green) chimera is associated with the AJs, monitored by  $\beta$ -cat immunostaining (red); **b**) –**d**) IEM pictures where Tkv-GFP was stained with an anti-GFP antibody. **b**) Tkv-GFP (stars) associated with the AJs (arrow); **c**) Tkv-GFP (stars) associated with the SJs (arrows); **d'**), **d''**) examples of Tkv-GFP-positive multivesicular bodies; **e**) IEM data: the density of Tkv in different regions of the cell (normalized for the area of the plasma membrane), numbers at the bottom of the columns represent number of EM pictures analyzed; \* $p$  < 0.05, \*\* $p$  < 0.001 (genotype: *hh-GAL4/UAS Tkv-GFP*) (scale bars: **a**: 5 $\mu$ m, **b**–**e**: 100nm)

To address if the association of Tkv with the cell junctions is ligand-dependent, the localization of the receptor was monitored in *dpp<sup>d8</sup>/dpp<sup>d12</sup>* mutant. This mutant combination lacks Dpp expression in the wing imaginal disc (St Johnston et al., 1990). The receptors are still preferentially associated with the junctions in the absence of the ligand (Fig. 17a, a' arrows), indicating that Tkv targeting to the junctional area is independent of the signaling event.

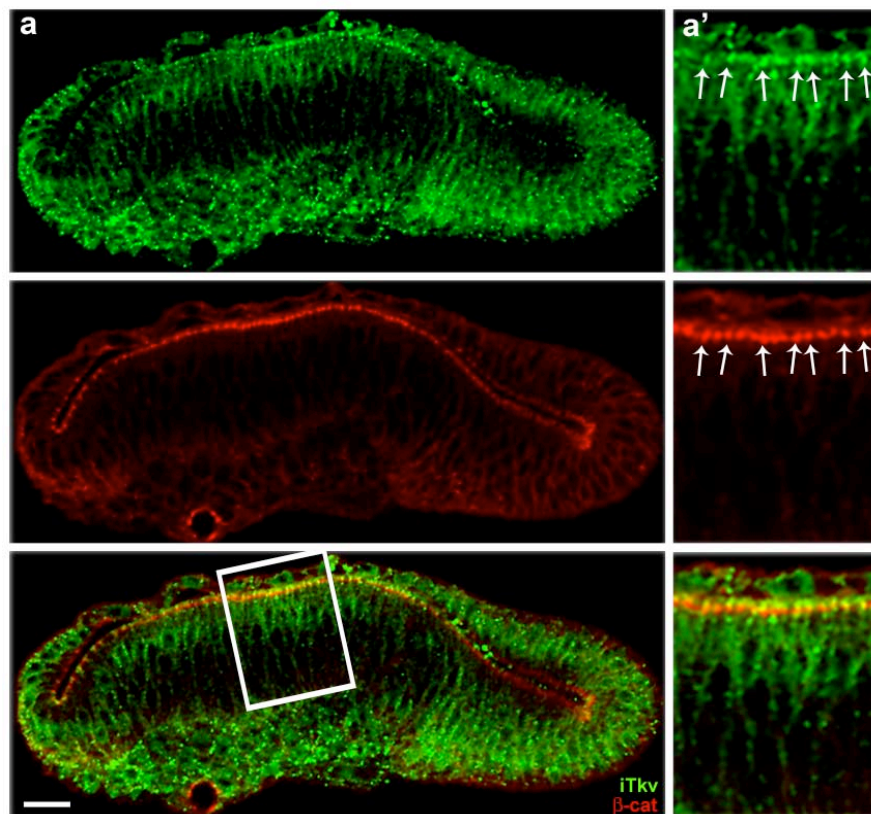


**Figure 17. Tkv junctional localization is ligand-independent.** **a)** cryostat XZ section of a *dpp<sup>d8</sup>/dpp<sup>d12</sup>* wing imaginal disc stained for the whole Tkv population (green) and  $\beta$ -cat (red); **a')** magnification of the region boxed in **a**, arrows point to the Tkv associated with the AJs (scale bar: 15 $\mu$ m)

### Junctional localization of the morphogen Dpp

The fact that the plasma membrane associated Tkv is concentrated at the junctional area of the wing imaginal disc cells raises the possibility that its ligand is targeted to the same area.

No antibody for Dpp immunofluorescence detection in the receiving cells is currently available. Instead, a functional GFP-Dpp fusion protein (Entchev et al., 2000) was used to study the localization of the ligand. Like the receptor, the GFP-

Dpp chimera accumulates in the apical region of the cells (Fig. 18a, a' arrows). To distinguish the extracellular ligand pool from the internalized pool, an extracellular staining (see above) was performed using an anti-GFP antibody (Kruse et al., 2004). Like the receptor, the extracellular ligand is found in a subapical region of the wing epithelium, at the level of the junctions (Fig. 18b).

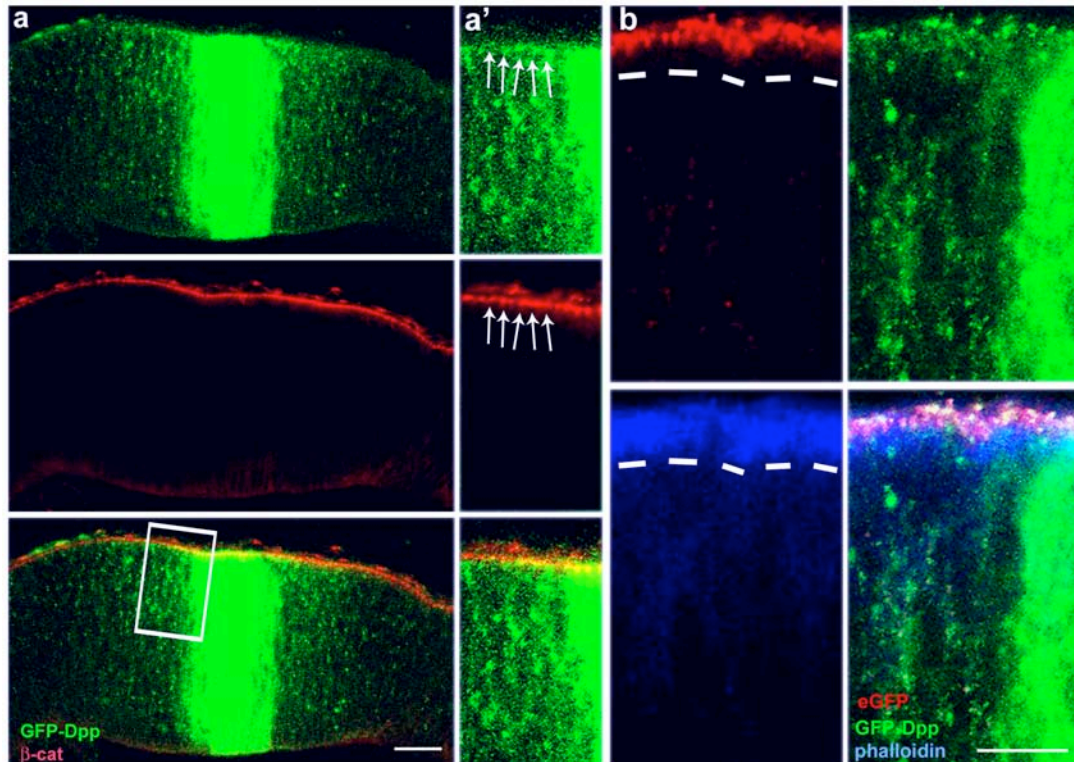


**Figure 18. The extracellular Dpp morphogen is confined to the junctions.** Cryostat XZ sections of imaginal wing discs expressing GFP-Dpp. **a)** GFP-Dpp (green) accumulates in an apical region of the cell,  $\beta$ -cat (red) labels the AJs; **a')** magnification of the region boxed in **a**, colocalization of GFP-Dpp and  $\beta$ -cat marked by arrows; **b)** junctional localization of the extracellular ligand detected by the extracellular staining protocol with an anti-GFP antibody (red), phalloidin (blue), GFP-Dpp (green), lower limit of the junctions is marked by a dashed line (genotype: *dpp-GAL4/UAS GFP-Dpp*) (scale bars: **a**: 10 $\mu$ m, **b**: 5 $\mu$ m)

Dpp localization at the ultrastructural level was studied by monitoring GFP-Dpp by IEM and HRP-Dpp by electron-microcopy (EM). In HRP-Dpp the horseradish peroxidase (HRP) is inserted in the same position as GFP in GFP-Dpp. Both chimeras were detected in close proximity to the junctions (Fig. 19a, b). In order to detect the HRP, DAB (di-amino-benzidine) and  $H_2O_2$  were added, leading to DAB polymerization and formation of a precipitate visible at electron microscopy level. This method provides a higher sensitivity, since the detection is not limited just to the surface of the section, like it is in IEM. In the receiving cells, HRP-Dpp

is detected internalized in endosomal structures, including multivesicular bodies (Fig. 19a, arrowheads). At the plasma membrane, HRP-Dpp is detected concentrated at the junctions (Fig. 19a', arrow). This observation suggests that Dpp is specifically targeted to a distinct region of the plasma membrane in the junctional area, the same one where its receptor is concentrated.

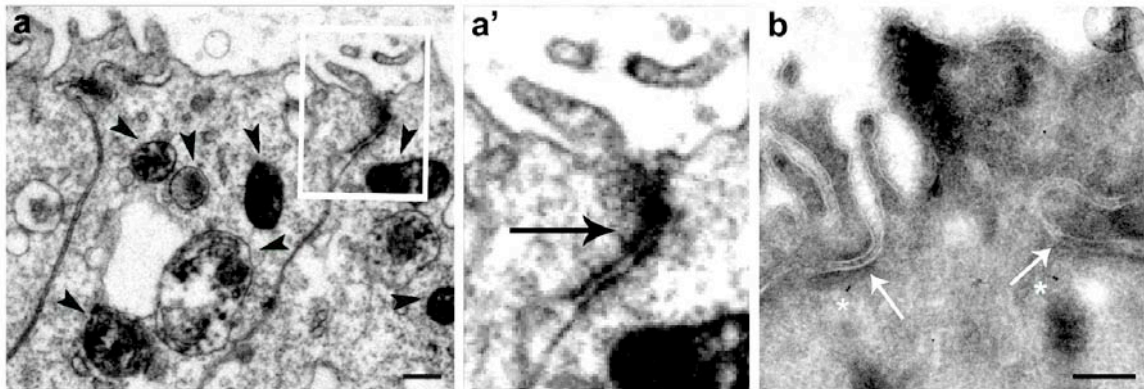


**Figure 19. Ultrastructural characterization of Dpp localization in wing imaginal disc cells.** **a)** EM picture showing HRP-Dpp (electron-dense precipitate) at the receiving tissue in endosomal and multivesicular structures (arrowheads); **a')** magnification of the region boxed in **a** showing Dpp concentrated at the AJs (arrow); **b)** IEM picture for GFP-Dpp detected with an anti-GFP antibody: Dpp (stars) is detected at the junctions (arrows) (genotypes: **a:** *apt-GAL4/ UAS HRP-Dpp*, **b:** *MS1096-GAL4/ UAS GFP-Dpp*) (scale bars: 200nm)

### Targeting of R-Smad Mad to the junctional area

The fact that both the TGF- $\beta$  ligand and its receptor are found enriched at the epithelial cells junctions raises the idea that the junctional area serves as a signaling domain in the plasma membrane. To explore this possibility, the localization of the R-Smad was studied. An antibody developed against the *Drosophila* R-Smad Mad (Sutherland et al., 2003) detects the transcription factor concentrated in the apical side of the epithelial disc cells, associated with the plasma membrane (Fig. 20c). To study at ultrastructural level the Mad localization, a GFP-chimera was generated. Functionality of GFP-Mad was confirmed by rescuing lethality of *mad*<sup>B1</sup> mutants (Wiersdorff et al., 1996). At light microscopy level, GFP-Mad is detected mainly in the nucleus (Fig. 20a N), but also at the apical junctions of the wing imaginal disc cells (Fig. 20a arrows, b), in a pattern similar to the TGF- $\beta$  ligand and its receptor.

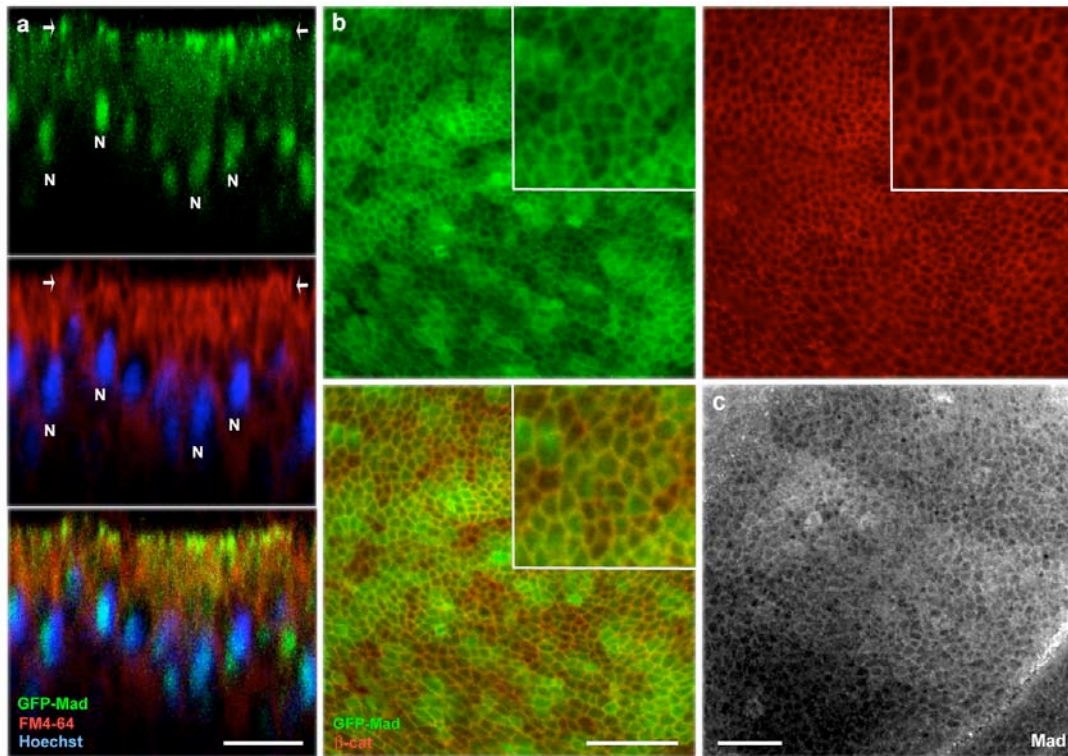


**Figure 20. The transcription factor Mad is associated with the plasma membrane at the junctions.** **a**) XZ section of a GFP-Mad (green) expressing disc, imaged in vivo, Hoechst (blue) labels the cells nuclei, FM4-64 (red) labels the cells membrane; GFP-Mad is present in both nuclei (N) and in an apical region of the plasma membrane (arrows); **b**) XY confocal section of a GFP-Mad (green) expressing disc taken at the level of the junctions, labeled by  $\beta$ -cat (red), inset shows a magnified region; **c**) XY confocal section at junctional level of a wild-type disc stained for Mad (genotypes: **a** and **b**: *tubGAL4/UAS GFP-Mad*, **c**: WT) (scale bars: **a**: 10 $\mu$ m, **b**, **c**: 15 $\mu$ m)

The localization of the protein to the junctions was confirmed at the ultrastructural level (Fig. 21). Of 43 junctions, 26 were Mad-positive. IEM data substantiated that, of the population associated with the plasma membrane, the fraction associated with the AJs and SJs is more concentrated than the one found along the basal membrane or at the apical microvilli (Fig. 21c).

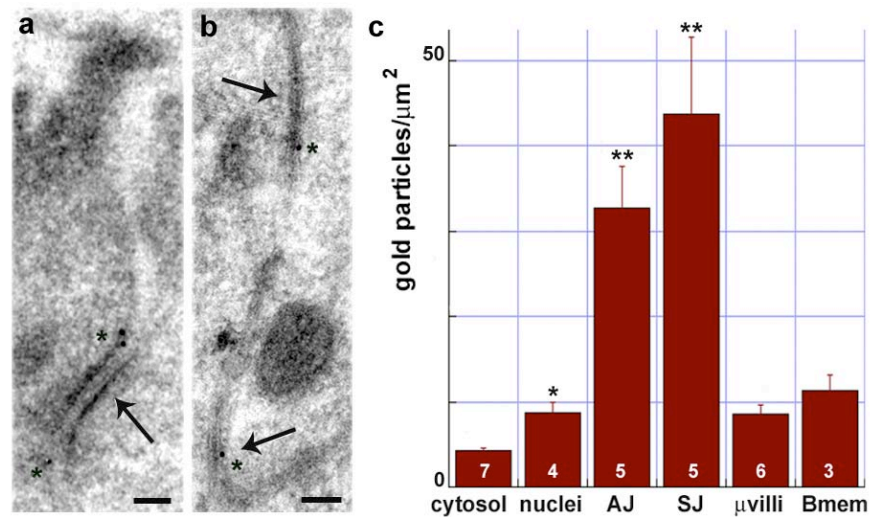


**Figure 21. Plasma membrane associated Mad is enriched at the junctions.** **a)** GFP-Mad (stars) associated with AJs (arrow); **b)** GFP-Mad (stars) associated with the SJs (arrows); **c)** quantification of Mad density associated with various regions of the wing disc cells (normalized to the membrane area); numbers at the bottom of the columns represent number of EM pictures analyzed; \* $p < 0.05$ , \*\* $p < 0.001$  (genotype: *tub-GAL4/ UAS GFP-Mad*) (scale bars: 50nm)

The observation that the transcription factor is associated with the junctions suggests that signaling occurs at the junctions. This prompts two questions: i) how is Mad targeted to the junctions? and ii) how would the disruption of the junctions affect Dpp signal transduction?

### $\beta$ -cat regulates Dpp signaling read-out

Mutants affecting the integrity of the AJs and SJs were used in order to study the effect of junctional disruption on signal transduction. In *shg<sup>IG29</sup>*, *shg<sup>IH</sup>*, *cora<sup>5</sup>*, *dlg<sup>m52</sup>* and *scrib<sup>1</sup>* mutant cells the seal of the junctions is compromised, while the apico-basal polarity is not affected (Le Borgne et al., 2002) (Woods and Bryant, 1991) (Lamb et al., 1998) (Bilder and Perrimon, 2000). None of these mutant conditions displayed defects in TGF- $\beta$  signaling read-out (not shown).

The level of Dpp signaling is affected in *arm<sup>XM19</sup>*, instead. In *arm<sup>XM19</sup>* mutants,  $\beta$ -cat is truncated at the C terminus, which leads to a reduction in its levels of about 30% of the wild-type protein (Cox et al., 1999). This reduction compromises the integrity of the AJs (Tolwinski and Wieschaus, 2001) (Tolwinski and Wieschaus, 2004). Dpp signal transduction is affected in the mutant cells: they display an increased level of Mad phosphorylation (PMad) (Fig. 22).

The Dpp signaling read-out phenotype in  $\beta$ -cat mutants could be explained by the involvement of  $\beta$ -cat at different steps of the pathway: i)  $\beta$ -cat could sequester the



R-Smad to the junctions impairing its translocation to the nucleus, ii)  $\beta$ -cat could bind to SARA, as a recent study suggests (Colland et al., 2004), impairing its Smad anchoring function, iii) similar to Wg signaling,  $\beta$ -cat could be part of a Smad complex that enters the nucleus and modulates Dpp target gene expression, iv) the effect on Dpp signaling could be an indirect one due to  $\beta$ -cat involvement in Wg signaling.

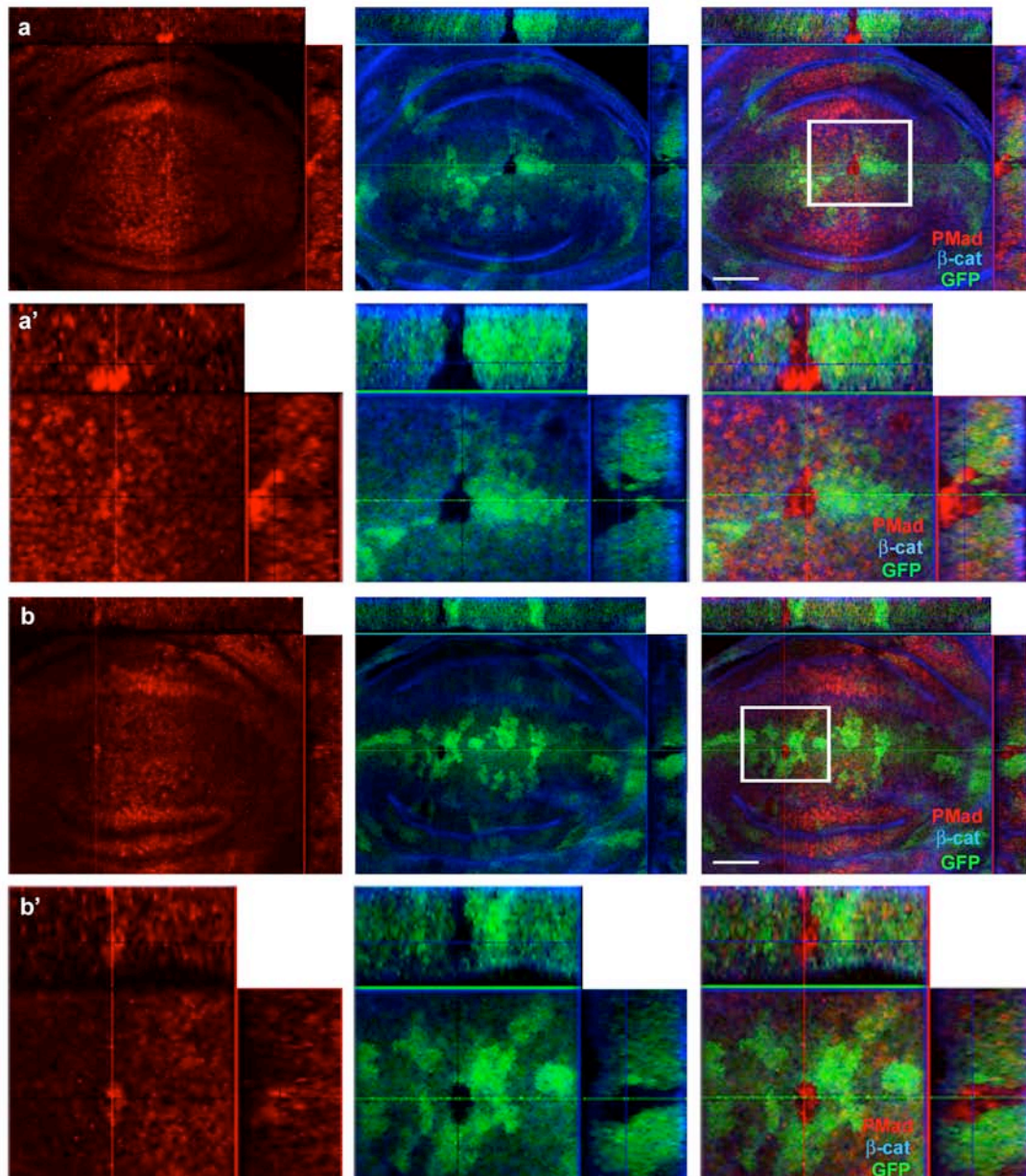


**Figure 22.  $\beta$ -cat regulates Dpp signal transduction.** Orthogonal projections of discs in which  $arm^{XM19}$  clones were induced.  $arm^{XM19}$  clones show increased PMad levels (red); the clones are labeled by the absence of GFP, as well as by the reduced  $\beta$ -cat staining (blue). **a)** a clone inside the PMad domain; **a')** magnification of the region boxed in **a**; **b)** a clone at the border of PMad domain; **b')** magnification of the region boxed in **b** (genotype:  $FRT101\ UbGFP/arm^{XM19}\ FRT101; hsFLP/+$ ) (scale bars:  $40\mu m$ )

### Mad forms a complex with $\beta$ -cat

Recent studies revealed physical interactions between TGF- $\beta$  and Wnt signaling components, involved in the transcriptional control of their target genes. In *Xenopus*,  $\beta$ -cat and TCF (downstream components of the Wnt signaling cascade) were shown to form a complex with Smad4 (Nishita et al., 2000). The complex modulates the expression of the homeobox gene *twi* during formation of the dorsal signaling center, the Spemann's organizer. Moreover, in renal human cell culture,  $\beta$ -cat was shown to associate to Smad3 and Smad4 upon TGF- $\beta$  signaling (Tian and Phillips, 2002), while in renal dysplastic tissues, a complex formed by Smad1,  $\beta$ -cat and TCF binds to the Myc promoter. This complex stimulates Myc transcription (Hu and Rosenblum, 2005), which does not happen in normal renal tissues, since Smad1 alone binds to Myc promoter and does inhibit the gene expression.

The cell culture studies and the fact that in the epithelial wing disc cells Mad is associated to the junctions, where a pool of  $\beta$ -cat is localized, prompted the possibility of an interaction between  $\beta$ -cat and Mad in *Drosophila*. Indeed, Mad immunoprecipitates  $\beta$ -cat, confirming that the proteins form a complex in vivo (Fig. 23a). Furthermore, this interaction is a direct one, as proved by in vitro pull-down experiments (Fig. 23b).

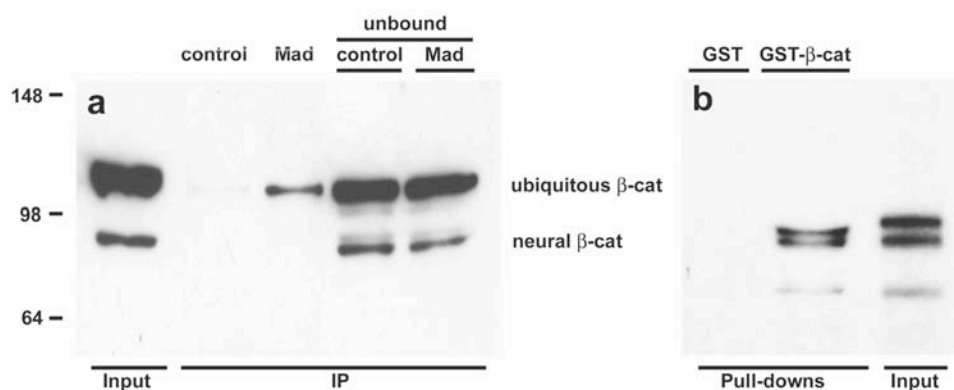


**Figure 23. The transcription factor Mad and the AJs component  $\beta$ -cat form a complex in epithelial cells. a)** The ubiquitous  $\beta$ -cat is pulled-down from an embryo extract by Mad; **b)**  $^{35}$ S-GFP-Mad is pulled down by bacterial expressed GST- $\beta$ -cat

It still remains to be shown which are the interacting domains of the two proteins and by which mechanism the complex regulates Dpp signaling.

## **TGF- $\beta$ signaling at *Drosophila* NMJ**

My results indicate that TGF- $\beta$  signaling machinery is targeted to the epithelial cell junctions. Moreover, TGF- $\beta$  signaling read-out is regulated by a component of the junctions,  $\beta$ -cat. Conversely, TGF- $\beta$  signaling was shown to be involved in the development and the plasticity of the neuromuscular junction (reviewed in Keshishian and Kim, 2004), processes mediated also by cell adhesion molecules like  $\beta$ -cat, Dlg and Scrib (Roche et al., 2002) (reviewed in Koh et al., 2000). To compare the situation at the epithelial cells and the synapse, I have studied the junctional localization of TGF- $\beta$  signaling molecules at the NMJ.

### **Postsynaptic TGF- $\beta$ signal transduction machinery**

TGF- $\beta$  signaling is involved in synaptic development and function. Mutants with impaired TGF- $\beta$  signaling are characterized at the level of the NMJ by reduced number of synaptic boutons and decreased synaptic strength (Marques et al., 2002) (Aberle et al., 2002) (Sweeney and Davis, 2002) (McCabe et al., 2003). These phenotypes are due to altered morphology of the presynaptic SVs release sites and postsynaptic defects of the SSR area opposed to the active zones. The mechanisms by which TGF- $\beta$  modulates NMJ development and function are, however, not yet clarified. A retrograde TGF- $\beta$  signaling occurs at the synapse, but there are indications of an anterograde TGF- $\beta$  signal as well.

In order to elucidate whether an anterograde TGF- $\beta$  signal acts at the synapse, the sub-cellular localization of TGF- $\beta$  signaling components at the synapse was studied. The expression of TGF- $\beta$  pathway components in the CNS and muscles was confirmed by RT-PCR. The TGF- $\beta$  superfamily BMP-like ligands (Dpp, Gbb, Scw) and activins (Activin- $\beta$ , Alp23B), type II (Wit, Put) and type I receptors (Tkv, Sax, Babo), R-Smads (Mad, Smox) and other transducing factors (SARA) transcripts are localized both in the muscles and CNS (Fig. 24). Therefore, these

proteins could in principle mediate TGF- $\beta$ -like signaling during synaptic development.

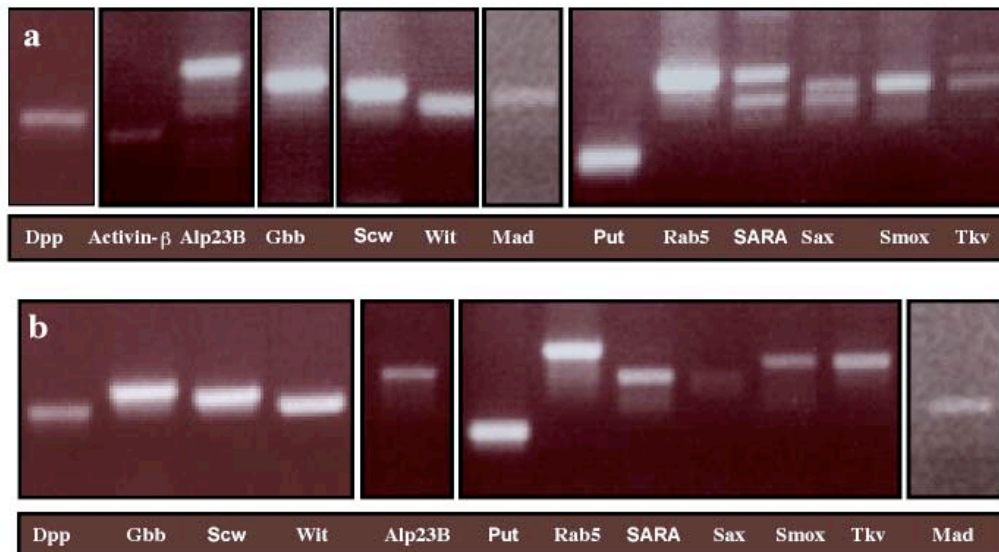


**Figure 24. TGF- $\beta$  superfamily ligands, receptors and transcription factors are expressed in *Drosophila* brain and muscles.** RT-PCR of 3<sup>rd</sup> instar larval a) brains and b) muscles

Indeed, the type I receptor Tkv is present at the NMJ, mainly localized to the SSR (Fig. 25a, a''). Tkv is also detected at low levels inside the presynaptic boutons, which are labeled by cystein string protein (CSP) immunostaining (Fig. 25a' circles). CSP is commonly used as marker of the presynaptic side of the NMJ (Zinsmaier et al., 1994) and they. Consistently, upon neuronal Tkv expression with the elav-GAL4 driver, positive Tkv structures can be detected in the presynaptic boutons (Fig. 25b, b' arrowheads). Conversely, upon expression of the functional Tkv-GFP transgene in the muscles using MHC-GAL4, the GFP-chimera is specifically targeted to the SSR surrounding the presynaptic terminal (Fig. 25c, c'').

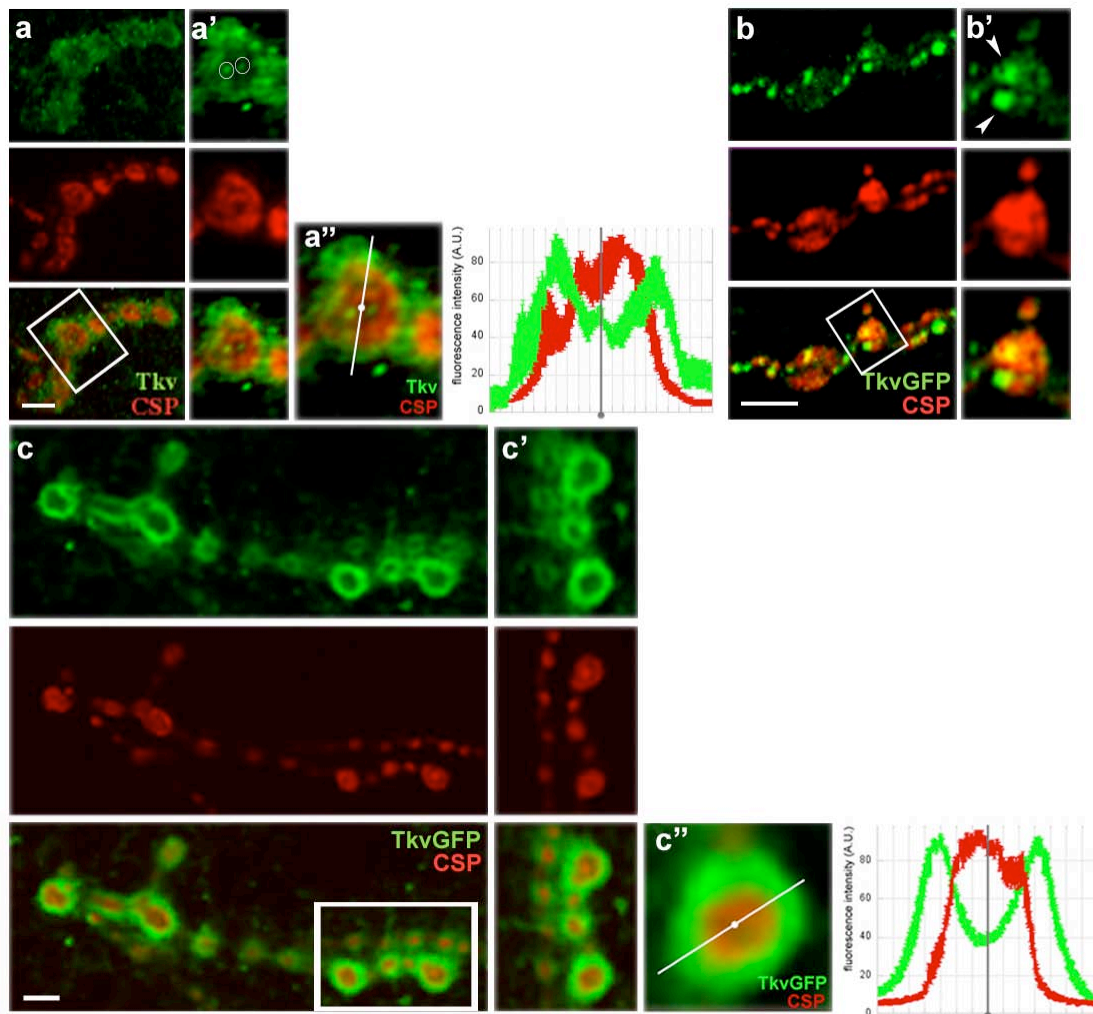


**Figure 25. TGF- $\beta$  type I receptor Tkv is enriched at the postsynaptic side of *Drosophila* larval NMJ.** **a)** Tkv (green) is mainly localized around the synaptic bouton, labeled by CSP (red); **a')** magnification of the region boxed in **a**: presynaptic Tkv-positive structures are encircled; **a'')** postsynaptic Tkv localization, quantification of Tkv (green) and CSP (red) fluorescence across the diameter of the boutons (arbitrary fluorescence units),  $n=5$  (white/ grey circle marks the center of the bouton); **b)** Tkv-GFP is targeted to presynaptic structures when expressed in the nervous system, CSP (red); **b')** magnification of the region boxed in **b**: presynaptic Tkv-positive structures (arrowheads); **c)** Tkv-GFP (green) is targeted to the SSR when expressed in the muscles, CSP (red); **c')** magnification of the region boxed in **c**; **c'')** postsynaptic targeting of Tkv-GFP, quantification of Tkv-GFP (green) and CSP (red) fluorescence across the diameter of the boutons (arbitrary fluorescence units),  $n=10$  (white/ grey circle marks the center of the bouton) (genotypes: **a**: WT, **b**: *elav-GAL4/ UAS Tkv-GFP*, **c**: *MHC-GAL4/ UAS Tkv-GFP*) (scale bars:  $5\mu\text{m}$ )

The presynaptic localization of the receptor is in accordance with a previously reported retrograde TGF- $\beta$  signaling event at the NMJ (Marques et al., 2002) (Aberle et al., 2002) (Sweeney and Davis, 2002) (McCabe et al., 2003). The SSR localization of Tkv raises, on the other hand, the possibility of an anterograde signaling event. It is therefore possible that both antero- and retrograde signaling take place at the synapse.

Which of the TGF- $\beta$  ligands mediates signaling at the NMJ? To address this question, GFP-fusions of Dpp, Gbb, Scw, Activin- $\beta$  and Alp23B have been generated and the transgenes were expressed either in the CNS, or in the muscles. If these ligands are responsible for the development/ function of the NMJ, then they should be targeted to this location. When expressed in the motoneurons, only the functional GFP-Alp23B and GFP-Activin- $\beta$  are targeted down to the presynaptic boutons (Fig. 26), whereas GFP-Scw and GFP-Gbb were not detected under our experimental conditions. Functionality of GFP-Alp23B chimera was confirmed by rescuing lethality of *alp*<sup>22c2</sup>/*Df*(11) mutants (Maximilian Fürthauer, personal communication).

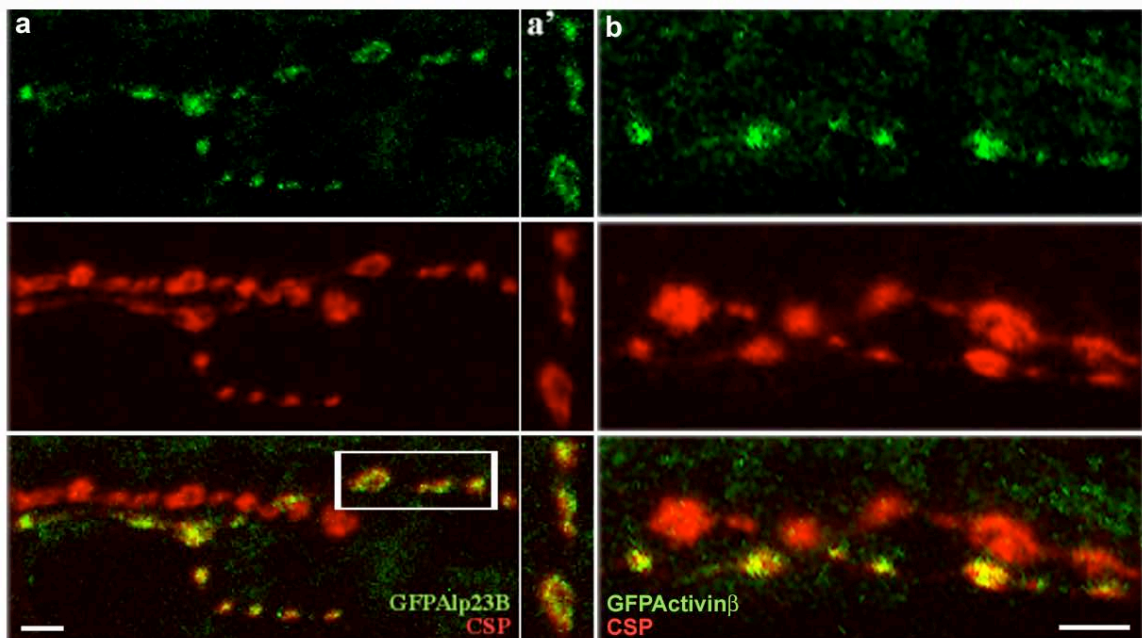


**Figure 26. Activins are targeted to the presynaptic boutons.** **a)** Functional GFP-Alp23B (green) is localized in presynaptic structures when expressed in the nervous system, CSP (red); **a')** magnification of the region boxed in **a**; **b)** GFP-Activin- $\beta$  (green) is localized in presynaptic structures when expressed in the nervous system, CSP (red) (genotype: **a:** *elav-GAL4/ UAS-GFP-Alp23B*, **b:** *elav-GAL4/ UAS-GFP-Activin- $\beta$* ); only a subset of the neurons expressed the chimeric proteins) (scale bars: 5 $\mu$ m)

The facts that a TGF- $\beta$  ligand can be specifically targeted to the presynaptic side of the terminal and that the receptor is mainly found postsynaptically suggest that an anterograde TGF- $\beta$  signal may occur at the *Drosophila* NMJ. If anterograde signaling takes place, the R-Smad should be recruited by the receptor to the postsynaptic side of the NMJ. Fig. 27a, a' shows that this is actually the case:

Mad is localized in the nuclei of the muscles (N), as well as at the postsynaptic side of the NMJ (inset), where Tkv is found, too.

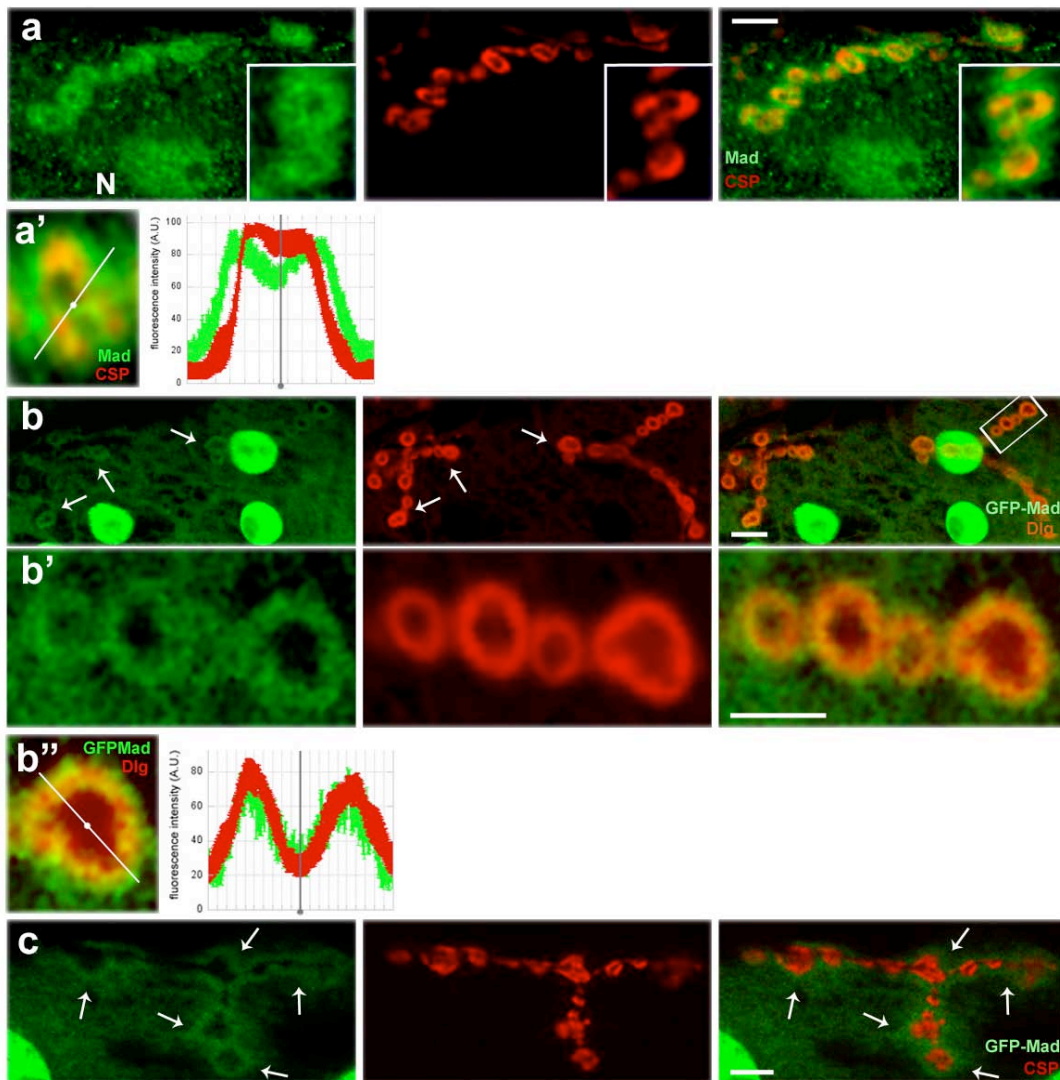


**Figure 27. The transcription factor Mad accumulates in the SSR, as well as in the nuclei of the muscles.** **a**) Mad (green) is localized at the postsynaptic side of the NMJ (inset with magnification) and in the muscle nuclei, CSP (red) labels the presynaptic side of the NMJ; **a'**) postsynaptic Mad localization, quantification of Mad (green) and CSP (red) fluorescence across the diameter of the boutons (arbitrary fluorescence units),  $n=7$  (white/ grey circle marks the center of the bouton); **b**) GFP-Mad (green) accumulates postsynaptically, Dlg (red) labels the SSR surrounding the synaptic boutons (arrows); **b'**) magnification of the region boxed in **b**, showing co-localization of Mad and Dlg in the SSR; **b''**) postsynaptic targeting of GFP-Mad, quantification of GFP-Mad (green) and CSP (red) fluorescence across the diameter of the boutons (arbitrary fluorescence units),  $n=8$  (white/ grey circle marks the center of the bouton); **c**) postsynaptic GFP-Mad (green) (arrows) and presynaptic CSP (red) (genotypes: **a**: WT, **b** and **c**: *MHC-GAL4/ UAS GFP-Mad*) (scale bars: **a**, **b'**, **c**:  $5\mu\text{m}$ , **b**:  $10\mu\text{m}$ )

Consistently, a functional GFP-Mad chimera, when expressed in the muscles is also targeted both to the nuclei and the subsynaptic region, as shown in fixed material and in vivo (Fig. 27b, b'', c).

The fact that R-Smad, like the receptor, is targeted to the SSR facing the presynaptic terminal raises the question whether the TGF- $\beta$ -like ligand released from the presynaptic bouton triggers the postsynaptic phosphorylation of Mad by the receptors localized in the muscle.

### **R-Smad postsynaptic phosphorylation**

An antibody recognizing the phosphorylated form of Mad, PMad (Tanimoto et al., 2000), was used to address whether signal transduction occurs indeed in the muscle. PMad is present at the synapse, in the SSR (Fig 28a), but it accumulates in the muscle nuclei as well. Conversely, in a *mad*<sup>12</sup> mutant background only residual PMad staining is detected in the muscle nuclei (Fig. 28b) (WT:  $5.4 \pm 0.85$ ; *mad*<sup>12</sup>:  $0.3 \pm 0.11$  arbitrary units of fluorescence intensity). The Mad<sup>12</sup> protein is truncated just before the conserved SSVS domain that is phosphorylated by the type I receptor and, therefore, it cannot be phosphorylated. Low levels of staining at NMJ (WT:  $5.7 \pm 0.58$ ; *mad*<sup>12</sup>:  $0.63 \pm 0.42$  arbitrary units of fluorescence intensity) are due to residual Mad maternal protein, which allows survival of the mutants until the third instar larval stage (Raftery et al., 1995). This result confirms that a TGF- $\beta$  signal coming from the NMJ is directed to the muscle nuclei and supports the idea of the transcription factor being phosphorylated in the muscle.



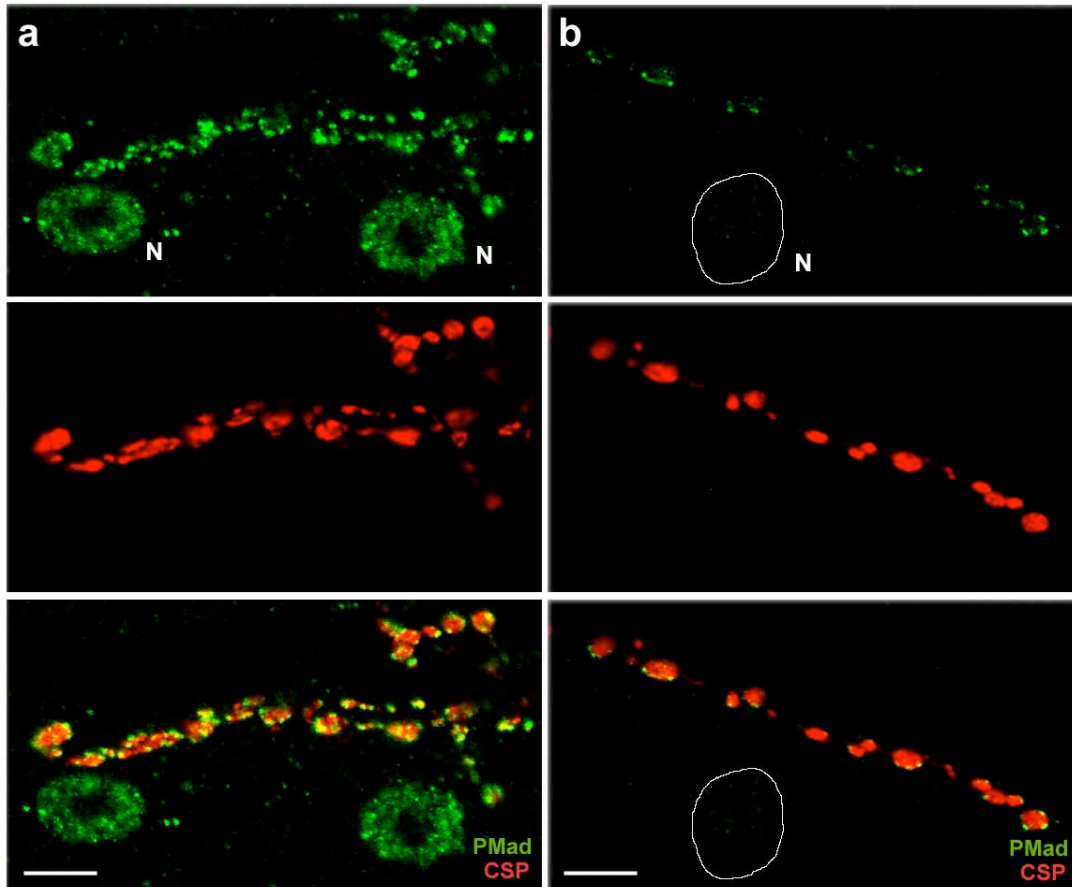


**Figure 28. Phospho-Mad staining specificity.** **a)** phospho-Mad (green) is detected postsynaptically and in the muscle nuclei, CSP (red); **b)** phospho-Mad (green) is drastically reduced at the synapse and in the muscle nuclei of *mad<sup>12</sup>* mutants (see text for quantification data), CSP (red) (N- muscle nucleus) (genotypes: **a:** WT, **b:** *mad<sup>12</sup>/mad<sup>12</sup>*) (scale bars: 10 $\mu$ m)

In *Drosophila*, Dad has been shown to function as an inhibitory Smad (Tsuneizumi et al., 1997). It represses Dpp activity by competing with Mad for binding to Tkv (Inoue et al., 1998), and overexpression of Dad rescues to wild-type the overgrowth caused by Mad overexpression (Tsuneizumi et al., 1997). In order to address if Mad is indeed phosphorylated in the muscles, the levels of PMad were monitored upon inhibiting TGF- $\beta$  signaling. In the wing discs, clones of cells overexpressing Dad have lower levels of PMad than the surrounding wild-type cells (Fig. 29a). Consistently, at the NMJ Mad phosphorylation is impaired by expression of Dad in the muscles, confirming that the transducing event occurs postsynaptically (WT:  $11.1 \pm 2.66$ ; *MHC-GAL4/ UAS-Dad*:  $2.96 \pm 0.43$  arbitrary units of fluorescence intensity) (Fig. 29, compare b with b').

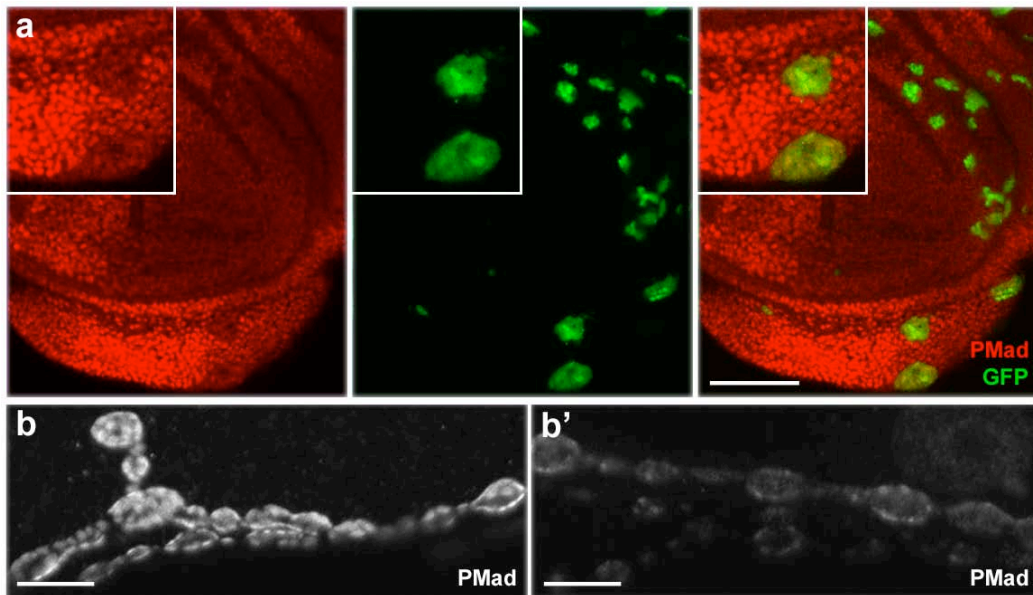


**Figure 29. Mad is phosphorylated postsynaptically.** **a)** wing disc clones expressing Dad (labeled by the presence of GFP, green) have decreased levels of PMad (red), inset shows a magnified region; **b')** phosphorylation of Mad is reduced by postsynaptic expression of Dad with respect to **b)** wild-type synapse (see text for quantification data) (genotypes: **a:** *yw-hsFlp*; *act > CD2 > GAL4*; *UAS-GFP/UAS-Dad*, **b:** WT, **b':** *MHC-GAL4/UAS-Dad*) (scale bars: **a:** 50 $\mu$ m, **b, b':** 5 $\mu$ m)

While the total pool of protein appears diffuse in the SSR (Fig. 27a), the pool of phosphorylated Mad concentrates in a punctate postsynaptic pattern (Fig. 29b). This pattern coincides with the pattern of glutamate receptor clusters in the muscle (Fig. 30a, a'). The postsynaptic glutamate receptor fields are juxtaposed to the presynaptic active zones (reviewed in Broadie and Richmond, 2002). Although the components of both secretion (the active zones) and reception units (neurotransmitter receptors) assemble autonomously, their alignment on both sides of the synaptic cleft requires intercellular signaling (Broadie and Bate, 1993) (Prokop et al., 1996). Consistently, PMad is detected opposite the active zones, labeled by nc82 immunostaining (Fig. 30b, b'). The nc82 antibody (Heimbeck et al., 1999) recognizes an antigen associated to the presynaptic active zones as monitored by the postsynaptic localization of the glutamate receptors at the active zones and the pattern of the centers of endocytosis around the active zones (Wucherpfennig et al., 2003).

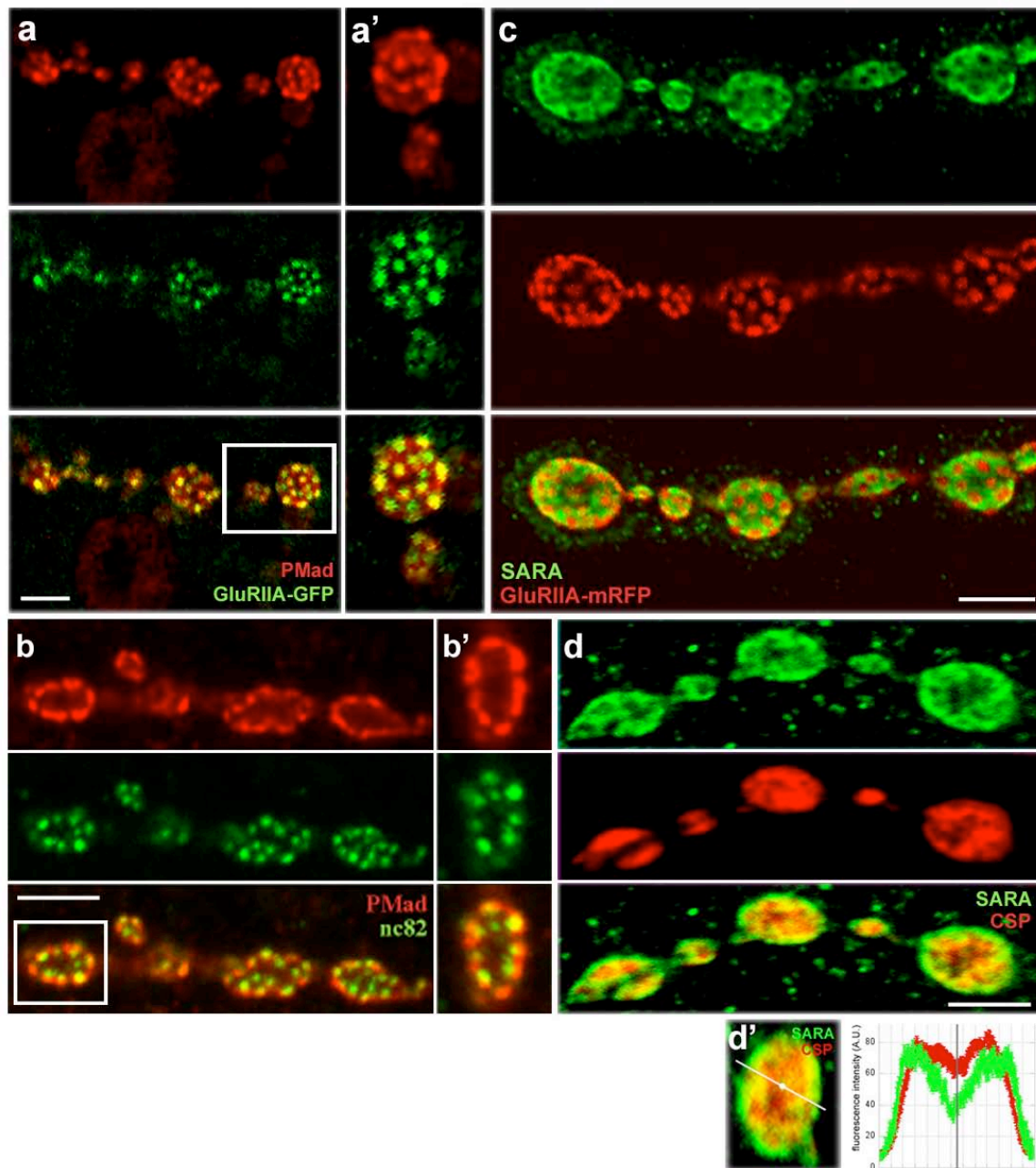


**Figure 30. TGF- $\beta$  signal transduction takes place opposite the synaptic release zones.** **a**) phospho-Mad (red) is present where the glutamate receptor clusters (GluRIIA-GFP) are localized in the muscle (green); **a'**) magnification of the region boxed in **a**; **b**) phospho-Mad (red) is detected postsynaptic facing the active zones labeled by nc82 (green); **b'**) magnification of the region boxed in **b**; **c**) SARA (green) is excluded from the areas where glutamate receptors (GluRIIA-mRFP) cluster in the muscle (red); **d**) SARA (green) is localized post-synaptically, CSP (red); **d'**) postsynaptic SARA localization, quantification of SARA (green) and CSP (red) fluorescence across the diameter of the bouton (arbitrary fluorescence units),  $n=9$  (white/ grey circle marks the center of the bouton) (genotypes: **a**: *MHC-GAL4/ UAS-GluRIIA-GFP*, **b**: WT, **c**: *MHC-GAL4/ UAS-GluRIIA-mRFP*, **d**: WT) (scale bars:  $5\mu\text{m}$ )

SARA is an adaptor protein that recruits R-Smads to the TGF- $\beta$  activated receptors (Tsukazaki et al., 1998) (Hayes et al., 2002). The activated receptors phosphorylate the R-Smads, decreasing thus their affinity for SARA and, as a consequence, the adaptor protein is detached from phospho-Smads (Xu et al.,

2000). At the NMJ, SARA is localized at the postsynaptic side of the terminal (Fig. 30d, d'). Postsynaptic SARA accumulates in a network-like pattern, excluded from the glutamate receptor clusters (Fig. 30c), where Mad is phosphorylated (Fig. 30a'). The absence of SARA from the areas where signal transduction occurs implies that, indeed, the phosphorylation of the transcription factor opposite the active zones triggers the detachment of the adaptor protein.

### R-Smad accumulation at the synapse depends on synaptic stimulation

GFP-Mad is targeted to the postsynaptic side of the NMJ (Fig. 27b, c). In order to address whether such accumulation is synaptic activity-dependent, *in vivo* imaging was performed. Upon stimulation with high  $K^+$  solution, which triggers the release of SVs, increased fluorescence of GFP-Mad in the SSR is detected (Fig. 31, compare a, a' with b, b', arrowheads). Quantification of the GFP fluorescence revealed that synaptic stimulation results in a 20-30% increase of GFP-Mad recruitment to the postsynaptic side of the NMJ (Fig. 31c). This result is consistent with a scenario where, during synaptic transmission, the transcription factor Mad is recruited from the cytoplasm to the receptors, at the SSR.

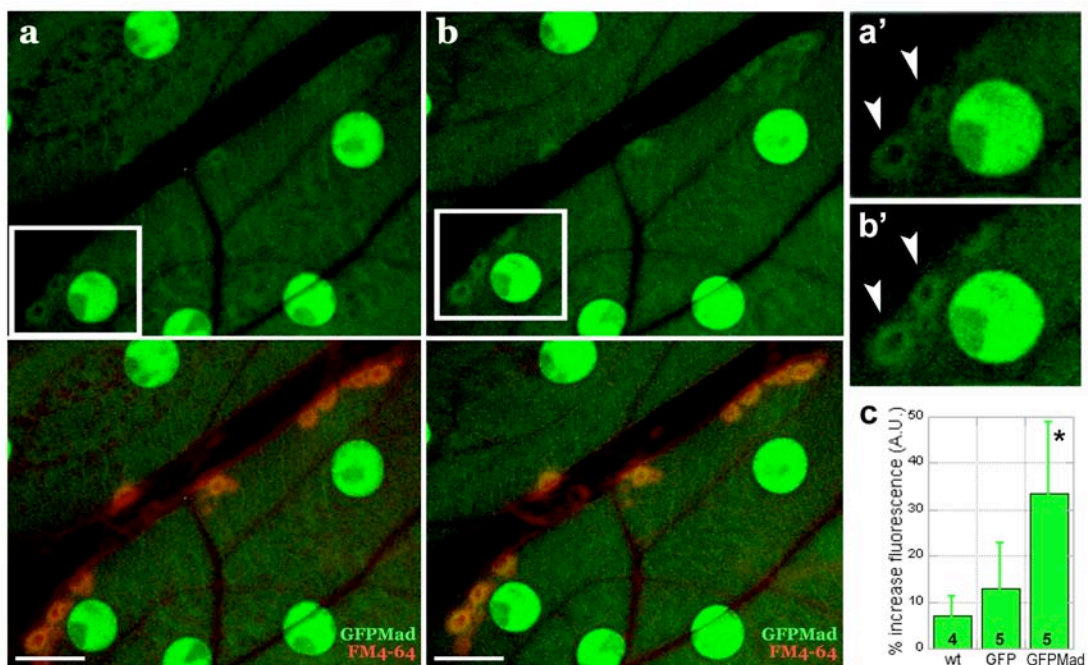


**Figure 31. Synaptic activity triggers Mad accumulation at the NMJ.** *In vivo* imaging of GFP-Mad at the synapse, **a**) before and **b**) after stimulation with high  $K^+$  solution. FM4-64 (red) labels the postsynaptic side of the terminal; **a')** and **b')** magnifications of the regions boxed in **a** and **b** (arrowheads point to two synaptic boutons); **c**) quantification of the fluorescence increase at the NMJ (arbitrary units) after stimulation (numbers at the bottom of the columns represent the number of synapses analyzed; \* $p < 0.05$ ) (scale bars: 20 $\mu$ m)

It remains to be addressed if the R-Smad nuclear import/ export rate depends on synaptic activity and whether ligand release is dependent on synaptic activity, key events in elucidating TGF- $\beta$  role during synaptic development and function.

## **DISCUSSION**

### **TGF- $\beta$ signaling at the epithelial cell junctions**

In the first part of this work, I have studied whether TGF- $\beta$  ligand Dpp and its receptor Tkv are localized at a specific area of the epithelial wing imaginal disc cells, namely the cellular junctions. Moreover, whether such localization is relevant for Dpp signaling read-out. The model of Dpp gradient formation by planar transcytosis implies that the morphogen is secreted by the producing cells and diffuses extracellularly only at short-range. The long-range distribution requires Dpp internalization and re-secretion at the cells of the target tissue. The ligand internalization is receptor-mediated, and is followed by intracellular traffic through endosomal compartments with the consequence that the non-degraded ligand is released to signal in the neighboring cells. The rate of transcytosis is dependent among other parameters on the rate of endocytosis, which is determined not by the absolute number of receptors, but by their concentration. Since a single molecule of Dpp travels very fast across a single cell, the rate of endocytosis must also be very fast to account for the transport by planar transcytosis. A possible scenario in which a fast endocytosis rate could be achieved is by concentrating the receptors to a specific area of the cells. Thus the ligand, while trafficking from one cell to the next, should be secreted also at the same specific area of the cell where the receptors are concentrated.

My results show that, indeed, extracellular Dpp is targeted to a specific area of the cell, the junctional area, where plasma membrane-associated Tkv is localized. Mad is recruited to the same area, probably by the interaction with the AJs component,  $\beta$ -cat.

### **Extracellular Dpp is targeted to the junctional area of receiving cells**

The apical concentration of Dpp raised the possibility that the trafficking of the growth factor to the receiving cells is confined to the apical side of the cell. My results show that, indeed, Dpp is asymmetrically distributed along the apico-basal

axis of the cells, concentrating in an area at the level of AJs (Fig. 18a). Dpp localization at the junctions was confirmed by EM studies (Fig. 19). From the total pool of the ligand, the extracellular one is found associated to the junctions (Fig. 18b). These observations indicate a specific targeting of Dpp to a restricted region of the cell, the junctional area.

### **Cell-surface TGF- $\beta$ type I receptor accumulates at the junctions**

The fact that extracellular Dpp is targeted to the junctional region could imply that its receptor is also localized in the same area. Indeed, cell-surface Tkv receptors are localized at the junctions. The total Tkv population is enriched in an apical region of the cell, where it associates with the junctional area of the plasma membrane. Of the total pool of Tkv, the plasma membrane associated Tkv is concentrated at the junctional level (Fig. 14). The junctional localization of the TGF- $\beta$  receptor was confirmed by EM studies: the surface receptors are six fold concentrated at the junctions with respect to other plasma membrane domains (i. e. microvilli) (Fig. 16).

These facts are in concordance with our model, according to which a fast endocytosis rate of the morphogen into the receiving cells is dependent, among other factors, on the concentration of the receiving proteins to one part of the cell. Cell culture studies suggested that polarized cells regulate signaling by expressing the receptors and secreting the ligand in spatially defined areas of the cell. In adhering MDCK cells, the TGF- $\beta$  ligand was found to be secreted from the apical surface of the polarized cells (Murphy et al., 2004). Similarly, in a polarized tissue, the wing imaginal disc, Dpp is apically secreted at the level of cell-cell junctions. In MDCK cells, the TGF- $\beta$  receptors are localized to the lateral membranes, but adjacent to the zonula adherens (Murphy et al., 2004). In the wing disc cells, plasma membrane associated Tkv receptors are associated with the AJs. These findings imply a general feature of polarized cells in optimizing the transport rate of the secreted signal.

Moreover, the association of Tkv with the cell junctions is ligand-independent. In *dpp<sup>d8</sup>/dpp<sup>d12</sup>* mutants that lack Dpp expression in the wing imaginal disc, the receptors are still associated with the junctions (Fig. 17). This result implies that the targeting of the receptors to the junctional area is not dependent of an initial TGF- $\beta$  signaling event.

### **The R-Smad Mad is recruited to the junctional area**

After binding the ligand, the TGF- $\beta$  receptors propagate the signal through the phosphorylation of R-Smads, which translocate to the nucleus to regulate the transcription of target genes (Lagna et al., 1996). The R-Smad Mad is enriched in the apical side of the wing disc cells, associated to the AJs (Fig. 20). The junctional concentration of the Smad was confirmed by EM studies (Fig. 21). From the population found at the plasma membrane, the one associated with the junctions is 3-4 times more concentrated than the one found along the basolateral membrane or at the microvilli.

The fact that both cell-surface Tkv and Mad are found enriched at the junctions suggests that, upon ligand binding, Mad is phosphorylated by the receptor and then targeted to the nucleus. By now, I have not detected phosphorylated Mad at the junctions. The release of the activated Mad from the ligand/receptor complex in the epithelial wing disc cells could be very rapid following its phosphorylation; therefore, in a steady state situation the phospho-Mad pool still present at the junctions might be under our current detection ability.

### **$\beta$ -cat regulates Dpp signaling read-out**

In *arm*<sup>XM19</sup> mutants,  $\beta$ -cat levels are low and the AJs are disrupted. Dpp signal transduction is affected in these mutant cells: they display an increased level of Mad phosphorylation (Fig. 22). The Dpp signaling read-out phenotype in  $\beta$ -cat mutants could be explained by the involvement of  $\beta$ -cat at different steps of the pathway: i)  $\beta$ -cat could sequester the R-Smad to the junctions impairing its translocation to the nucleus, ii)  $\beta$ -cat could bind to SARA, impairing its function of anchoring the Smads, iii)  $\beta$ -cat could be part of the Smad complex that enters the nucleus and modulates Dpp target gene expression, iv) the effect on Dpp signaling could be an indirect effect of the Wg signaling pathway.

Recent studies revealed physical interactions between TGF- $\beta$  and Wnt signaling components, involved in the transcriptional control of their target genes. In *Xenopus*,  $\beta$ -cat and TCF (downstream components of the Wnt signaling cascade) were shown to form a complex with Smad4 (Nishita et al., 2000). The complex modulates the expression of the homeobox gene *twin* during formation of the dorsal signaling center, the Spemann's organizer. In renal human cell culture,  $\beta$ -



cat was shown to become associated to Smad3 and Smad4 after TGF- $\beta$  stimulation (Tian and Phillips, 2002). In renal dysplastic tissues, a complex formed by Smad1,  $\beta$ -cat and TCF binds to the Myc promoter, thus stimulating Myc transcription (Hu and Rosenblum, 2005). The complex does not form in normal renal tissues, since Smad1 alone binds to Myc promoter and does inhibit the gene expression.

Indeed, Mad is directly interacting with  $\beta$ -cat in vivo (Fig. 23), forming a complex that might be responsible for regulating Dpp signaling read-out. On the other hand, if Dpp and Wg signaling networks are connected intracellularly, availability of a limited pool of the possibly shared component  $\beta$ -cat could affect the efficacy of one of the cascades. It still remains to be shown which are the interacting domains of the two proteins ( $\beta$ -cat and Mad) and by which mechanism the complex regulates Dpp signaling.

### **TGF- $\beta$ signaling at the neuromuscular junction**

In the second part of the work I have studied whether anterograde TGF- $\beta$  signaling occurs at the NMJ. Three results support this possibility: i) the presynaptic localization of the ligand vs. the postsynaptic localization of the receptor; ii) the postsynaptic phosphorylation of the R-Smad; iii) recruitment of the R-Smad to the NMJ during synaptic transmission. Likewise, the specific sub-cellular localization of the pathway components suggests a scenario in which anterograde TGF- $\beta$  signaling is coupled with synaptic transmission. Such a scenario implies that within the synaptic terminal there are synaptic vesicles containing both neurotransmitter and growth factors. During synaptic transmission the terminal would release not just quanta of neurotransmitter, but also quanta of growth factors that bind to the receptor present in the muscle. These quanta of growth factor would then modulate the synaptic development in an activity-dependent manner. Since the synaptic vesicles are released at the active zones, signaling would occur through Smads phosphorylation in the area opposed to the active zones, where also the glutamate receptors are clustered. From here the signal would be targeted to the nuclei of the muscles, where the activity of unknown genes involved in synaptic development and function would be modulated.

### **Presynaptic TGF- $\beta$ localization**

In accordance with the idea of an anterograde TGF- $\beta$  signaling at the NMJ, TGF- $\beta$  ligands were found localized to the presynaptic boutons. In order to detect their localization, I have generated GFP chimeras of TGF- $\beta$  ligands, since no functional antibodies for immunofluorescence are available. GFP-Alp23B and GFP-Activin- $\beta$  are targeted down to the presynaptic side of the NMJ when expressed in the neurons (Fig. 26). None of the other TGF- $\beta$  ligands (Gbb, Dpp, Scw) were detected at the NMJ, when the GFP chimeras were expressed either in the neurons, or in the muscles. However, when driven in the wing imaginal disc, the chimeras are detected in the expressing cells. The fact that they are not found at the NMJ could be due to low expression, under our current detection level.

### **Postsynaptic pool of TGF- $\beta$ type I receptor**

The type I receptor Tkv is mainly localized to the SSR. Consistently, upon expression of a functional Tkv-GFP transgene in the muscles, the GFP-chimera is specifically targeted to the SSR surrounding the presynaptic terminal (Fig. 25). Tkv can also be detected at low levels inside the presynaptic boutons. Likewise, upon neuronal Tkv expression in the neurons, positive Tkv structures can be detected in the presynaptic boutons (Fig. 25).

The presynaptic localization of the receptor is in accordance with a retrograde TGF- $\beta$  signaling event at the NMJ, as previously reported (Marques et al., 2002) (Aberle et al., 2002) (Sweeney and Davis, 2002) (McCabe et al., 2003). The SSR localization of Tkv, together with the fact that the ligand is detected presynaptically, suggests the possibility of an anterograde signaling or an autocrine event.

Why would activins signal through a BMP receptor? A cross-talk between the two pathways could occur at the synapse, alternatively Tkv could signal in the activin pathway as well. Our antibodies generated against Babo and Put or a commercial Wit antibody (Hybridoma Bank) did not detect these receptors at the NMJ, while they did detect the receptors in the wing imaginal disc cells. On the other hand, I have found that a Babo-GFP chimeric protein is targeted to the SSR, in the same manner like Tkv-GFP, when expressed in the muscles (not shown).

### **An anterograde TGF- $\beta$ signal at the synapse**

Evidence for the anterograde TGF- $\beta$  signaling was supported by three results: i) Mad is localized at the postsynaptic side of the terminal, ii) Mad is phosphorylated in the muscle SSR, iii) phosphorylated Mad is translocated from the SSR to the muscle nuclei.

Mad is detected in the nuclei of the muscles, as well as at the postsynaptic side of the NMJ. Consistently, a functional GFP-Mad chimera, when expressed in the muscles is also targeted both to the nuclei and the subsynaptic region (Fig. 27). The active Mad is detected at the synapse, in the SSR, and in the muscle nuclei (Fig 28a), suggesting that TGF- $\beta$  signaling takes place at the muscle. Indeed, Mad phosphorylation is impaired when TGF- $\beta$  signaling is inhibited by the expression of i-Smad Dad in the muscles (Fig. 29). The fact that the transducing event occurs postsynaptically is supported also by the absence of the PMad in the muscle nuclei of the *mad*<sup>12</sup> mutant larvae (Fig. 28). The mutant protein cannot be phosphorylated, but the mutants manage to survive until the third instar stage on the account of residual Mad maternal protein. Low PMad levels of staining are still detected at the NMJ, probably too low to allow detection also at the nuclei of the muscles.

### **Sub-cellular localization of TGF- $\beta$ components indicative of their role at the synapse?**

While the total pool of synaptic Mad appears diffuse in the SSR, the pool of phosphorylated Mad concentrates in a punctate postsynaptic pattern. This pattern coincides with the pattern of glutamate receptor clusters in the muscle, opposite the active zones (Fig. 30). The fact that Mad phosphorylation takes place where the glutamate receptors are clustered supports the idea of a synaptic activity-dependent signal transduction event, according to which quanta of growth factor are released to signal postsynaptically. Moreover, SARA, an adaptor protein thought to recruit R-Smads to the TGF- $\beta$  activated receptors, is localized at the postsynaptic side (Fig. 30d) of the terminal in an interesting pattern: SARA accumulates in a network-like pattern, excluded from the glutamate receptor clusters, where Mad is phosphorylated (Fig. 30). The absence of SARA from the areas where signal transduction occurs suggests that phosphorylation of the

transcription factor opposite the active zones lowers the affinity of the adaptor protein for the Smad and triggers its detachment.

### **R-Smad accumulation at the synapse is dependent on synaptic activity**

The fact that Mad phosphorylation takes place where the glutamate receptors are clustered suggests a synaptic activity-dependent signal transduction event. Indeed, Mad accumulation to the postsynaptic side of the NMJ is synaptic activity-dependent (Fig. 31). There is a 20-30% increase in Mad levels at the SSR when the release of SVs is induced with high  $K^+$  solution. This result is consistent with our model according to which, during synaptic transmission, the ligand released from the synaptic bouton would bind to the postsynaptic receptor. This event would then trigger the recruitment of Mad from the cytoplasm to the receptors, at the SSR.

It remains still to be addressed if the R-Smad nuclear import/ export rate depends on synaptic activity and whether ligand release is dependent on synaptic activity, key events in elucidating TGF- $\beta$  role during synaptic development and function.

In summary, in this study the relevance of the sub-cellular localization of the TGF- $\beta$  pathway core components for the signal transduction in the context of communication processes in polarized cells was analyzed. In the epithelial cells of wing imaginal discs, during morphogenetic signaling, and at the NMJ, during synaptic transmission, TGF- $\beta$  ligands, receptors and R-Smads show a polarized localization. My results indicate that TGF- $\beta$  signaling is confined to the junctional area between the secreting and the receiving cell. In the context of epithelial cells, the AJs seem to play a role in TGF- $\beta$  signaling through their component  $\beta$ -cat. A complex forms between  $\beta$ -cat and the R-Smad Mad, but the mechanism by which  $\beta$ -cat modulates signaling is not yet understood. Further studies are necessary in order to determine the interacting domains of the two molecules and to address how the complex regulates Dpp signaling read-out. In the context of NMJ, the sub-cellular localization of TGF- $\beta$  pathway components indicates an anterograde signal occurring at the synapse. The phosphorylation of the R-Smad Mad opposite the active zones of neurotransmitter release suggests a dependency of the signaling on synaptic activity. Quanta of growth factor, released together with neurotransmitter quanta, might send signals to the muscle

---

that would control the maturation and physiology of the synapse. The possibility of a coupling between TGF- $\beta$  signaling and synaptic transmission can be addressed by FRAP (fluorescence recovery after photobleaching) experiments: a faster recovery of the GFP-Mad fluorescence at photobleached synapses and nuclei of the muscle should occur upon synaptic stimulation.

## ABBREVIATIONS

Additional abbreviations are introduced and explained in the text. Symbols of multiples (e. g.  $\mu$ , n, etc.) and SI units are not listed.

<b>act</b>	actin
<b>AJ</b>	adherens junction
<b>Alp23B</b>	Activin-like protein at 23B
<b>arm</b>	<i>Armadillo</i>
<b><math>\beta</math>-cat</b>	$\beta$ -catenin
<b>Babo</b>	Baboon
<b>Bmem</b>	basal membrane
<b>Cora</b>	Coracle
<b>CSP</b>	Cystein string protein
<b>Dad</b>	Daughters against Dpp
<b>Dlg</b>	Discs large
<b>Dpp</b>	Decapentaplegic
<b>E-Cad</b>	E-Cadherin
<b><i>E.coli</i></b>	<i>Escherichia coli</i>
<b>EM</b>	electron microscopy
<b>FRT</b>	FLPase recombination target
<b>Gbb</b>	Glass bottom boat 60A
<b>GFP</b>	green fluorescent protein
<b>GluRIIA</b>	Glutamate receptor subunit IIA
<b>GST</b>	glutathione-S-transferase
<b>HRP</b>	horseradish peroxidase
<b>IEM</b>	immuno-electron microscopy
<b>Int</b>	Integrin
<b>IP</b>	immunoprecipitation
<b>LB</b>	Luria-Bertani medium
<b><math>\mu</math>villi</b>	microvilli
<b>Mad</b>	Mothers against Dpp
<b>MHC</b>	myosin heavy chain
<b>NMJ</b>	neuromuscular junction
<b>PMad</b>	phosphorylated Mad
<b>Put</b>	Punt
<b>Rab</b>	Ras-related in the brain
<b>RFP</b>	red fluorescent protein
<b>RT</b>	room temperature
<b>RT-PCR</b>	reverse-transcriptase polymerase chain reaction
<b>SARA</b>	Smad anchor for receptor activation
<b>Scw</b>	Screw
<b>Scrib</b>	Scribble
<b><i>shg</i></b>	<i>shot-gun</i>
<b>SJ</b>	septate junction
<b>Smox</b>	Smad on X
<b>SSR</b>	subsynaptic reticulum
<b>SV</b>	synaptic vesicle
<b>TGF</b>	transforming growth factor
<b>TJ</b>	tight junction
<b>Tkv</b>	Thick veins
<b>tub</b>	Tubulin
<b>Wit</b>	Wishful thinking
<b>WT</b>	wild-type

## **ACKNOWLEDGEMENTS**

I wish to thank my supervisor, Dr. Marcos González-Gaitán, for the innovative ideas, for the discussions about my data, and for the encouragement during the long PhD years. Thank you for backing me up when I had to change the project.

I am thankful to the members of my thesis advisory committee (TAC), Prof. Dr. Gerold Barth and Prof. Dr. Marino Zerial, for their scientific input.

I am grateful to Michaela Wilsch-Bräuninger (Electron Microscopy Facility, Dresden) for everything concerning electron microscopy. Also, to Penny Hayward (Alfonso Martinez Arias lab, University of Cambridge) for setting up the conditions for the  $\beta$ -cat/ Mad immunoprecipitation and for sharing results and advises.

I would like to thank to all the past and present lab members (Ani, Anja, Antje, Christian, Claudia, Eugeni, Franck, Maximilian, Naomi, Olivier, Tanja) for the lively atmosphere. Especially thank you, Dana and Laki, for being there for me on unaccounted number of times when things went wrong or did not go at all (thanks for being there when sun was shining, too).

A big thanks to Giovanna, Mirko and Sylke for their scientific help, as well as for the 'every-day life' help.

Thank you, Lars, for making and breaking things better.

Multe multumiri parintilor mei care, desi departe, au fost tot timpul alaturi de mine si m-au incurajat. Multumesc, Andreea, pentru rabdarea cu care mi-ai repetat de atatea ori 'lasa, ca mai e putin si vii..'.  
.



**REFERENCES**

- Aberle, H., Haghighi, A. P., Fetter, R. D., McCabe, B. D., Magalhaes, T. R. and Goodman, C. S. (2002).** *wishful thinking* encodes a BMP type II receptor that regulates synaptic growth in *Drosophila*. *Neuron* **33**, 545-558.
- Allan, D. W., St Pierre, S. E., Miguel-Aliaga, I. and Thor, S. (2003).** Specification of neuropeptide cell identity by the integration of retrograde BMP signaling and a combinatorial transcription factor code. *Cell* **113**, 73-86.
- Anderson, M. S., Halpern, M. E. and Keshishian, H. (1988).** Identification of the neuropeptide transmitter proctolin in *Drosophila* larvae: characterization of muscle fiber-specific neuromuscular endings. *Journal of Neuroscience* **8**, 242-255.
- Arora, K., Levine, M. S. and O'Connor, M. B. (1994).** The *screw* gene encodes a ubiquitously expressed member of the TGF-beta family required for specification of dorsal cell fates in the *Drosophila* embryo. *Genes and Development* **8**, 2588-2601.
- Atwood, H. L., Govind, C. K. and Wu, C. F. (1993).** Differential ultrastructure of synaptic terminals on ventral longitudinal abdominal muscles in *Drosophila* larvae. *Journal of Neurobiology* **24**, 1008-1024.
- Bachmann, A., Schneider, M., Theilenberg, E., Grawe, F. and Knust, E. (2001).** *Drosophila* Stardust is a partner of Crumbs in the control of epithelial cell polarity. *Nature* **414**, 638-643.
- Bate, M. (1990).** The embryonic development of larval muscles in *Drosophila*. *Development* **110**, 791-804.
- Bate, M., Landgraf, M. and Ruiz Gomez Bate, M. (1999).** Development of larval body wall muscles. *International Review of Neurobiology* **43**, 25-44.
- Baumgartner, S., Littleton, J. T., Broadie, K., Bhat, M. A., Harbecke, R., Lengyel, J. A., Chiquet-Ehrismann, R., Prokop, A. and Bellen, H. J. (1996).** A *Drosophila* neurexin is required for septate junction and blood-nerve barrier formation and function. *Cell* **87**, 1059-1068.
- Benveniste, R. J. and Taghert, P. H. (1999).** Cell type-specific regulatory sequences control expression of the *Drosophila* FMRF-NH2 neuropeptide gene. *Journal of Neurobiology* **38**, 507-520.
- Beumer, K. J., Rohrbough, J., Prokop, A. and Broadie, K. (1999).** A role for PS integrins in morphological growth and synaptic function at the postembryonic neuromuscular junction of *Drosophila*. *Development* **126**, 5833-5846.
- Bienz, M. (2005).** beta-Catenin: A Pivot between Cell Adhesion and Wnt Signalling. *Current Biology* **15**, R64-67.

- Bilder, D. and Perrimon, N.** (2000). Localization of apical epithelial determinants by the basolateral PDZ protein Scribble. *Nature* **403**, 676-680.
- Blair, S. S.** (1992). Engrailed expression in the anterior lineage compartment of the developing wing blade of *Drosophila*. *Development* **115**, 21-33.
- Bollenbach, T., Kruse, K., Pantazis, P., González-Gaitán, M. and Julicher, F.** (2005). Robust Formation of Morphogen Gradients. *Phys Rev Lett* **94**, 018103.
- Brand, A. H. and Perrimon, N.** (1993). Targeted gene expression as a means of altering cell fates and generating dominant phenotypes. *Development* **118**, 401-415.
- Broadie, K. and Bate, M.** (1993). Activity-dependent development of the neuromuscular synapse during *Drosophila* embryogenesis. *Neuron* **11**, 607-619.
- Broadie, K. and Richmond, J.** (2002). Establishing and sculpting the synapse in *Drosophila* and *C. elegans*. *Current Opinion in Neurobiology* **12**, 491.
- Brower, D. L., Brabant, M. C. and Bunch, T. A.** (1995). Role of the PS integrins in *Drosophila* development. *Immunol Cell Biol* **73**, 558-564.
- Brummel, T. J., Twombly, V., Marques, G., Wrana, J. L., Newfeld, S. J., Attisano, L., Massague, J., O'Connor, M. B. and Gelbart, W. M.** (1994). Characterization and relationship of Dpp receptors encoded by the *saxophone* and *thick veins* genes in *Drosophila*. *Cell* **78**, 251-261.
- Bryant, P. J.** (1975). Pattern formation in the imaginal wing disc of *Drosophila melanogaster*: fate map, regeneration and duplication. *J Exp Zool* **193**, 49-77.
- Bryant, P. J.** (1997). Junction genetics. *Dev Genet* **20**, 75-90.
- Budnik, V., Koh, Y. H., Guan, B., Hartmann, B., Hough, C., Woods, D. and Gorczyca, M.** (1996). Regulation of synapse structure and function by the *Drosophila* tumor suppressor gene *dlg*. *Neuron* **17**, 627-640.
- Budnik, V., Zhong, Y. and Wu, C. F.** (1990). Morphological plasticity of motor axons in *Drosophila* mutants with altered excitability. *Journal of Neuroscience* **10**, 3754-3768.
- Cantera, R., Hansson, B. S., Hallberg, E. and Nassel, D. R.** (1992). Postembryonic development of leucokinin I-immunoreactive neurons innervating a neurohemal organ in the turnip moth *Agrotis segetum*. *Cell and Tissue Research* **269**, 65-77.
- Chacko, B. M., Qin, B., Correia, J. J., Lam, S. S., de Caestecker, M. P. and Lin, K.** (2001). The L3 loop and C-terminal phosphorylation jointly define Smad protein trimerization. *Nat Struct Biol* **8**, 248-253.
- Chiba, A.** (1999). Early development of the *Drosophila* neuromuscular junction: a model for studying neuronal networks in development. *International Review of Neurobiology* **43**, 1-24.
- Colland, F., Jacq, X., Trouplin, V., Mouglin, C., Groizeleau, C., Hamburger, A., Meil, A., Wojcik, J., Legrain, P. and Gauthier, J. M.** (2004). Functional proteomics mapping of a human signaling pathway. *Genome Res* **14**, 1324-1332.

- Cox, R. T., Pai, L. M., Kirkpatrick, C., Stein, J. and Peifer, M.** (1999). Roles of the C terminus of Armadillo in Wingless signaling in *Drosophila*. *Genetics* **153**, 319-332.
- Cubas, P., de Celis, J. F., Campuzano, S. and Modolell, J.** (1991). Proneural clusters of achaete-scute expression and the generation of sensory organs in the *Drosophila* imaginal wing disc. *Genes and Development* **5**, 996-1008.
- Derynck, R., Jarrett, J. A., Chen, E. Y., Eaton, D. H., Bell, J. R., Assoian, R. K., Roberts, A. B., Sporn, M. B. and Goeddel, D. V.** (1985). Human transforming growth factor-beta complementary DNA sequence and expression in normal and transformed cells. *Nature* **316**, 701-705.
- DiAntonio, A., Haghghi, A. P., Portman, S. L., Lee, J. D., Amaranto, A. M. and Goodman, C. S.** (2001). Ubiquitination-dependent mechanisms regulate synaptic growth and function. *Nature* **412**, 449-452.
- Diaz-Benjumea, F. J. and Cohen, S. M.** (1995). Serrate signals through Notch to establish a Wingless-dependent organizer at the dorsal/ventral compartment boundary of the *Drosophila* wing. *Development* **121**, 4215-4225.
- Doctor, J. S., Jackson, P. D., Rashka, K. E., Visalli, M. and Hoffmann, F. M.** (1992). Sequence, biochemical characterization, and developmental expression of a new member of the TGF-beta superfamily in *Drosophila melanogaster*. *Developmental Biology* **151**, 491-505.
- Ebisawa, T., Fukuchi, M., Murakami, G., Chiba, T., Tanaka, K., Imamura, T. and Miyazono, K.** (2001). Smurf1 interacts with transforming growth factor-beta type I receptor through Smad7 and induces receptor degradation. *Journal of Biological Chemistry* **276**, 12477-12480.
- Entchev, E. V., Schwabedissen, A. and González-Gaitán, M.** (2000). Gradient formation of the TGF-beta homolog Dpp. *Cell* **103**, 981-991.
- Estes, P. S., Roos, J., van\_der\_Bliek, A., Kelly, R. B., Krishnan, K. S. and Ramaswami, M.** (1996). Traffic of dynamin within individual *Drosophila* synaptic boutons relative to compartment-specific markers. *Journal of Neuroscience* **16**, 5443-5456.
- Faucheux, M., Netter, S., Bloyer, S., Moussa, M., Boissonneau, E., Lemeunier, F., Wegnez, M. and Theodore, L.** (2001). Advantages of a P-element construct containing MtnA sequences for the identification of patterning and cell determination genes in *Drosophila melanogaster*. *Mol Genet Genomics* **265**, 14-22.
- Fischer, J. A., Giniger, E., Maniatis, T. and Ptashne, M.** (1988). GAL4 activates transcription in *Drosophila*. *Nature* **332**, 853-856.
- Garcia-Bellido, A., Ripoll, P. and Morata, G.** (1973). Developmental compartmentalisation of the wing disc of *Drosophila*. *Nat New Biol* **245**, 251-253.

- Gentry, L. E., Liubin, M. N., Purchio, A. F. and Marquardt, H.** (1988). Molecular events in the processing of recombinant type 1 pre-pro-transforming growth factor beta to the mature polypeptide. *Mol Cell Biol* **8**, 4162-4168.
- González-Gaitán, M.** (2003). Signal dispersal and transduction through the endocytic pathway. **4**, 213-224.
- Goold, R. G., Owen, R. and Gordon-Weeks, P. R.** (1999). Glycogen synthase kinase 3beta phosphorylation of microtubule-associated protein 1B regulates the stability of microtubules in growth cones. *Journal of Cell Science* **112 ( Pt 19)**, 3373-3384.
- Gorczyca, M., Augart, C. and Budnik, V.** (1993). Insulin-like receptor and insulin-like peptide are localized at neuromuscular junctions in *Drosophila*. *Journal of Neuroscience* **13**, 3692-3704.
- Greco, V., Hannus, M. and Eaton, S.** (2001). Argosomes: a potential vehicle for the spread of morphogens through epithelia. *Cell* **106**, 633-645.
- Guichet, A., Wucherpfennig, T., Dudu, V., Etter, S., Wilsch-Bräuninger, M., Hellwig, A., González-Gaitán, M., Huttner, W. B. and Schmidt, A. A.** (2002). Essential role of endophilin A in synaptic vesicle budding at the *Drosophila* neuromuscular junction. *Embo Journal* **21**, 1661-1672.
- Guillen, I., Mullor, J. L., Capdevila, J., Sanchez-Herrero, E., Morata, G. and Guerrero, I.** (1995). The function of engrailed and the specification of *Drosophila* wing pattern. *Development* **121**, 3447-3456.
- Halpern, M. E., Chiba, A., Johansen, J. and Keshishian, H.** (1991). Growth cone behavior underlying the development of stereotypic synaptic connections in *Drosophila* embryos. *Journal of Neuroscience* **11**, 3227-3238.
- Hartenstein, V.** (1993). Atlas of *Drosophila* Development. *Cold Spring Harbor Laboratory Press*.
- Hata, A., Lagna, G., Massague, J. and Hemmati-Brivanlou, A.** (1998). Smad6 inhibits BMP/Smad1 signaling by specifically competing with the Smad4 tumor suppressor. *Genes and Development* **12**, 186-197.
- Hayes, S., Chawla, A. and Corvera, S.** (2002). TGF beta receptor internalization into EEA1-enriched early endosomes: role in signaling to Smad2. *Journal of Cell Biology* **158**, 1239-1249.
- Heimbeck, G., Bugnon, V., Gendre, N., Haberman, C. and Stocker, R. F.** (1999). Smell and taste perception in *Drosophila melanogaster* larva: toxin expression studies in chemosensory neurons. *Journal of Neuroscience* **19**, 6599-6609.
- Henderson, K. D. and Andrew, D. J.** (1998). Identification of a novel *Drosophila* SMAD on the X chromosome. *Biochem Biophys Res Commun* **252**, 195-201.
- Hoang, B. and Chiba, A.** (2001). Single-cell analysis of *Drosophila* larval neuromuscular synapses. *Developmental Biology* **229**, 55-70.

- Hu, M. C. and Rosenblum, N. D.** (2005). Smad1, {beta}-catenin and Tcf4 associate in a molecular complex with the Myc promoter in dysplastic renal tissue and cooperate to control Myc transcription. *Development* **132**, 215-225.
- Hulsken, J., Birchmeier, W. and Behrens, J.** (1994). E-cadherin and APC compete for the interaction with beta-catenin and the cytoskeleton. *Journal of Cell Biology* **127**, 2061-2069.
- Inoue, H., Imamura, T., Ishidou, Y., Takase, M., Udagawa, Y., Oka, Y., Tsuneizumi, K., Tabata, T., Miyazono, K. and Kawabata, M.** (1998). Interplay of signal mediators of decapentaplegic (Dpp): molecular characterization of mothers against dpp, Medea, and daughters against dpp. *Mol Biol Cell* **9**, 2145-2156.
- Jan, L. Y. and Jan, Y. N.** (1976). L-glutamate as an excitatory transmitter at the *Drosophila* larval neuromuscular junction. **262**, 215-236.
- Jia, X. X., Gorczyca, M. and Budnik, V.** (1993). Ultrastructure of neuromuscular junctions in *Drosophila*: comparison of wild type and mutants with increased excitability. *Journal of Neurobiology* **24**, 1025-1044.
- Johansen, J., Halpern, M. E., Johansen, K. M. and Keshishian, H.** (1989). Stereotypic morphology of glutamatergic synapses on identified muscle cells of *Drosophila* larvae. *Journal of Neuroscience* **9**, 710-725.
- Kadowaki, T., Wilder, E., Klingensmith, J., Zachary, K. and Perrimon, N.** (1996). The segment polarity gene porcupine encodes a putative multitransmembrane protein involved in Wingless processing. *Genes and Development* **10**, 3116-3128.
- Kavsak, P., Rasmussen, R. K., Causing, C. G., Bonni, S., Zhu, H., Thomsen, G. H. and Wrana, J. L.** (2000). Smad7 binds to Smurf2 to form an E3 ubiquitin ligase that targets the TGF beta receptor for degradation. *Mol Cell* **6**, 1365-1375.
- Keshishian, H., Broadie, K., Chiba, A. and Bate, M.** (1996). The *Drosophila* neuromuscular junction: a model system for studying synaptic development and function. *Annu Rev Neurosci* **19**, 545-575.
- Keshishian, H. and Kim, Y. S.** (2004). Orchestrating development and function: retrograde BMP signaling in the *Drosophila* nervous system. *Trends Neurosci* **27**, 143-147.
- Kim, J., Irvine, K. D. and Carroll, S. B.** (1995). Cell recognition, signal induction, and symmetrical gene activation at the dorsal-ventral boundary of the developing *Drosophila* wing. *Cell* **82**, 795-802.
- Kim, J., Sebring, A., Esch, J. J., Kraus, M. E., Vorwerk, K., Magee, J. and Carroll, S. B.** (1996). Integration of positional signals and regulation of wing formation and identity by *Drosophila vestigial* gene. *Nature* **382**, 133-138.
- Knust, E. and Bossinger, O.** (2002). Composition and formation of intercellular junctions in epithelial cells. *Science* **298**, 1955-1959.

- Koh, Y. H., Gramates, L. S. and Budnik, V.** (2000). *Drosophila* larval neuromuscular junction: molecular components and mechanisms underlying synaptic plasticity. *Microsc Res Tech* **49**, 14-25.
- Kretzschmar, M., Liu, F., Hata, A., Doody, J. and Massague, J.** (1997). The TGF-beta family mediator Smad1 is phosphorylated directly and activated functionally by the BMP receptor kinase. *Genes and Development* **11**, 984-995.
- Kruse, K., Pantazis, P., Bollenbach, T., Julicher, F. and González-Gaitán, M.** (2004). Dpp gradient formation by dynamin-dependent endocytosis: receptor trafficking and the diffusion model. *Development* **131**, 4843-4856.
- Kutty, G., Kutty, R. K., Samuel, W., Duncan, T., Jaworski, C. and Wiggert, B.** (1998). Identification of a new member of transforming growth factor-beta superfamily in *Drosophila*: the first invertebrate activin gene. *Biochem Biophys Res Commun* **246**, 644-649.
- Lagna, G., Hata, A., Hemmati-Brivanlou, A. and Massague, J.** (1996). Partnership between DPC4 and SMAD proteins in TGF-beta signalling pathways. *Nature* **383**, 832-836.
- Lamb, R. S., Ward, R. E., Schweizer, L. and Fehon, R. G.** (1998). *Drosophila* coracle, a member of the protein 4.1 superfamily, has essential structural functions in the septate junctions and developmental functions in embryonic and adult epithelial cells. *Mol Biol Cell* **9**, 3505-3519.
- Lander, A. D., Nie, Q. and Wan, F. Y.** (2002). Do morphogen gradients arise by diffusion? **2**, 785-796.
- Lane, N. J. and Swales, L. S.** (1982). Stages in the assembly of pleated and smooth septate junctions in developing insect embryos. *Journal of Cell Science* **56**, 245-262.
- Le Borgne, R., Bellaiche, Y. and Schweisguth, F.** (2002). *Drosophila* E-cadherin regulates the orientation of asymmetric cell division in the sensory organ lineage. *Current Biology* **12**, 95-104.
- Lecuit, T., Brook, W. J., Ng, M., Calleja, M., Sun, H. and Cohen, S. M.** (1996). Two distinct mechanisms for long-range patterning by Decapentaplegic in the *Drosophila* wing. *Nature* **381**, 387-393.
- Letsou, A., Arora, K., Wrana, J. L., Simin, K., Twombly, V., Jamal, J., Staehling-Hampton, K., Hoffmann, F. M., Gelbart, W. M., Massague, J. et al.** (1995). *Drosophila* Dpp signaling is mediated by the punt gene product: a dual ligand-binding type II receptor of the TGF beta receptor family. *Cell* **80**, 899-908.
- Lo, P. C. and Frasch, M.** (1999). Sequence and expression of *myoglianin*, a novel *Drosophila* gene of the TGF-beta superfamily. *Mechanisms of Development* **86**, 171-175.

- Macias-Silva, M., Abdollah, S., Hoodless, P. A., Pirone, R., Attisano, L. and Wrana, J. L.** (1996). MADR2 is a substrate of the TGF beta receptor and its phosphorylation is required for nuclear accumulation and signaling. *Cell* **87**, 1215-1224.
- Marques, G., Bao, H., Haerry, T. E., Shimell, M. J., Duchek, P., Zhang, B. and O'Connor, M. B.** (2002). The *Drosophila* BMP type II receptor Wishful Thinking regulates neuromuscular synapse morphology and function. *Neuron* **33**, 529-543.
- Martinez Arias, A.** (2003). Wnts as morphogens? The view from the wing of *Drosophila*. *Nat Rev Mol Cell Biol* **4**, 321-325.
- Maschat, F., Serrano, N., Randsholt, N. B. and Geraud, G.** (1998). engrailed and polyhomeotic interactions are required to maintain the A/P boundary of the *Drosophila* developing wing. *Development* **125**, 2771-2780.
- Massague, J.** (2000). How cells read TGF-beta signals. *Nat Rev Mol Cell Biol* **1**, 169-178.
- McCabe, B. D., Hom, S., Aberle, H., Fetter, R. D., Marques, G., Haerry, T. E., Wan, H., O'Connor, M. B., Goodman, C. S. and Haghghi, A. P.** (2004). Highwire regulates presynaptic BMP signaling essential for synaptic growth. *Neuron* **41**, 891-905.
- McCabe, B. D., Marques, G., Haghghi, A. P., Fetter, R. D., Crotty, M. L., Haerry, T. E., Goodman, C. S. and O'Connor, M. B.** (2003). The BMP homolog Gbb provides a retrograde signal that regulates synaptic growth at the *Drosophila* neuromuscular junction. *Neuron* **39**, 241-254.
- Monastirioti, M., Gorczyca, M., Rapus, J., Eckert, M., White, K. and Budnik, V.** (1995). Octopamine immunoreactivity in the fruit fly *Drosophila melanogaster*. *Journal of Comparative Neurology* **356**, 275-287.
- Murphy, S. J., Dore, J. J., Edens, M., Coffey, R. J., Barnard, J. A., Mitchell, H., Wilkes, M. and Leof, E. B.** (2004). Differential trafficking of transforming growth factor-beta receptors and ligand in polarized epithelial cells. *Mol Biol Cell* **15**, 2853-2862.
- Nellen, D., Affolter, M. and Basler, K.** (1994). Receptor serine/threonine kinases implicated in the control of *Drosophila* body pattern by decapentaplegic. *Cell* **78**, 225-237.
- Nellen, D., Burke, R., Struhl, G. and Basler, K.** (1996). Direct and long-range action of a DPP morphogen gradient. *Cell* **85**, 357-368.
- Neumann, C. J. and Cohen, S. M.** (1996). Distinct mitogenic and cell fate specification functions of *wingless* in different regions of the wing. *Development* **122**, 1781-1789.
- Nguyen, M., Parker, L. and Arora, K.** (2000). Identification of *maverick*, a novel member of the TGF-beta superfamily in *Drosophila*. *Mechanisms of Development* **95**, 201-206.

- Nishita, M., Hashimoto, M. K., Ogata, S., Laurent, M. N., Ueno, N., Shibuya, H. and Cho, K. W.** (2000). Interaction between Wnt and TGF-beta signalling pathways during formation of Spemann's organizer. *Nature* **403**, 781-785.
- Oda, H., Uemura, T., Harada, Y., Iwai, Y. and Takeichi, M.** (1994). A *Drosophila* homolog of cadherin associated with armadillo and essential for embryonic cell-cell adhesion. *Developmental Biology* **165**, 716-726.
- Omer, C. A., Miller, P. J., Diehl, R. E. and Kral, A. M.** (1999). Identification of Tcf4 residues involved in high-affinity beta-catenin binding. *Biochem Biophys Res Commun* **256**, 584-590.
- Orsulic, S. and Peifer, M.** (1996). An in vivo structure-function study of armadillo, the beta-catenin homologue, reveals both separate and overlapping regions of the protein required for cell adhesion and for wingless signaling. *Journal of Cell Biology* **134**, 1283-1300.
- Packard, M., Koo, E. S., Gorczyca, M., Sharpe, J., Cumberledge, S. and Budnik, V.** (2002). The *Drosophila* Wnt, wingless, provides an essential signal for pre- and postsynaptic differentiation. *Cell* **111**, 319-330.
- Parker, L., Stathakis, D. G. and Arora, K.** (2004). Regulation of BMP and activin signaling in *Drosophila*. *Prog Mol Subcell Biol* **34**, 73-101.
- Penton, A., Chen, Y., Staehling-Hampton, K., Wrana, J. L., Attisano, L., Szidonya, J., Cassill, J. A., Massague, J. and Hoffmann, F. M.** (1994). Identification of two bone morphogenetic protein type I receptors in *Drosophila* and evidence that Brk25D is a decapentaplegic receptor. *Cell* **78**, 239-250.
- Perrimon, N. and Mahowald, A. P.** (1987). Multiple functions of segment polarity genes in *Drosophila*. *Developmental Biology* **119**, 587-600.
- Prokop, A., Landgraf, M., Rushton, E., Brodie, K. and Bate, M.** (1996). Presynaptic development at the *Drosophila* neuromuscular junction: assembly and localization of presynaptic active zones. *Neuron* **17**, 617-626.
- Rafferty, L. A., Twombly, V., Wharton, K. and Gelbart, W. M.** (1995). Genetic screens to identify elements of the decapentaplegic signaling pathway in *Drosophila*. *Genetics* **139**, 241-254.
- Rawson, J. M., Lee, M., Kennedy, E. L. and Selleck, S. B.** (2003). *Drosophila* neuromuscular synapse assembly and function require the TGF-beta type I receptor saxophone and the transcription factor Mad. *Journal of Neurobiology* **55**, 134-150.
- Roche, J. P., Packard, M. C., Moeckel-Cole, S. and Budnik, V.** (2002). Regulation of synaptic plasticity and synaptic vesicle dynamics by the PDZ protein Scribble. *Journal of Neuroscience* **22**, 6471-6479.



- Roos, J., Hummel, T., Ng, N., Klambt, C. and Davis, G. W.** (2000). *Drosophila* Futsch regulates synaptic microtubule organization and is necessary for synaptic growth. *Neuron* **26**, 371-382.
- Ruberte, E., Marty, T., Nellen, D., Affolter, M. and Basler, K.** (1995). An absolute requirement for both the type II and type I receptors, punt and thick veins, for dpp signaling in vivo. *Cell* **80**, 889-897.
- Salinas, P. C. and Hall, A. C.** (1999). Lithium and synaptic plasticity. *Bipolar Disord* **1**, 87-90.
- Sanicola, M., Sekelsky, J., Elson, S. and Gelbart, W. M.** (1995). Drawing a stripe in *Drosophila* imaginal discs: negative regulation of *decapentaplegic* and *patched* expression by engrailed. *Genetics* **139**, 745-756.
- Schuster, C. M., Davis, G. W., Fetter, R. D. and Goodman, C. S.** (1996). Genetic dissection of structural and functional components of synaptic plasticity. I. Fasciclin II controls synaptic stabilization and growth. *Neuron* **17**, 641-654.
- Sekelsky, J. J., Newfeld, S. J., Raftery, L. A., Chartoff, E. H. and Gelbart, W. G.** (1995). Genetic characterization and cloning of Mothers against dpp, a gene required for decapentaplegic function in *Drosophila melanogaster*. *Genetics* **139**, 1347--1358.
- Shi Y., M. J.** (2003). Mechanisms of TGF-beta signaling from cell membrane to the nucleus. *Cell* **113**, 685-700.
- Sink, H. and Whittington, P. M.** (1991). Location and connectivity of abdominal motoneurons in the embryo and larva of *Drosophila melanogaster*. *Journal of Neurobiology* **22**, 298-311.
- Skeath, J. B. and Carroll, S. B.** (1992). Regulation of proneural gene expression and cell fate during neuroblast segregation in the *Drosophila* embryo. *Development* **114**, 939-946.
- Spencer, F. A., Hoffmann, F. M. and Gelbart, W. M.** (1982). Decapentaplegic: a gene complex affecting morphogenesis in *Drosophila melanogaster*. *Cell* **28**, 451-461.
- St Johnston, R. D., Hoffmann, F. M., Blackman, R. K., Segal, D., Grimaila, R., Padgett, R. W., Irick, H. A. and Gelbart, W. M.** (1990). Molecular organization of the decapentaplegic gene in *Drosophila melanogaster*. *Genes and Development* **4**, 1114-1127.
- Strigini, M. and Cohen, S. M.** (1997). A Hedgehog activity gradient contributes to AP axial patterning of the *Drosophila* wing. *Development (Cambridge, England)* **124**, 4697-4705.
- Strigini, M. and Cohen, S. M.** (2000). Wingless gradient formation in the *Drosophila* wing. *Current Biology* **10**, 293-300.

- Sutherland, D. J., Li, M., Liu, X. Q., Stefancsik, R. and Raftery, L. A.** (2003). Stepwise formation of a SMAD activity gradient during dorsal-ventral patterning of the *Drosophila* embryo. *Development* **130**, 5705-5716.
- Suzuki, C., Murakami, G., Fukuchi, M., Shimanuki, T., Shikauchi, Y., Imamura, T. and Miyazono, K.** (2002). Smurf1 regulates the inhibitory activity of Smad7 by targeting Smad7 to the plasma membrane. *Journal of Biological Chemistry* **277**, 39919-39925.
- Sweeney, S. T. and Davis, G. W.** (2002). Unrestricted synaptic growth in spinster-a late endosomal protein implicated in TGF-beta-mediated synaptic growth regulation. *Neuron* **36**, 403-416.
- Tabata, T. and Kornberg, T. B.** (1994). Hedgehog is a signaling protein with a key role in patterning *Drosophila* imaginal discs. *Cell* **76**, 89-102.
- Tajima, Y., Goto, K., Yoshida, M., Shinomiya, K., Sekimoto, T., Yoneda, Y., Miyazono, K. and Imamura, T.** (2003). Chromosomal region maintenance 1 (CRM1)-dependent nuclear export of Smad ubiquitin regulatory factor 1 (Smurf1) is essential for negative regulation of transforming growth factor-beta signaling by Smad7. *Journal of Biological Chemistry* **278**, 10716-10721.
- Tanimoto, H., Itoh, S., ten Dijke, P. and Tabata, T.** (2000). Hedgehog creates a gradient of DPP activity in *Drosophila* wing imaginal discs. *Mol Cell* **5**, 59-71.
- Teleman, A. A. and Cohen, S. M.** (2000). Dpp gradient formation in the *Drosophila* wing imaginal disc. *Cell* **103**, 971-980.
- Tepass, U., Gruszynski-DeFeo, E., Haag, T. A., Omatyar, L., Torok, T. and Hartenstein, V.** (1996). *shotgun* encodes *Drosophila* E-cadherin and is preferentially required during cell rearrangement in the neurectoderm and other morphogenetically active epithelia. *Genes and Development* **10**, 672-685.
- Tian, Y. C. and Phillips, A. O.** (2002). Interaction between the transforming growth factor-beta type II receptor/Smad pathway and beta-catenin during transforming growth factor-beta1-mediated adherens junction disassembly. *Am J Pathol* **160**, 1619-1628.
- Tolwinski, N. S. and Wieschaus, E.** (2001). Armadillo nuclear import is regulated by cytoplasmic anchor Axin and nuclear anchor dTCF/Pan. *Development* **128**, 2107-2117.
- Tolwinski, N. S. and Wieschaus, E.** (2004). A Nuclear Function for Armadillo/beta-Catenin. *PLoS Biol* **2**, E95.
- Tsukazaki, T., Chiang, T. A., Davison, A. F., Attisano, L. and Wrana, J. L.** (1998). SARA, a FYVE domain protein that recruits Smad2 to the TGF beta receptor. *Cell* **95**, 779-791.
- Tsuneizumi, K., Nakayama, T., Kamoshida, Y., Kornberg, T. B., Christian, J. L. and Tabata, T.** (1997). Daughters against dpp modulates dpp organizing activity in *Drosophila* wing development. *Nature* **389**, 627-631.

- Turing, A. M.** (1952). The Chemical Basis of Morphogenesis. *Philosophical Transactions of the Royal Society of London Series B-Biological Sciences* **237**, 37-72.
- Vervoort, M., Crozatier, M., Valle, D. and Vincent, A.** (1999). The COE transcription factor Collier is a mediator of short-range Hedgehog-induced patterning of the *Drosophila* wing. *Current Biology* **9**, 632-639.
- Wan, H. I., DiAntonio, A., Fetter, R. D., Bergstrom, K., Strauss, R. and Goodman, C. S.** (2000). Highwire regulates synaptic growth in *Drosophila*. *Neuron* **26**, 313-329.
- Wang, Q. T. and Holmgren, R. A.** (1999). The subcellular localization and activity of *Drosophila* cubitus interruptus are regulated at multiple levels. *Development* **126**, 5097-5106.
- Ward, R. E. t., Schweizer, L., Lamb, R. S. and Fehon, R. G.** (2001). The protein 4.1, ezrin, radixin, moesin (FERM) domain of *Drosophila* Coracle, a cytoplasmic component of the septate junction, provides functions essential for embryonic development and imaginal cell proliferation. *Genetics* **159**, 219-228.
- Wharton, K. A., Thomsen, G. H. and Gelbart, W. M.** (1991). *Drosophila* 60A gene, another transforming growth factor beta family member, is closely related to human bone morphogenetic proteins. *Proceedings of the National Academy of Sciences of the United States of America* **88**, 9214-9218.
- Wiersdorff, V., Lecuit, T., Cohen, S. M. and Mlodzik, M.** (1996). Mad acts downstream of Dpp receptors, revealing a differential requirement for *dpp* signaling in initiation and propagation of morphogenesis in the *Drosophila* eye. *Development* **122**, 2153-2162.
- Wodarz, A., Ramrath, A., Grimm, A. and Knust, E.** (2000). *Drosophila* atypical protein kinase C associates with Bazooka and controls polarity of epithelia and neuroblasts. *Journal of Cell Biology* **150**, 1361-1374.
- Wolpert, L.** (1969). Positional information and the spatial pattern of cellular differentiation. *J Theor Biol* **25**, 1-47.
- Woods, D. F. and Bryant, P. J.** (1991). The *discs-large* tumor suppressor gene of *Drosophila* encodes a guanylate kinase homolog localized at septate junctions. *Cell* **66**, 451-464.
- Woods, D. F., Hough, C., Peel, D., Callaini, G. and Bryant, P. J.** (1996). Dlg protein is required for junction structure, cell polarity, and proliferation control in *Drosophila* epithelia. *Journal of Cell Biology* **134**, 1469-1482.
- Wrana, J. L., Attisano, L., Wieser, R., Ventura, F. and Massague, J.** (1994). Mechanism of activation of the TGF-beta receptor. *Nature* **370**, 341-347.
- Wucherpennig, T., Wilsch-Bräuninger, M. and González-Gaitán, M.** (2003). Role of *Drosophila* Rab5 during endosomal trafficking at the synapse and evoked neurotransmitter release. *The Journal of Cell Biology* **161**, 609-624.

- Xie, T., Finelli, A. L. and Padgett, R. W.** (1994). The *Drosophila saxophone* gene: a serine-threonine kinase receptor of the TGF-beta superfamily. *Science* **263**, 1756-1759.
- Xu, L., Chen, Y. G. and Massague, J.** (2000). The nuclear import function of Smad2 is masked by SARA and unmasked by TGF beta-dependent phosphorylation. *Nat Cell Biol* **2**, 559-562.
- Zecca, M., Basler, K. and Struhl, G.** (1996). Direct and long-range action of a wingless morphogen gradient. *Cell* **87**, 833-844.
- Zheng, X., Wang, J., Haerry, T. E., Wu, A. Y., Martin, J., O'Connor, M. B., Lee, C. H. and Lee, T.** (2003). TGF-beta signaling activates steroid hormone receptor expression during neuronal remodeling in the *Drosophila* brain. *Cell* **112**, 303-315.
- Zhong, Y., Budnik, V. and Wu, C. F.** (1992). Synaptic plasticity in *Drosophila* memory and hyperexcitable mutants: role of cAMP cascade. *Journal of Neuroscience* **12**, 644-651.
- Zhu, H., Kavsak, P., Abdollah, S., Wrana, J. L. and Thomsen, G. H.** (1999). A SMAD ubiquitin ligase targets the BMP pathway and affects embryonic pattern formation. *Nature* **400**, 687-693.
- Zinsmaier, K. E., Eberle, K. K., Buchner, E., Walter, N. and Benzer, S.** (1994). Paralysis and early death in *cysteine string protein* mutants of *Drosophila*. *Science* **263**, 977-980.

**Statement / Versicherung**

I herewith declare that I have produced this paper without the prohibited assistance of third parties and without making use of aids other than those specified; notions taken over directly or indirectly from other sources have been identified as such. This paper has not previously been presented in identical or similar form to any other German or foreign examination board. The thesis work was conducted from 15.06.2001 to 22.02.2005 under the supervision of Dr. Marcos González-Gaitán at the Max Planck Institute of Molecular Cell Biology and Genetics in Dresden.

Hiermit versichere ich, dass ich die vorliegende Arbeit ohne unzulässige Hilfe Dritter und ohne Benutzung anderer als der angegebenen Hilfsmittel angefertigt habe; die aus fremden Quellen direkt oder indirekt übernommenen Gedanken sind als solche kenntlich gemacht. Die Arbeit wurde bisher weder im Inland noch im Ausland in gleicher oder ähnlicher Form einer anderen Prüfungsbehörde vorgelegt. Die vorgelegte Arbeit wurde vom 15.06.2001 bis 22.02.2005 unter der Aufsicht von Dr. Marcos González-Gaitán am Max Planck Institut für Molekulare Zellbiologie und Genetik in Dresden durchgeführt.

Dresden,  
22.02.2005

## Publications during PhD

**Guichet, A., Wucherpfennig, T., Dudu, V., Etter, S., Wilsch-Bräuninger, M., Hellwig, A., González-Gaitán, M., Huttner, W.B. and Schmidt, A.A. (2002).** Essential role of endophilin A in synaptic vesicle budding at the *Drosophila* neuromuscular junction. *EMBO Journal* **21**, 1661-1672.

**Dudu, V.\*, Pantazis, P.\* and González-Gaitán, M. (2004).** Membrane traffic during embryonic development: epithelial formation, cell fate decisions and differentiation. *Current Opinion in Cell Biology* **16**, 407-414.

\* equally contributed